

EUR 3113.e

EUROPEAN ATOMIC ENERGY COMMUNITY - EURATOM

FIAT S. p. A., Sezione Energia Nucleare - Torino

Società ANSALDO S. p. A. - Genova

**FORCED CONVECTION BURNOUT AND
HYDRODYNAMIC INSTABILITY
EXPERIMENTS FOR WATER AT HIGH
PRESSURE**

PART III: COMPARISON BETWEEN EXPERIMENTAL BURNOUT DATA AND
THEORETICAL PREDICTION FOR UNIFORM AND NON-UNIFORM
HEAT FLUX DISTRIBUTION

by

G. PREVITI, P. GRILLO

(FIAT, Sezione Energia Nucleare, Torino, Italia)

and

A. CAMPANILE, G. GALIMI, M. GOFFI

(SORIN, Centro Ricerche Nucleari, Saluggia, Italia)

1966



Contract No 008-61-12 PNII

LEGAL NOTICE

This document was prepared under the sponsorship of the Commission of the European Atomic Energy Community (EURATOM).

Neither the EURATOM Commission, its contractors nor any person acting on their behalf :

Make any warranty or representation, express or implied, with respect to the accuracy, completeness, or usefulness of the information contained in this document, or that the use of any information, apparatus, method, or process disclosed in this document may not infringe privately owned rights ; or

Assume any liability with respect to the use of, or for damages resulting from the use of any information, apparatus, method or process disclosed in this document.

This report is on sale at the addresses listed on cover page 4

at the price of FF 17.50 FB 175 DM 14.— Lit. 2180 Fl. 12.65

When ordering, please quote the EUR number and the title, which are indicated on the cover of each report.

Printed by Vanmelle
Brussels, August 1966

This document was duplicated on the basis of the best available copy.

EUR 3113.e

FORCED CONVECTION BURNOUT AND HYDRODYNAMIC INSTABILITY EXPERIMENTS FOR WATER AT HIGH PRESSURE PART III : COMPARISON BETWEEN EXPERIMENTAL BURNOUT DATA AND THEORETICAL PREDICTION FOR UNIFORM AND NON-UNIFORM HEAT FLUX DISTRIBUTION

by G. PREVITI, P. GRILLO (FIAT, Sezione Energia Nucleare, Torino, Italia) and A. CAMPANILE, G. GALIMI, M. GOFFI (SORIN, Centro Ricerche Nucleari, Saluggia, Italia)

European Atomic Energy Community - EURATOM

FIAT S.p.A., Sezione Energia Nucleare - Torino

Società ANSALDO S.p.A. - Genova

Contract No. 008-61-12 PNII

Brussels, August 1966 - 136 Pages - 51 Figures - FB 175

The increase of power output from a pressurized water reactor core with constant hot channel factors depends largely upon a more accurate

EUR 3113.e

FORCED CONVECTION BURNOUT AND HYDRODYNAMIC INSTABILITY EXPERIMENTS FOR WATER AT HIGH PRESSURE PART III : COMPARISON BETWEEN EXPERIMENTAL BURNOUT DATA AND THEORETICAL PREDICTION FOR UNIFORM AND NON-UNIFORM HEAT FLUX DISTRIBUTION

by G. PREVITI, P. GRILLO (FIAT, Sezione Energia Nucleare, Torino, Italia) and A. CAMPANILE, G. GALIMI, M. GOFFI (SORIN, Centro Ricerche Nucleari, Saluggia, Italia)

European Atomic Energy Community - EURATOM

FIAT S.p.A., Sezione Energia Nucleare - Torino

Società ANSALDO S.p.A. - Genova

Contract No. 008-61-12 PNII

Brussels, August 1966 - 136 Pages - 51 Figures - FB 175

The increase of power output from a pressurized water reactor core with constant hot channel factors depends largely upon a more accurate

EUR 3113.e

FORCED CONVECTION BURNOUT AND HYDRODYNAMIC INSTABILITY EXPERIMENTS FOR WATER AT HIGH PRESSURE PART III : COMPARISON BETWEEN EXPERIMENTAL BURNOUT DATA AND THEORETICAL PREDICTION FOR UNIFORM AND NON-UNIFORM HEAT FLUX DISTRIBUTION

by G. PREVITI, P. GRILLO (FIAT, Sezione Energia Nucleare, Torino, Italia) and A. CAMPANILE, G. GALIMI, M. GOFFI (SORIN, Centro Ricerche Nucleari, Saluggia, Italia)

European Atomic Energy Community - EURATOM

FIAT S.p.A., Sezione Energia Nucleare - Torino

Società ANSALDO S.p.A. - Genova

Contract No. 008-61-12 PNII

Brussels, August 1966 - 136 Pages - 51 Figures - FB 175

The increase of power output from a pressurized water reactor core with constant hot channel factors depends largely upon a more accurate

prediction of DNB conditions (Departure from Nuclear Boiling or burnout phenomenon).

The finality of the present work is to compare the experimental data obtained for conditions peculiar of small PWR cores with the predictions of several correlations chosen among the existing ones for their reliability.

The experimental data have been obtained from a research program supplementing the design study of a nuclear tanker performed under a contract between Euratom, Fiat and Ansaldo with the participation of CNEN.

The experiments have been carried out by SORIN Heat Transfer Laboratory. The data cover both uniform and non-uniform power distributions as well as unheated wall effect. Although a large fraction of the collected data have been obtained for the tanker reactor design conditions, a certain number of parameters such as pressure, mass flow rate, inlet enthalpy, and diameter have been investigated so that the comparison here presented will have a broader interest.

prediction of DNB conditions (Departure from Nuclear Boiling or burnout phenomenon).

The finality of the present work is to compare the experimental data obtained for conditions peculiar of small PWR cores with the predictions of several correlations chosen among the existing ones for their reliability.

The experimental data have been obtained from a research program supplementing the design study of a nuclear tanker performed under a contract between Euratom, Fiat and Ansaldo with the participation of CNEN.

The experiments have been carried out by SORIN Heat Transfer Laboratory. The data cover both uniform and non-uniform power distributions as well as unheated wall effect. Although a large fraction of the collected data have been obtained for the tanker reactor design conditions, a certain number of parameters such as pressure, mass flow rate, inlet enthalpy, and diameter have been investigated so that the comparison here presented will have a broader interest.

prediction of DNB conditions (Departure from Nuclear Boiling or burnout phenomenon).

The finality of the present work is to compare the experimental data obtained for conditions peculiar of small PWR cores with the predictions of several correlations chosen among the existing ones for their reliability.

The experimental data have been obtained from a research program supplementing the design study of a nuclear tanker performed under a contract between Euratom, Fiat and Ansaldo with the participation of CNEN.

The experiments have been carried out by SORIN Heat Transfer Laboratory. The data cover both uniform and non-uniform power distributions as well as unheated wall effect. Although a large fraction of the collected data have been obtained for the tanker reactor design conditions, a certain number of parameters such as pressure, mass flow rate, inlet enthalpy, and diameter have been investigated so that the comparison here presented will have a broader interest.

EUR 3113.e

EUROPEAN ATOMIC ENERGY COMMUNITY - EURATOM
FIAT S. p. A., Sezione Energia Nucleare - Torino
Società ANSALDO S. p. A. - Genova

**FORCED CONVECTION BURNOUT AND
HYDRODYNAMIC INSTABILITY
EXPERIMENTS FOR WATER AT HIGH
PRESSURE**

PART III : COMPARISON BETWEEN EXPERIMENTAL BURNOUT DATA AND
THEORETICAL PREDICTION FOR UNIFORM AND NON-UNIFORM
HEAT FLUX DISTRIBUTION

by

G. PREVITI, P. GRILLO

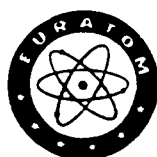
(FIAT, Sezione Energia Nucleare, Torino, Italia)

and

A. CAMPANILE, G. GALIMI, M. GOFFI

(SORIN, Centro Ricerche Nucleari, Saluggia, Italia)

1966



Contract No 008-61-12 PNII

LIST OF FIGURES

- FIG. 1 - Uniform heat flux distribution - DNB ratios obtained by q'' W-2 correlation versus exit quality - Test section No. 1B - 1C.
- FIG. 2 - Uniform heat flux distribution - DNB ratios obtained by ΔH -W 2 correlation versus exit quality - Test section No. 1B - 1C.
- FIG. 3 - Uniform heat flux distribution - DNB ratios obtained by W-3 correlation versus exit quality - Test section No. 1 - 1B - 1C.
- FIG. 4 - Uniform heat flux distribution - DNB ratios obtained by Ferrel's correlation versus exit quality - Test section No. 1 - 1B - 1C.
- FIG. 5 - Uniform heat flux distribution - DNB ratios obtained by CISE correlation versus exit quality - Test section No. 1 - 1B - 1C.
- FIG. 6 - Uniform heat flux distribution - DNB ratios obtained by ΔH -FIAT correlation versus exit quality - Test section No. 1 - 1B - 1C.
- FIG. 7 - Effect of power distribution on burnout-Critical power versus inlet subcooling.
- FIG. 8 - Effect of power distribution on burnout-Critical power versus inlet subcooling.
- FIG. 9 - Effect of power distribution on burnout-Critical power versus inlet subcooling.
- FIG. 10 - Effect of power distribution on burnout-Critical power versus quality at DNB location.
- FIG. 11 - Effect of power distribution on burnout-Critical power versus quality at DNB location.
- FIG. 12 - Effect of power distribution on burnout-Critical power versus quality at DNB location.
- FIG. 13 - Effect of power distribution on burnout-Critical power versus quality at DNB location.
- FIG. 14 - Effect of power distribution on burnout-Critical power versus quality at DNB location.
- FIG. 15 - Effect of power distribution on burnout-Critical power versus exit quality.
- FIG. 16 - Effect of power distribution on burnout-Critical power versus exit quality.
- FIG. 17 - Effect of power distribution on burnout-Critical power versus exit quality.
- FIG. 18 - Effect of power distribution on burnout-Critical power versus exit quality.

- FIG.19 - Effect of power distribution on burnout-Critical power versus exit quality.
- FIG.20 - Effect of local "hot patch" on burnout.
- FIG.21 - Non uniform heat flux distribution - Highly subcooled region-DNB ratios obtained by Ferrel's correlation versus exit quality - Test section No. 2 - 2B - 2C.
- FIG.22 - Non uniform heat flux distribution - Highly subcooled region-DNB ratios obtained by $q'' W^2$ correlation versus exit quality - Test section No. 2B - 2C.
- FIG.23 - Simmetrical cosine heat flux distribution - Intermediate region DNB ratios obtained by memory effect method applied to W-3 correlation (Ref.15) versus exit quality - Test section No. 2.
- FIG.24 - Asymmetrical cosine heat flux distribution - Intermediate region DNB ratios obtained by memory effect method applied to W-3 correlation (Ref.15) versus exit quality - Test section No. 2B-2C.
- FIG.25 - Simmetrical cosine heat flux distribution. Comparison between predicted and measured DNB locations.
- FIG.26 - Asymmetrical sine skewed toward the bottom heat flux distribution. Comparison between predicted and measured DNB locations.
- FIG.27 - Asymmetrical sine skewed toward the top heat flux distribution. Comparison between predicted and measured DNB locations.
- FIG.28 - Comparison between critical heat fluxes obtained by W-3 correlation with and without the use of F factor.
- FIG.29 - Comparison between critical heat fluxes obtained by W-3 correlation with and without the use of F factor.
- FIG.30 - Non uniform heat flux distribution - Intermediate region - DNB ratios obtained by Ferrel's correlation versus exit quality - Test section No. 2.
- FIG.31 - Non uniform heat flux distribution - Intermediate region - DNB ratios obtained by Ferrel's correlation versus exit quality - Test section No. 2B - 2C.
- FIG.32 - Non uniform heat flux distribution - Intermediate region - DNB ratios obtained by CISE correlation versus exit quality - Test section No. 2 - 2B - 2C.
- FIG.33 - Non uniform heat flux distribution - Intermediate region - DNB ratios obtained by ΔH -FIAT correlation versus exit quality - Test section No. 2 - 2B - 2C.
- FIG.34 - Non uniform heat flux distribution - High quality region - DNB ratios obtained by Ferrel's correlation versus exit quality - Test section No. 2 - 2B - 2C.

- FIG.35 - Non uniform heat flux distribution - High quality region - DNB ratios obtained by ΔH -W 2 correlation versus exit quality - Test section No. 2B - 2C.
- FIG.36 - Non uniform heat flux distribution - High quality region - DNB ratios obtained by CISE correlation versus exit quality - Test section No. 2 - 2B - 2C.
- FIG.37 - Non uniform heat flux distribution - High quality region - DNB ratios obtained by ΔH -FIAT correlation versus exit quality - Test section No. 2, 2B, 2C.
- FIG.38 - Comparison of predictions from W-2 q'' DNB correlation with heater rod in square duct DNB data.
Nominal pressures: 84, 126, 132 ata
- FIG.39 - Comparison of predictions from W-2 q'' DNB modified correlation with heater rod in square duct DNB data.
Nominal pressures: 84, 126, 132 ata
- FIG.40 - Comparison of predictions from W-2 ΔH_{DNB} correlations with heater rod in square duct DNB data.
Nominal pressures: 84, 126, 132 ata
- FIG.41 - Comparison of predictions from W-3 correlations with heater rod in square duct DNB data.
Nominal pressures: 84, 126, 132 ata
- FIG.42 - Comparison of predictions from CISE correlation with heater rod in square duct DNB data. L and \hat{W} parameters correlation.
Nominal pressures: 84, 126, 132 ata
- FIG.43 - Comparison of predictions from CISE correlation with heater rod in square duct DNB data. L_g and \hat{W}_g parameters correlation.
Nominal pressures: 84, 126, 132 ata
- FIG.44 - DNB ratio versus exit quality for heater rod in square duct data obtained with W-2 modified correlations.
Nominal pressure : 84 ata
- FIG.45 - DNB ratio versus exit quality for heater rod in square duct data obtained with W-2 modified correlations.
Nominal pressures: 126 - 132 ata
- FIG.46 - DNB ratio versus exit quality for heater rod in square duct data obtained with W-3 correlation.
Nominal pressure : 84 ata
- FIG.47 - DNB ratio versus exit quality for heater rod in square duct data obtained with W-3 correlation.
Nominal pressures : 126 - 132 ata
- FIG.48 - DNB ratio versus exit quality for heater rod in square duct data obtained with W-3 modified correlation.
Nominal pressures : 126 - 132 ata

- FIG.49 - DNB ratio versus exit quality for heater rod in square duct data obtained with CISE generalized correlation.
Nominal pressure : 84 ata
- FIG.50 - DNB ratio versus exit quality for heater rod in square duct data obtained with CISE generalized correlation.
Nominal pressures: 126 - 132 ata
- FIG.51 - Equivalent enthalpy rises of "local and system parameters" correlations.

LIST OF TABLES

- TABLE I - Thermal and hydraulic core data.
- TABLE II - Test sections data.
- TABLE III - Comparison between measured and predicted critical powers for uniform heat flux distribution (test section no. 1)
- TABLE IV - Comparison between measured and predicted critical powers for uniform heat flux distribution (test section no. 1B)
- TABLE V - Comparison between measured and predicted critical powers for uniform heat flux distribution (test section no. 1C)
- TABLE VI - Comparison between measured and predicted critical powers for non uniform heat flux distribution - Highly subcooled region.
- TABLE VII - Comparison between measured and predicted critical powers for non uniform heat flux distribution - Intermediate quality region.
- TABLE VIII - Comparison between measured and predicted critical powers for non uniform heat flux distribution - High quality region.
- TABLE IX - Comparison of DNB data in square annular test section with DNB correlations - Heated length 560 mm. Nominal pressure 84 ata.
- TABLE X - Comparison of DNB data in square annular test section with DNB correlations - Heated length 560 mm. Nominal pressure 126 ata.
- TABLE XI - Comparison of DNB data in square annular test section with DNB correlations - Heated length 560 mm. Nominal pressure 132 ata.
- TABLE XII - Comparison of DNB data in square annular test section with DNB correlations - Heated length 1183 mm. Nominal pressure 84 ata.
- TABLE XIII - Comparison of DNB data in square annular test section with DNB correlations - Heated length 1183 mm. Nominal pressure 132 ata.
- TABLE XIV - General data of the normal unit cell.

I N T R O D U C T I O N (*)

The increase of power output from a pressurized water reactor core with constant hot channel factors depends largely upon a more accurate prediction of DNB conditions (Departure from Nucleate Boiling or burnout phenomenon).

The finality of the present work is to compare the experimental data obtained for conditions peculiar of small PWR cores with the predictions of several correlations chosen among the existing ones for their reliability.

The experimental data have been obtained from a research program supplementing the design study of a nuclear tanker performed under a contract between Euratom, Fiat and Ansaldo with the participation of CNEN (1) (2).

The experiments have been carried out by SORIN Heat Transfer Laboratory. The data cover both uniform and non uniform power distributions as well as unheated wall effect. Although a large fraction of the collected data have been obtained for the tanker reactor design conditions, a certain number of parameters such as pressure, mass flow rate, inlet enthalpy, and diameter have been investigated so that the comparison here presented will have a broader interest.

In Table I the actual thermal and hydraulic design conditions for the tanker reactor core are reported to be compared with the test conditions of the various test sections up to now investigated.

(*) Manuscript received on July 11, 1966

A. TUBULAR TEST SECTIONS

A.1. Uniform power distribution

Three test sections have been used to investigate the DNB conditions with uniform axial heat flux distribution. A detailed description of the test sections is given in Ref.(1). In Table II are given the dimensions of the heaters and the range of parameters tested with each configuration. The uniform heat flux heaters were tested in the earlier stage of the contract when a comparison study was conducted between a boiling and a pressurized water reactor; hence some of the tested conditions are peculiar of a BWR solution.

A.1.a. Review of existing DNB correlations

At present a vast number of DNB correlations exists. A preliminary analysis was made in order to choose the most reliable and general ones among the correlations for upward forced water flow.

In Ref.(3) a comparison between experimental data and predictions shows that Griffith, Bernath, Gambill, Weatherhead and Macbeth correlations are not accurate enough for design purpose. The Zenkevich correlation, limited to subcooled conditions only, yields acceptable results. Westinghouse, in 1962, developed two correlations (W-2) applicable in the subcooled region ($q''W-2$) and in the quality region ($\Delta H W-2$) (Ref.3). Lately (Ref.4) a new correlation, called W-3 correlation, has been developed covering the quality range $-15\% < X < +15\%$. Within these limits, it is suggested to use the W-3 correlation instead of the W-2 ones since, with these correlations, a discontinuity generally occurred at the saturation condition.

The other correlations used for comparison purpose are :

- CISE (Ref.5) and FIAT (Ref.6) (for the quality region)
- Ferrel's (Ref.7) (for both quality and subcooled conditions).

Here after the correlations used are presented and discussed in some details.

./. .

1) W-2 Correlations

As result of a parametric study of DNB experimental data, Westinghouse developed two DNB correlations for the subcooled and for the quality region respectively. The first one determines the critical conditions by a local heat flux, the other assumes local enthalpy to be the limiting condition for DNB. The critical power P_{DNB} is expressed, in each correlation, as a function of the following terms :

$$P_{DNB} = F(H_{IN}, L/De, De, p, G)$$

The W-2 q'' and ΔH correlations expression are as follows :

$$q''_{DNB} = (0,23 \times 10^6 + 0,094 G) (3 + 0,01 \Delta T_{sub})$$

$$(0,435 + 1,23 e^{-0,0093 L/De}) (1,7 - 1,4 e^{-a})$$

$$\text{where: } a = 0,532 \left[(H_f - H_{IN}) / H_{fg} \right]^{3/4} \left(\frac{\rho_g}{\rho_f} \right)^{-1/3} \quad (1)$$

and :

$$\begin{aligned} \Delta H_{DNB} &= 0,529 (H_f - H_{IN}) + (0,825 + 2,36 e^{-204 De}) H_{fg} e^{-1,5 G/10^6} \\ &- 0,41 H_{fg} e^{-0,0048 L/De} - 1,12 H_{fg} \rho_g / \rho_f + 0,548 H_{fg} \end{aligned}$$

For the q'' correlation, the ranges of parameters of the correlated experimental data are as follows :

Mass velocity = 0,2 to 8×10^6 lb/hr.ft²

Pressure = 800 to 2750 psia

L/De = 21 to 365

Inlet subcooling ($H_f - H_{IN}$) = 0 to 700 BTU/lb

Subcooling at DNB, ΔT_{SC} = 0 to 228 °F

Local heat flux = 0,4 to $4,0 \times 10^6$ BTU/hr.ft²

Equivalent diameter = 0,1 + 0,54 in

Axial heat flux distribution: uniform

Geometries : circular tube, rectangular channel, rod bundle.

The analogous ranges of parameters for the ΔH correlation are:

Mass velocity = $0,2 \times 10^6$ to $4,0 \times 10^6$ lb/hr.ft²

Pressure = 800 to 2750 psia

L/De = 21 to 656

Inlet subcooling $H_{IN} \geq 400$ BTU/lb

Local heat flux = $0,1 \times 10^6$ to $1,8 \times 10^5$ BTU/hr.ft²

Exit quality = 0 to 0,90 (by weight)

Equivalent diameter = 0,1 to 0,54 in

Axial heat flux distribution: uniform and non-uniform

Geometries : circular tube, rectangular channel, rod bundle

The saturation point is the dividing line between the regions in which the two correlations applies.

2) W-3 Correlation

Critical heat flux, q''_{DNB} , is expressed in this correlation as a function of the following parameters :

$$q''_{DNB} = f(P, De, G, H_{IN}, H_{loc} \text{ or local quality } X_{loc})$$

The correlations constants have been determined by fitting DNB data points available in the quality range $-15\% < X < +15\%$.

The expression is given as follows :

$$\begin{aligned} q''_{DNB}/10^6 = & [(2,022 - 0,0004302 P) + (0,1722 - 0,0000984 P) \cdot \\ & \cdot e^{(18,177 - 0,004129 P) X}] [(0,1484 - 1,595 X + \\ & + 0,1729 X \cdot G/10^6 + 1,037) [1,157 - 0,869 X]] \\ & [0,2664 + 0,8357 e^{-3,151 De}] [0,8252 + 0,000794 (H_{SAT} - H_{IN})] \end{aligned}$$

The heat flux is in BTU/hft² and the units are as listed below.

The ranges of parameters of the correlated experimental data are as follows :

Pressure P = 800 + 2000 psia

Mass velocity G = 0,5 x 10⁶ + 5 x 10⁶ lb/hft²

Equivalent diameter De = 0,2 + 0,7 in

Exit quality X = - 0,15 + 0,15

Inlet enthalpy H_{IN} > 400 BTU/lb

Length L = 10 + 79 inches

As derived, W-3 correlation applies to uniform heat flux distribution; whenever used for non uniform cases it gives equivalent critical fluxes.

;) Ferrel's Correlation

Wilson and Ferrel (Ref.7) have developed an empirical DNB correlation for subcooled and bulk boiling regions and for circular and rectangular cross sections.

The critical heat flux is expressed as a function of pressure, mass velocity, inlet subcooling, and diameter over length ratio.

The final expression for round channels is as follows :

$$q''_{DNB} = 90.000 F_p \left[\frac{G}{240} - \frac{De}{Z} \right]^a \quad \text{where :}$$

$$F_p = 1,83 - 0,415 \times 10^{-3} p$$

$$a = 0,3987 + 1,036 \times 10^{-3} [T_{SAT} - T_{IN}] - 1,027 \times 10^{-6} [T_{SAT} - T_{IN}]^2$$

The range of variables for the data compared by Wilson and Ferrel with the above equation are :

$$0,25 \leq Z \leq 2,28 \text{ ft}$$

$$0,00625 \leq De \leq 0,037 \text{ ft}$$

$$0,02 \times 10^6 \leq G \leq 7,8 \times 10^6 \text{ lb/hr-ft}^2$$

$$0 \leq T_{SAT} - T_{IN} \leq 564^\circ\text{F}$$

$$1000 \leq p \leq 2000 \text{ psia}$$

4) Zenkevich's Correlation

Zenkevich has developed a DNB correlation where the critical heat flux is expressed as a function of pressure, quality, mass velocity and some physical properties of liquid. This correlation applies to subcooled DNB only and its constants were determined by empirically fitting DNB data points.

The correlation is :

$$q''_{DNB} = R H_{fg} \sqrt{\frac{G \times \rho_f \times g \times 4,1697 \times 10^8}{\mu}}$$

where :

$$R = 10^{-5} \left[\frac{\rho_g}{\rho_f} \right]^{0,65} \left[95-420 \frac{H-H_{SAT}}{H_{fg}} \right] \left[1 + \frac{0,32 \times 10^6}{N^a} \right]$$

$$a = 1,1 + 2,6 \frac{\rho_g}{\rho_f} - 0,9 \frac{H - H_{SAT}}{H_{fg}}$$

$$N = \frac{G}{\mu} \sqrt{\frac{G}{\rho_f - \rho_g}}$$

The ranges of parameters are :

$$1400 \leq p \leq 3000 \text{ psia}$$

$$0,3 \times 10^6 \leq G \leq 5,2 \times 10^6 \text{ lb/hr.ft}^2$$

$$0,61 \leq z \leq 5,25 \text{ ft}$$

$$3,6 \leq T_{SAT} - T(z) \leq 180^\circ\text{F}$$

5) CISE Correlation

The CISE Heat Transfer Laboratory staff developed a correlation applicable only to quality DNB conditions. It has to be pointed out that in this correlation the actual length of the heated section has been eliminated as a parameter and the crisis is expressed as a relationship between critical power \dot{W}_S and length L_s for the particular case $x_{IN} = 0$.

./. .

The expression is given as follows :

$$\frac{\hat{W}_S}{\Gamma_{Hg1}} = x_{EX} = \frac{1 - P/P_{CR}}{\left(\frac{G}{100}\right)^{1/3}} \times \frac{L_S}{L_S + 0,315 \left(\frac{P_{CR}}{P} - 1\right)^{0,4} \cdot De^{1,4} \cdot G}$$

The ranges of parameters in which the correlation is applicable is defined as follows :

Equivalent diameter $De > 0,7$ cm

Pressure $P = 45 \div 150$ kg/cm²

Mass velocity $G = 100 \left(1 - \frac{P}{P_{CR}}\right)^3 \div 400$ g/cm²s

Exit quality : $x_{EX} > 0$

6) FIAT Correlation

Lately a correlation applicable only in the quality DNB region for forced convection upward flowing water mixtures has been developed by Previti, Riccardi and Valtancoli (Ref.6).

A choice among physical parameters, that can be used to describe the DNB phenomenon, and a systematic (as much as possible) study of the pattern presented by the available data as function of each of the selected parameters led to the following expression:

$$\frac{H_{ex} - H_{IN}}{H_{fg}} = 0,084848 \alpha \left(\frac{H_f - H_{IN}}{H_{fg}} \right) + 0,153945 \left(0,45 - 0,3 \frac{P - P_0}{10^3} \right)$$

$$\left(\frac{G}{10^6} \right)^{-0,874} + 0,119932 L^{0,5} + 1,088892 (e^{-8,13} De^{0,85})$$

$$+ 0,067711 \left(\frac{G}{10^6} \right)^{-0,874} \left(\frac{\rho_g}{\rho_f} \right)^{0,533} - 0,892651$$

where: $\alpha = \left[1-3 \left(\frac{G}{10^6} - 1,1 \right) 10^{-4} (2000-P) \right] \frac{L^{0,3}}{D^{0,5}}$ and $P_0 = 1000$ psia

The ranges of parameters of the correlated experimental data are as follows :

./. .

Pressure $P = 1000 + 2000$ psia

Heated length $L = 17 + 79$ inches

Equivalent diameter $D_e = 0,22 + 1,475$ inches

Mass velocity $G = 0,35 \times 10^6 + 2,5 \times 10^6$ lb/hft²

Inlet enthalpy $H_{IN} > 370$ BTU/lb

The correlation has been developed using british units since it is used in digital codes developed in the USA.

A.1.b. Results and comments

1) W-2 Correlations

The parameter's ranges of the experimental data used to find out the correlations constants are given in Ref.12; however the field of applicability of the W-2 correlations has not been expressly limited to these ranges. Therefore both q'' and ΔH correlations have been tentatively used also outside of these ranges, particularly for diameter D_e (since much of the uniform distribution data have been obtained with a 17,1 mm diameter test section) and, in a few cases, also for other parameters such as G and H_{IN} .

The results obtained in terms of DNBR are reported in Tables III, IV and V and shown in Figg. 1 and 2.

Hereafter the DNB Ratio (DNBR) is intended as the ratio of predicted to measured values at DNB location.

It can be seen that the diameter range given in Ref.12 ($0,1 < D_e < 0,54$ in) has to be intended as a real applicability limitation for both q'' and ΔH correlation; this is particularly true for pressures higher than 84 kg/cm² since most of the calculated critical powers at 126 and 140 kg/cm² deviate more than 25% from the experimental data obtained with the test section No.1 (Table III). This limitation appears to be more critical for q'' than for ΔH .

Limiting the analysis to test sections 1C and 1B, the results obtained with the q'' correlation (used within the parameter ranges given in Ref.12) present a maximum deviation over the experimental data of +20%, with the calculated critical flux always higher than the actual one (Tables IV and V, Fig.1).

As far as W-2 ΔH correlation is concerned, applied to the quality range only, almost 50% of the processed points (all falling within the above parameter ranges), present a deviation higher than 25%. This percentage becomes even higher if the exit quality is above 15% (Tables IV and V, Fig.2).

Important conclusions cannot certainly be drawn from this comparison since the number of the available data falling within the parameter ranges given in Ref.12 is quite small.

However care shall be used in applying both W-2 correlations outside the diameter range $0,1 < D < 0,54$ in.

2) W-3 Correlation

The new Westinghouse correlation has been applied to all the experimental point presenting exit quality within the range $-15\% < X_{EX} < +15\%$.

The results are reported on Tables III, IV and V and in Fig.3.

The W-3 correlation, even if applied with an inlet enthalpy H_{IN} lower than the limiting value specified in Ref.4 yields, for almost all the points, DNB ratios within $\pm 2\%$ of the theoretical value. Actually only three points present DNBR higher than 1,25.

For most of the evaluated points the correlation gives a conservative value for the critical heat flux and hence a DNB ratio lower than one.

At 140 kg/cm^2 all the cases, besides the three pointed out above, fall within $\pm 15\%$ of $\text{DNBR} = 1$ line.

The W-3 correlation presents a larger scatter of DNB ratio as exit quality increases. However the correlation perform quite satisfactory in all the ranges of pressures and geometries tested.

3) Ferrel's Correlation

This correlation seems to present (Ref.7) quite a narrow range of application as far as diameter and length of the heated sections are concerned ($0,075 < De < 0,44$ in and $6 < L < 27$ in). However the authors do not limit the applicability of their correlation to this field but only state that the ranges of variables for the data compared with their correlation fall within the above limits.

Therefore the correlation was applied to the experimental data given in Ref.1, even if none of them did fall, as far as geometry is concerned, within the cited limits.

It can be pointed out that this application seems allowable from the results obtained, given in Tables III, IV and V and shown in Fig.4.

About one sixth of the points processed gives DNB ratios higher than 1,25. However the correlation yields non conservative values since the large majority of DNB ratios obtained is above one. In general this correlation behaves satisfactory in the quality as well as in the subcooled regions for all ranges of pressures and geometries tested.

4) Zenkewich's Correlation

This correlation has been applied only in the subcooled region. However, in this region, also diameters outside the given parameter range have been explored (Tables III, IV and V).

The results show that this extrapolation does not seem allowable. Furthermore also for the data obtained with the sections of 10,2 and 11,6 mm diameter the results do not look promising.

The great majority of the processed cases, presents a DNB ratio higher than 1,25.

This deviation seems to increase with exit subcooling.

5) CISE Correlation

This correlation has been applied to all the experimental data with positive exit quality.

The results obtained are reported in Tables III, IV and V and shown in fig.5.

At 84 kg/cm² almost all the processed points are within $\pm 2\%$ of the theoretical DNB ratio. The correlation seems to yield higher discrepancies as the mass flow rate increases and exit quality decreases. At 126 and 140 kg/cm² the number of points having DNBR outside the $\pm 2\%$ range increases, with maximum deviations at 140 kg/cm².

At all pressures the correlation seems unconservative since for the great majority of the processed cases the DNB ratios obtained are higher than one.

6) FIAT Correlation

This correlation has also been applied to all experimental data with positive exit quality.

Also the points with inlet enthalpy lower than the limiting value given in Ref.6 ($H_{IN} = 370$ BTU/lb) have been processed.

Only a few points fall outside the $\pm 20\%$ range around the theoretical DNB ratio. These points are taken at 140 kg/cm² while at all other tested pressures no points fall outside the cited range (Tables III, IV and fig.6).

The correlation seems conservative at 126 and 140 kg/cm² while at 84 kg/cm² and low mass velocity it yields unconservative values.

However it has to be pointed out (Ref.6) that the correlation should be applied having as lower limiting value the exit quality for which the inverse mass velocity effect takes place. This limiting quality varies with pressure, i.e. increases with pressure.

A.2. Non uniform power distribution

Actually in the nuclear reactor core thermal design only non-uniform axial heating must be considered. The shape of the heat flux distribution varies over the core lifetime; therefore it is very important to be able to correctly predict the effect of non-uniform axial flux distribution on DNB in order to assure at any time of the core life a safe reactor performance.

A.2.a. Influence of non-uniform heat flux distribution on DNB

Recent tests conducted by various laboratories (Ref. 8,1,9,10,11) have shown a marked influence of power distribution on both burnout power and location.

This may be easily pointed out plotting, as function of both inlet and outlet quality, the critical power for uniform and non uniform heat flux distribution test sections of identical geometry.

Quite interesting is also the plot of the critical power of the whole test section versus quality at the DNB location (X_{DNB}).

Since this report is dealing with the results obtained in Ref.(1) the plots of Figg. 7 through 19 concern only with the experimental data reported in(Ref. 1).

However similar plots may be obtained from all other references above mentioned (Ref. 8,9,10,11).

The following comments can be given :

- at constant inlet subcooling the total critical power is maximum for uniform flux distribution; however this deviation approaches zero as the inlet condition approaches the saturation one. This statement is correct over the entire range of mass velocity tested at 132 ata ($90 < G < 313 \text{ g/cm}^2\text{s}$); however the lowest the mass velocity the smallest becomes the difference between critical powers obtained with different heat flux distributions (Figg. 7,8,9).

./. .

- at constant critical enthalpy (that is for uniform and non uniform couples of data presenting the same quality X_{DNB} at DNB location) the total critical power is maximum for uniform flux distribution. The difference between critical powers tends to vanish as X_{DNB} reaches high values while it increases for subcooled DNB conditions (Figg. 10,11,12,13,14).
- at constant exit quality the total critical power is also maximum for the uniform heat flux distribution. The behaviour of the difference between critical power follows the same pattern as for constant critical enthalpy reported above (Figg. 15,16,17,18,19).

As far as critical location is concerned, it can be generally stated that, while for uniform heat flux distribution DNB always occurs at the test section exit, for flux distributions with the flux peak at any location except the exit, the critical condition can occur upstream depending on inlet subcooling and peak to average fluxes ratio. The DNB point tends to move upstream toward the peak location when the subcooling and the peak to average flux ratio increases, while for high exit qualities burnout occurs usually at the section exit (Ref.1).

A.2.b. Considerations on possible evaluation methods for critical heat fluxes in non-uniform power distribution

For the uniform heat flux distribution the parameters universally accepted in defining the burnout phenomenon are H_{eX} , H_{IN} , L , De , G , p and q'' . Hence we can write :

$$q''_{DNB} = f(X_{eX}, H_{IN}, L, De, G, p) \quad (a)$$

But since :

$$q''_{DNB} \cdot \pi De \cdot L = G \cdot \frac{\pi \cdot D^2}{4} \cdot (H_{eX} - H_{IN})$$

the number of independent variables of equation (a) can be reduced by one. Therefore two types of empirical DNB correlations have been developed using the so called "system" (H_{IN} , L , De , G and p) or "local" (X_{eX} or H_{loc} , L , De , G and p) parameters as independent variables.

In both cases the correlations, developed mainly from uniform heat fluxes DNB data, were used to predict critical conditions for non uniform heat flux distribution cases. This application is generally uncorrect and usually yields not acceptable predictions for total critical power as well as for critical heat flux and position.

This will be demonstrated applying the DNB correlations discussed in Section A.1.a (that have given satisfactory results for the uniform DNB data processing) to the non-uniform heat flux distributions.

Although some attempt has been made to predict non uniform critical heat fluxes from local parameters only (Ref.12), the usual approach is to consider the equivalence between the average heat flux for the non uniform power distribution and the critical uniform heat flux under the same test condition (Ref.8).

However, although the average heat flux versus exit quality for the cosine and peak near the bottom flux distributions reasonably agree with the same data for uniform power, for the peak-near the top distribution the data fall much below the uniform one.

This appears clearly from both Ref.1 and 9 data at all pressures and mass velocities tested.

These results indicate that the apparent success sometimes obtained by comparing with the uniform flux the average value of the heat flux over the heated section for cosine distribution presenting rather small peak to average flux ratio, cannot be generalized. For the very important case of outlet peaked distributions (usual for PWR at the end of core lifetime) this method fails, thus indicating an incorrect interpretation of the DNB phenomenon.

In conclusion, since the DNB powers of uniform and non uniform test sections having same H_{IN} , P , L , D_e and G have been found approximately equal only in the high quality region, and quite different in the low qualities and subcooled region (particularly with a outlet peaked flux distribution), the "system parameter" correlations are not adequate to predict DNB occurrence.

Again, experimental evidence indicates that, neglecting any upstream

effect and using only local conditions, the "local parameter" correlations are also inadequate to predict DNB occurrence in non uniform heat flux distribution.

Hence it is conceivable to think DNB affected by both local and upstream conditions and this assumes particular interest in the case of non uniform power distribution.

It is interesting to point out, for various flux distributions and quality regions, the relative importance of local versus integrated conditions.

The hot patch tests performed at Bettis at pressure 140 kg/cm^2 and over a wide quality range ($-26,5 < x_{ex} < 53,3\%$) are adequate to show this behaviour (Ref.13).

The comparison between uniform and patched flux distribution (Fig.20) for the same exit enthalpy and geometry suggests that local conditions are of prime importance in the subcooled region, while integrated conditions prevails in the high quality regions; in the intermediate regions the relative importance of local versus integrated conditions is weighted as a function of local conditions.

Therefore a method that takes into account both "local" and "system" parameters (therefore including local and upstream effects) should be used to predict DNB conditions for non uniform heat flux distribution.

A.2.c. Method used to predict critical conditions for non-uniform heat flux distribution

Since DNB is a phenomenon originating at the interface between fluid and heated surface, it has been proposed in a recent work (14) that the critical condition occurs when the enthalpy of the superheated liquid layer adjacent to the heated surface reaches a limiting value. It is conceivable that the limiting enthalpy of the superheated layer be the same both for uniform and non uniform heat flux distribution presenting the same geometry and local conditions at DNB location. (that is quality x_{DNB} , pressure, mass flow rate).

Therefore a correction factor was developed in order to enable prediction of non uniform behaviour from existing uniform data. In reference 14 a physical model is proposed, that seems justified from experimental evidence, where a bubbly layer separates the main stream from the superheated water layer close to the wall. The energy balance of the superheated layer over the heated length should yield the critical enthalpy value for DNB onset. Solving the energy equation for both uniform and non uniform heat flux distribution up to DNB point we have :

$$q''_{DNB\ EU} (1 - e^{-C l_{DNB}}) = C \int_0^{l_{DNB}} q''(z) e^{-C(l_{DNB}-z)} dz$$

Now the correction factor $F = \frac{q''_{DNB}, \text{ equivalent to uniform flux}}{q''_{DNB}, \text{ local in non uniform flux}}$

can be defined as function of C (empirical constant function of mass velocity and local quality at DNB) and of the integral of heat fluxes over the critical length weighted by the factor $e^{-C(l_{DNB}-z)}$.

Hence the factor F combines local and integrated effects in such a way that in subcooled and low quality regions (where the factor C is large), local conditions are primarily determining the critical conditions while, for high qualities, C becomes small and the integrated conditions are prevailing in determining the crisis onset.

This result is in agreement with the experiments as shown in pertinent figures and discussed in paragraphs A.2.a and A.2.b.

The method actually used in predicting both DNB flux and locations is presented in Ref.15. The paper defines the field of applicability of the theoretical approach reported in Ref.14 and points out the role of some important parameters such as the length to which the integration should be extended and the test pressure.

Two expressions for the factor C have been derived theoretically in Ref.15 for the bubbly flow region C_p and for the annular flow region C_a . As the test indicates (Fig.20), the field has been divided into three

./. .

regions, namely the highly subcooled, the low subcooled and low quality (bubbly flow region) and the high quality region. Highly subcooled is the region where the bubbles do not detach from the wall as defined in Ref.16. The high quality region onset can be defined according to Baker's plot (Ref.17) or by the inverse mass velocity effect occurrence. The intermediate region or bubbly flow region, where the memory effect on the superheated liquid layer close to the heated wall takes place, lies between the highly subcooled and the annular regions as defined above.

In the first region, where mainly the local conditions should influence DNB, correlations such as W-3, and Zenkewitch, should be successful. However, because of the lower quality limit (-1%) of correlation W-3, also other correlation like q"-W2 and Ferrel's have been used.

Although also in this region a certain memory effect should be expected, the difficulty of defining the actual bubble detachment point and the very short lenght over which usually, in this subcooled condition, the memory effect could takes place, has lead to apply directly the above mentioned correlations point by point after the peak until the minimum DNB ratio was reached.

For the intermediate range the following method, derived from the analysis of Ref.15, was used for each non uniform power test section:

- Step 1 - The bubble detachment point, Z'_{BD} is evaluated as per Ref.16 (Z' is the current abscissa from channel inlet)
- Step 2 - For the selected point Z' , following Z'_{BD} , where DNBR will be evaluated, local quality $X(Z')$ and the distance $l_{DNB,NU}$ from Z'_{BD} are determined ($l_{DNB,NU} = Z' - Z'_{BD}$)
- Step 3 - The factor $C_F = \frac{8.23 \times 10^3 (1-X)^a}{G \times f(T_{SAT})} (\text{ft}^{-1})$ is evaluated.

In the C_F expression :

$$a = 6,105 + 0,44 \times 10^{-3} (P-1000)$$

P = test pressure (psia)

$$f(T_{SAT}) = 39,74836 \times 10^{-15} T_{SAT}^4 - 64,83156 \times 10^{-12}$$

$$T_{SAT}^3 = 38,6336 T_{SAT}^2 \times 10^{-9} + 47,189 \times 10^{-6}$$

$$T_{SAT} = 1,9452 \times 10^{-3}$$

T_{SAT} = saturation temperature ($^{\circ}\text{F}$)

G = mass flow rate (lb/hft^2)

x = local quality

- Step 4 - Being Z the distance from the bubble detachment point,

(that is $Z = 0$ for $Z' = Z'_{BD}$) the expression

$$C_F \cdot \int_{0}^{l_{DNB,NU}} q''(z) \cdot e^{-C_F(l_{DNB,NU} - z)} dz \quad .$$

- Step 5 - Introducing $x'(z)$, G , De , P , H_{SAT} , H_{IN} in the W-3 correlation, the equivalent uniform critical flux $q''_{DNB,EU}$ is calculated.

- Step 6 - Through the enthalpy balance $\frac{(H_{loc} - H_{IN}) \cdot G \cdot De}{4 q''_{DNB,EU}} = l_{EU}$

the total length associated with $q''_{DNB,EU}$ will be found.

- Step 7 - Steps 1 and 2 will be repeated for the equivalent uniform case, thus evaluating $l_{DNBU} = L_U - Z'_{BDU}$, distance between test section exit and bubble detachment point.

- Step 8 - Expression $q''_{DNBEU} (1 - e^{-C_F l_{DNBU}})$ will be found

- Step 9 - The ratio $R = \frac{q''_{DNB,EU} (1 - e^{-C_F l_{DNBU}})}{C_F \int_{0}^{l_{DNB,NU}} q''(z) \cdot e^{-C_F(l_{DNB,NU} - z)} dz}$

representing the DNB ratio will be evaluated.

If $R = 1$ the burnout location coincides with the selected point.

Otherwise the calculation may proceed along the channel until a minimum value of R is reached. As far as the high quality region is

concerned, a method similar to the one outlined above should be used. The factor C_p should be replaced by

$$Ca = \frac{9,7 \times 10^{-4}}{X \cdot Vg \cdot (\frac{G}{10^6})^{1,5} D} \quad (\text{ft}^{-1})$$

where : D = equivalent diameter (ft)
 G = mass flow rate (lb/h ft^2)
 X = quality
 Vg = steam specific volume (ft^3/lb) (Ref.15)

and the bubbly region limiting point rather than local boiling inception shall be considered.

However, since the maximum to average flux ratio is not high, also an evaluation of DNB as a global phenomenon has been tentatively done. In this case correlations such as CISE, ΔH FIAT, ΔH W-2, and Ferrel's have been used.

A.2.d. Results and comments

The evaluation of critical power and position has been carried out by the methods outlined in the proceeding paragraph A.2.c, for the simmetrical cosine, and assymetrical skewed to the top and to the bottom power distributions.

The geometrical and heat flux distribution data are of test sections, reported on Ref.(1) and, sintetically, in Table II.

The results have been separately reported as function of the quality at DNB location.

A.2.d.1. Highly subcooled region

Within this region, defined as the region where the bubble detachment, evaluated as per Ref.10, does not occur, the experimental points have been processed using the Ferrel, Zenkewich and W-2 " correlations.

The results obtained are reported on Table VI and Figures 21 and 22. In general the following considerations can be done :

- the Ferrel correlation shows a fairly good agreement with the experimental burnout power to within $\pm 2\%$, preferable leading to conservative predictions. It gives also an accurate prediction of DNB location.

Both Zenkewich and $q''-W_2$ correlations offer satisfactory evaluation of DNB position. As far as the critical flux prediction is concerned, the agreement with Zenkewich correlation is poor in all cases, whereas $q''-W_2$ predicts well for the upward skewed sine distribution and is unconservative for the other flux shapes.

- maximum deviations on both critical heat flux and location are observed for the symmetrical cosine flux distribution.

A.2.d.2. Intermediate quality region or bubbly flow region

The lower limit of this region is empirically defined by the bubble detachment occurrence, since from then on a memory effect can take place.

More difficult is to correctly define the upper limit of this region. Tentatively this limit should be set at the quality, function of pressure, where the inverse mass velocity effect takes place. It is suggested (Ref.18) that this point may represent the onset of annular flow region.

In this case the crisis takes place at the exit section and the memory effect, if applied, as for the bubbly flow region should yield unsatisfactory results.

1) Memory effect method.

The results obtained by the application of the method derived from Ref.15 and briefly described on paragraph A.2.c, are reported on Tables VII and shown on Figs. 23 and 24.

All data points presenting the experimental determination of DNB location and quality at DNB in a range approximately $-15\% \leftrightarrow +15\%$ have been processed.

The following comments can be made :

- the method gives very good results as far as critical heat flux is concerned if applied in the correct quality range. The great majority of the processed points presents a maximum DNB ratio within the range 1,20 to 0,9;
- the DNB location presents an almost fixed position for each flux distribution considered; however small deviation around this position have been found. The predicted burnout position falls, for the great majority of the cases, within the lenght where sudden rise of wall temperature was detected (Figg.25, 26 e 27);
- for the lowest values of X_{DNB} , particularly at high mass flow rates ($G > 1 \times 10^6$ lb/hft²), a few points present a DNB ratio within the range 1,25 to 1,15. This is due to the uncertainty of the bubble detachment location. Since the distance between this point and the critical location is, for this quality, very small, a mistake in defining the bubble detachment location yields the higher deviation.

This statement is proved by the fact that using the Bowring method (Ref.19) to define the bubble detachment point (that usually is upstream than the detachment location obtained as per Ref.(16), the results become in excellent agreement with the theoretical ones (Table VII).

- When the crisis takes place at the exit section the method, if applied with the modality of the bubble flow region (that is, with the coefficient C_F and starting to consider the memory effect from the bubble detachment point) gives unsatisfactory and not conservative results both for critical power and location.

This is particularly true at high mass flow rate where the inverse mass flow rate effect gives a rapid drop of the critical heat flux for small increase in exit quality. Evidence to this fact offered in Fig.24 in which the highest deviations are

attained for the points corresponding to the highest mass flow rates which presented the experimental DNB location at channel exit.

The inconsistency of using the bubbly flow region approach in the cases presenting high exit quality and DNB location at the exit of test section is also proved by the fact that correlations such as CISE and FIAT, considering the crisis as a global phenomenon, usually give satisfactory results (Table VI).

These correlations proved to predict correctly the critical power for the uniform cases within the quality and geometry range tested (Tables III, IV and V).

It is interesting to observe how the use of the correction factor F modifies, the critical heat flux obtained using a correlation such W-3. In Fig.28 are reported for the particular case No.149, both the critical heat fluxes given by W-3 and by the factor F. While the first one indicates a well defined critical position, the use of factor F tends to indicate DNB occurrence possible over a certain lenght, since the DNB ratios are, in this region, not much different.

This is what actually happens in the tested case (No.149-9/12/64) where a sudden rise of wall temperature has been detected over a certain lenght (that is the DNB did not occur at a unic location but over a certain lenght of the heater). For a slightly sub-cooled point such as No. 79 (7/12/64) the DNB position is defined quite precisely plotting DNB ratios versus lenght. In this case also the experiments show the burnout located on a short lenght (Fig.29).

2) Direct approach method

The application of correlation such as Ferrel's and Zenkevich has been carried out calculating the DNB ratio along the lenght from the peak heat flux to the exit. A minimum value of DNBR was usually reached at a fixed position for each investigated power distribution. The maximum deviations of DNBR are, for Ferrel cor-

relation, usually lower than 1,3; however for the cosine distribution there are several points presenting an higher value. The results are reported on Tables VII and shown on Figg. 30 and 31. Zenkevich correlation's results are in poor agreement with experimental values as for the uniform heat flux distribution case. It has to be pointed out that the DNB location given by both correlations is usually upstream of the detected position.

In the quality range of this intermediate region ($0 < X_{DNB} < +0,15$) correlation such as CISE, Ferrel and ΔH FIAT have been used.

In the quality range $+10\% < X_{DNB} < +15\%$ both CISE and FIAT correlations give satisfactory results, particularly when the DNB is located at the section exit (Figg. 32-33 and Tables VII).

A.2.d.3. High quality region

Correlations such as CISE, ΔH FIAT, ΔH -W2 and Ferrel have been used to process the data following in this region.

These points present always DNB location at channel exit.

The Ferrel's correlation, although predicting critical powers close to the experimental ones, gives DNB location always upstream than the detected (Fig.34).

The ΔH -W2 correlation generally yields unconservative values as for the uniform distribution, while both CISE and ΔH Fiat predict critical power in good agreement with the experiments (Tables VIII and Figg. 35, 36 and 37).

B. TESTS WITH HEATER IN CLOSE PROXIMITY OF COLD SURFACES

B.1. General aspects of the problem

Examination of the core lattices of water reactors with fuel elements generally in the form of rod bundles, poses the problem of studing channels of different shapes and conditions that may be reduced to two fundamental types :

- a) Channels with the totality of the wetted physical surfaces transfer ring heat to the coolant. This type includes cells of the flow area associated to fuel rods symmetrically surrounded by other fuel rods. Generally this is the case of all the cells of a rod bundle not sited at the assembly periphery.
- b) Annular channels having only part of the wetted perimeter heated. This is the case of rods facing structural members that form annular channels with perimetral unheated surfaces.

Characterization of the last channels may be best achieved through the introduction of a modified form of the purely hydraulic concept of equivalent diameter that would account for the heated part of the wetted perimeter only.

Calling D_e and D_h the two diameter respectively, their definition is as follows :

$$D_e = 4 \times \frac{\text{Flow Area}}{\text{Wetted Perimeter}}$$

$$D_h = 4 \times \frac{\text{Flow Area}}{\text{Heated Perimeter}}$$

A logical criterion of similarity between channels of any shape could be established by resorting to the D_h concept.

Actually, in channels having equal D_h and heated length, the fluid stream would receive the same enthalpy rise for the same heat flux, all other physical conditions of the fluid being equal.

Without knowing the real mechanism of the thermal crisis, the parameters representing the system (geometry of the channels, heated length, steam

quality, critical heat flux, mass flow rate, pressure) are generally used to describe the phenomenon by means of correlations in which they appear differently grouped.

Consequently the introduction of the parameter D_h may reasonably allow the extension of the use of correlations originally developed for tubes to annular geometry.

However, this procedure does not cover entirely the effects induced by a cold wall in close proximity to the heater to the extent to which flow distribution in the interspaces and actual coolant conditions at the DNB point are affected. Considering coolant cells of the types previously referred to as a) and b), one can see that their boundary conditions are quite different. Actually the external contour of cells of the first type is an ideal line, whereas in the second case it is partially replaced by physical walls. In this connection it is worth to note that the flow distribution within the two cells is subject to different boundary conditions, the fluid velocity in the first case attaining the maximum value at the external contour, whereas here in the second case the fluid is at rest. Therefore, where physical unheated surfaces replace the ideal contour there is a fraction of the total flow that is not utilized for the heat removal.

It seems reasonable to expect that the critical conditions are somehow affected by the presence of an unheated wall facing the surface on which burnout occurs, particularly for the cases of narrow gaps and low local steam quality.

Lack of a clear insight of the actual effect induced by the materialization of the cell contours, stress the need of providing experimental evidences produced by tests with and without cold wall effects and performed in comparable physical conditions.

To this purpose, great interest seems to have the possibility of comparing tests made in channels having cold walls with experiments performed in annular channels of same D_h and heated length in which the ambiguity between D_h and D_e is removed.

Data obtained with a square annular test section could be compared with results of tests performed on a suitable rod bundle assembly. More simply, a comparison could be made between data referring to circular annulus of same D_h but with both or only a single wall heated.

B.2. Comparison of data with DNB correlation

Four existing DNB correlations have been used to predict, within their ranges of validity, critical power for experiments performed on the square annular test section. The tests were conducted on a square annular channel consisting of a 10,2 mm O.D. heater rod centered in a 15 x 15 mm unheated square duct cooled by water at high pressure flowing upward. The lengths of the heater tested were 560 mm and 1183 mm. The tested geometry has been selected to reproduce the actual condition of corner rods of the second pass fuel assemblies proposed for the nuclear tanker core (Ref.17). Detailed information on these experiments can be found in the referenced report (2).

The correlations were originally developed for round tubes and have been suitably modified for adaptation to the conditions of annular geometry.

B.2.1. Westinghouse Correlations

For tests having negative or positive exit quality, W-2 q''_{DNB} and W-2 ΔH_{DNB} correlations have been used respectively (3).

Tests with exit quality within $-15\% +15\%$ have been also compared with predictions based on the W-3 q''_{DNB} correlation (4).

These correlations, formerly developed for geometries in which there is no ambiguity between D_e and D_h , have been modified to account for the effect of unheated surfaces in annular geometry (3).

The modification common to all three correlations consists in replacing the equivalent diameter D_e with its modified form D_h .

The limitation on L , D_e and $\frac{L}{D_e}$, as far as applicability range of the correlations is concerned, has been maintained.

In reference (3) a reducing empirical factor of 0,9 has been suggested for the W-2 q''_{DNB} because an overprediction of the burnout heat flux should be expected since the correlation in its original form does not account for flow partialization with respect to heat removal. Concerning the W-2 ΔH_{DNB} correlation, a correction "mixing factor" has been proposed to account for the non uniformity of the enthalpy across the flow area. Accordingly the critical enthalpy rise becomes:

$(\Delta H_{DNB})_{\text{modif.}}$ =

$$= \left[\frac{R}{(1,11 - 0,42 \cdot X_{DNB}) (0,484 + 0,697 e^{-0,0109 \frac{L}{D_e}})} \right] (\Delta H_{DNB})_{\text{using } D_h}$$

where :

$$R = \frac{P_h}{P_h + P_c}$$

P_h = heated perimeter

P_c = unheated perimeter

X_{DNB} = steam quality at the DNB point

Similarly, a correction factor for the burnout heat flux predicted by W-3 correlation, has been suggested for the case of cold wall in proximity of heating surfaces (4) :

$$(q''_{DNB})_{W-3 \text{ modified}} = (1,36 + 0,12 e^{9 X_{DNB}}) (q''_{DNB})_{W-3 \text{ using } D_h}$$

B.2.2. CISE Correlation

The correlation generalized for complex geometries has been applied within its range of validity (5).

This correlation predicts the critical power measured only on the heated surface on which burnout occurs, and differs from the one developed for tubes simply in that the expression given in paragraph A.1.a.5) is corrected by the factor $\frac{P_h}{P_h + P_c}$ already defined.

The comparison with the experimental data has been made with predicted total power as well as with the power fed along the saturation lenght.

B.2.3. Results Tabulation

Predicted critical values obtained with the employed correlations, have been divided by corresponding measured values at DNB thus defining the DNB ratios reported in Tables IX through XIII.

The tables report also the values of other physical parameters relevant to the identification of the runs.

B.3. Remarks on the comparison study

Predicted DNB fluxes, critical enthalpy rises or power obtained according to the correlations employed as well as to their modified forms, have been plotted against measured values in Figg. 38 through 43.

The comparison with W-2 q''_{DNB} correlation, applied using D_h , shows that data obtained with the long heater are predicted fairly well whereas the agreement is poor with the data referring to the short heater.(Fig. 38). For these last runs the prediction is slightly improved through the application of the 0,9 empirical correction factor while it becomes worse for the long heater (Fig.39).

Fig.40 shows that the "mixing factor", introduced to correct the values given by the W-2 ΔH_{DNB} correlation, generally leads to a substantial improvement of the prediction although it appears to be in most cases too conservative. Considering the real improvement introduced by the correction factor, only modified values have been reported in further graphical representations.

Because of the limited number of runs falling within the range of validity of the correction factor suggested for the W-3 q''_{DNB} , no definitive conclusion could be drawn in this case. It appeared, however, that for the shorter heater, the prediction was generally improved by

the correction factor (Fig.41). As far as CISE generalized correlation is concerned, Fig.42 shows that if the comparison is made with the predicted total power based on actual values of the inlet enthalpy and total lenght of the heater the agreement is satisfactory in most cases. Fig.43 indicate that the agreement between predicted and experimental values of the power referring to the same saturation lenght is poor in most cases.

It ought to be pointed out however, that the worst deviations refer to tests performed with the highly unsaturated inlet conditions.

In Fig.44 through 50, the trends of the DNB ratios referring to total power over the explored quality ranges, have been represented for each pressure, with mass flow rate and heated length assumed as parameters.

C. INFLUENCE OF TEST RESULTS AND OF THE NEW THEORETICAL APPROACH ON CORE THERMAL DESIGN

In the preceding paragraphs it has been practically demonstrated that the use of DNB correlations developed from uniform heat flux data to predict non uniform heat flux distribution can give relevant errors both in critical power and DNB location.

In ref.20 is shown how the use of both "system" and "local" parameter DNB correlations to non uniform heat flux distribution leads to a wrong result. The former has as independent variables inlet enthalpy, mass velocity, equivalent diameter, core lenght and pressure while the dependent variable is either DNB flux or DNB enthalpy.

The equivalent enthalpy rise of a test section having the same system parameter is a straight line starting from reactor inlet enthalpy, being the correlation developed from uniform heat flux data (Fig.5').

For the local parameter case the equivalent enthalpy rise of the uniform power test section (having the same lenght as the DNB location-distance from inlet sections in the non uniform heat flux test section) is a straight line too.

This line do not coincide with the line joining local and inlet reactor enthalpy unless the average heat flux for both uniform and non uniform case coincide. This can happen for small values of maximum to average heat flux and high DNB qualities only, certainly not in the case of PWR design as demonstrated in Figures 7 through 20.

Therefore the inlet enthalpy of the equivalent uniform test section, H'_{IN} , is lower than the reactor inlet enthalpy H_{IN} in order to yield the same local DNB enthalpy. The enthalpy line of the local parameter correlation is lower than the same line of the system parameter correlation. Hence the DNB heat flux predicted by a "local parameter" correlation will be higher than that obtained by using a "system parameter" correlation for at a lower coolant enthalpy the DNB heat flux is higher.

In order to show how the test results and the derived new theoretical approach influence the core thermal design, the correlations results obtained

using a system parameter correlation ($q''W-2$) and the memory effect method have been reported in Table XIV.

The channel taken into consideration is the hot channel of the second pass of the core designed for the nuclear tanker reactor (Ref.20).

The heat flux distribution is peaked toward the exit (similar to the test section 2-B Distribution - Table II) with a maximum to average flux ratio of 1.7. The design condition, as specified in Table XIV, represents the worst reactor transient condition as far as critical power is concerned. The minimum DNB ratio obtained by using the memory effect method is 1.35 while the allowable value is 1.3. This demonstrates that the margin on DNB kept using the system parameter correlation $q''W-2$ was amply justified. However it has to be pointed out that these results cannot be extrapolated to other reactor cores since each case shall be handled on individual basis.

The influence of non uniform power distribution and cold wall has been studied admitting that the effect can be superimposed.

A corner rod of the core second pass has been considered.

The calculation was performed using the coolant mass flow rate of the corner cell, function of its hydraulic resistance as obtained from the pressure drop evaluation reported in Ref.20.

The equivalent diameter used was based on the heated perimeter and the heat flux distribution was unasymmetrical sine upward skewed having the same average value as for the "hot channel".

The inlet flow maldistribution factor was still chosen equal to 1.13. In these conditions, the DNB ratio resulted of 1.47 (Table XV). From the comparison between the measured and experimental values (as reported in the Figg. 44, 45, 46) it appears that a reduction factor should be applied in the application of W-3 correlation to a channel with unheated walls. The expression of this factor, function of some parameters influencing DNB, is still in elaboration.

D. WORK PROSECUTION

The assumption that separated effects such as non uniform heat flux distribution and cold wall can be superimposed should be experimentally proved.

Other effects like the presence and the particular design of spacing grids and the mixing between adjacent heated channels presenting power gradient should also be investigated. In general it has to be pointed out that care shall be exercised in extrapolating to reactor cores where different effects on DNB may be simultaneously presents, the results obtained in simple geometries set up to study single effects separately.

A gradual approach to investigate more complex test section is needed with the target to arrive to geometries and conditions near as much as possible to actual core working conditions.

A graduality in the effort to reach core conditions is suggested by two main reasons:

- the possibility to follow more closely basic phenomena thus allowing an advancement in the theoretical stage;
- the design and operational difficulties of a quite complicated test section like a tube bundle presenting the characteristics of the actual core.

The research program on heat transfer supporting the nuclear ship propulsion studies performed by Fiat and Ansaldo under Euratom contract will continue following as closely as possible the path above outlined with the double aim to improve the basic understanding of the DNB phenomenon in PWR conditions and to find out the real limitation to power output of the proposed core.

R E F E R E N C E S

- 1) BIANCONE, CAMPANILE, CALIMI et COFFI - "Forced convection burnout and hydrodynamic instability experiments for water at high pressure" Part I "Presentation of data for round tubes with uniform and non uniform power" - EUR.2490.e (1965).
- 2) CAMPANILE, CALIMI, COFFI - "Forced convection burnout and hydrodynamic instability experiments for water at high pressure - Part II: Presentation of data for water flowing upward along a uniformly heated rod in a square unheated duct", to be published as Euratom report.
- 3) L.S. TONG, H.B. CURRIN, F.C. ENGEL - "DNB (Burnout) studies in an open lattice core" - Vol.I - WCAP 3736 - August 1964.
- 4) L.S. TONG - "DNB predictions for an axially non uniform heat flux distribution" - WCAP 2815 Rev.1 - September 1965.
- 5) S.BERTOLETTI et alii - "Heat transfer crisis with steam-water mixtures" Energia Nucleare - Vol.12 No.3, March 1965.
- 6) G.PREVITI, R.RICCARDI, A.VALTANCOLI - "Critical heat fluxes prediction for forced convection boiling fluid flow " - FIAT-Sezione Energia Nucleare to be published as Euratom report.
- 7) WILSON, R.H. and FERREL, J.K. - "Correlation of critical heat flux for boiling water in forced circulation at elevated pressures" - BAW-168, November 1961.
- 8) LEE, D.H. and OBERTELLI J.D. - "An experimental investigation of forced convection burnout in high pressure water. Part II: Preliminary results for round tubes with non uniform axial heat flux distribution" AEEW-R-309 Winfrith 1963.
- 9) IUDD, D. et alii - "Non uniform heat generation experimental program" BAW-3238-5 (1964)
- 10) STEVENS, G.F., ELLIOT, D.F. and WOOD R.W. - "An experimental between forced convection burnout in Freon 12 following vertically upwards through uniformly and non uniformly heated tubes" * AEEW-R-426 (1965).
- 11) SMITH, O.C. - "Non uniform heat flux burnout with upward water flow" WCAP - 2795 (1965)
- 12) JANSSEN E. and KERVINEN J.A. - "Burnout conditions for non uniformly heated rod in annular geometry water at 1000 psia" - GEAP 3755 - June 1963

- 13) DE BORTOLI, R.A. GREEN, S.J. et alii - "Forced convection heat transfer burnout studies for water in rectangular channels and round tubes at pressure above 500 psia" WAED-188 (1958)
- 14) TONG L.S., CURRIN H.B., LARSEN P.S. and SMITH O. - "Influence of axially non uniform heat flux on DNB" - AIChE Preprint 17, Eight National Heat Transfer Conference, Los Angeles (1965).
- 15) G.PREVITI and M.DE BERNARDI - "An investigation on same parameters influencing non uniform heat flux DNB prediction" - FIAT-Sesione Energia Nucleare to be published as Euratom report.
- 16) GRIFFITH P., CLARK M.A., and ROHSENOW, W.N. - "Void volumes in subcooled boiling systems" - ASME Paper No.58-HT-19 (1958)
- 17) BAKER, O. - "Simultaneous flow of oil and gas" - Oil and Gas Journal 53, 185-190 (1954)
- 18) GRIFFEL, J. and BONILLA, C.F. - "Forced-convection boiling burnout for water in uniformly heated tubular test sections" - Nuclear Structural Engineering 2 (1965) 1-35.
- 19) BOWRING, R-W - "Physical model, based on bubble detachment, and calculation of steam voidage in the subcooled region of a heated channel" - HPR-10 (1962)
- 20) "Nave cisterna a propulsione nucleare - Progetto intermedio"
Giugno 1965 - EUR-2629 I - Vol.1°.

ACKNOWLEDGMENTS

The authors are indebted to A. Molino, R. Riccardi and A. Valtancoli of FIAT - Sezione Energia Nucleare and to G. Fumero of the SORIN Heat Transfer Laboratory for their contribution to the data processing and the effort in editing the report.

The assistance of the FIAT - Sezione Energia Nucleare and SORIN computing staffs is deeply appreciated.

TABLE I - THERMAL AND HYDRAULIC CORE DATA

Total power output,	MWt	82,00
Mass flow rate,	gr/cm ² sec	172,20
Heat transfer surface area,	m ²	212,20
Average heat flux,	w/cm ²	38,66
Maximum heat flux,	w/cm ²	125,67
Nominal coolant inlet temperature to internal core region,	°C	289,40
Active length,	mm	1180,00
Equivalent hydraulic diameter of unit cell,	mm	11,58
Exit quality at the outlet of the hot channel,	weight per cent (%)	-1,00
Coolant nominal pressure	ata	126,80

TABLE II - TEST SECTIONS DATA

Test section n°1

Heated tube inside diameter,	mm	17,1
Heated tube outside diameter,	mm	21,3
Heated length,	mm	1317,0
Length to diameter ratio,	-	77,0
Axial flux distribution,	-	nominally uniform.

Test section n°1B

Heated tube inside diameter,	mm	10,2
Heated tube outside diameter,	mm	13,6
Heated length,	mm	785,0
Length to diameter ratio,	-	77,0
Axial flux distribution,	-	nominally uniform.

Test section n°1C

Heated tube inside diameter,	mm	11,6
Heated tube outside diameter,	mm	15,0
Heated length,	mm	1183,0
Length to diameter ratio,	-	102,0
Axial flux distribution,	-	nominally uniform.

Test section n°2

Heated tube inside diameter,	mm	17,1
Heated length,	mm	1317,0
Length to diameter ratio	-	77,0
Axial flux distribution	-	symmetrical cosine

$$1,7 \frac{\phi_s}{\phi_{max}} = 0,7 \cos 2\pi \left(\frac{z}{L} - 0,5 \right) + 1$$

Test section n°2B

Heated tube inside diameter,	mm	11,6
Heated length,	mm	1183,0
Length to diameter ratio	-	102,0
Axial flux distribution	-	upward skewed asymmetrical sine

$$\frac{\phi_z}{\phi_{max}} = 0,5\pi \frac{z}{L} \operatorname{sen} \pi \frac{z}{L} + 0,088$$

./.

TABLE II (follows)

Test section n°2C

Heated tube inside diameter,	mm	11,6
Heated length,	mm	1183,0
Length to diameter ratio	-	102,0
Axial flux distribution	-	downward skewed asymmetrical sine

$$\frac{\phi_z}{\phi_{\max}} = 0,5\pi \frac{L-z}{L} \sin \pi \frac{L-z}{L} + 0,088$$

For Test Sections No.2, 2B, 2C the equations given above represent the nominal heat flux distribution. For the actual values, see reference (1).

SQUARE ANNULUS TEST SECTION

Square duct,	mm	15x15
Heater outside diameter	mm	10.2
Heater lengths	mm	560,0 and 1183
Axial flux distribution	-	nominally uniform

TABLE III DNB DATA FOR TEST SECTION N° 1 -

Pressure = 84 atm (Nominal)

Run	Mass flow rate g/cm sec^2	Inlet temperature $^{\circ}\text{C}$	Average heat flux W/cm^2	Exit quality %	(DNBR) $q''-\text{W}_2$	(DNBR) $\Delta H-\text{W}_2$	(DNBR) W_3	(DNBR) CISE	(DNBR) $\Delta H-\text{FIAT}$	(DNBR) Ferrel	(DNBR) Zankovich
178 (7-2-64)	49,3	265,5	154,00	63,04	-	1,03 ++	-	0,95	1,18	0,86	-
184 (7-2-64)	49,1	279,5	157,11	62,66	-	1,05 ++	-	0,96	1,22	0,87	-
170 (7-2-64)	49,8	274,0	160,36	60,86	-	1,03 ++	-	0,98	1,17	0,88	-
160 (19-12-63)	46,5	271,3	163,19	66,24	-	0,97 ++	-	0,91	1,15	0,85	-
156 (7-2-64)	49,8	263,5	160,01	59,70	-	1,02 ++	-	0,96	1,16	0,89	-
137 (7-2-64)	49,8	258,7	167,42	58,52	-	1,02 ++	-	0,97	1,17	0,91	-
55 (13-2-64)	74,0	280,5	169,12	43,56	-	1,21	-	1,06	1,14	0,96	-
46 (13-2-64)	73,4	282,5	166,72	43,42	-	1,20	-	1,05	1,11	0,96	-
42 (13-2-64)	73,7	275,6	173,64	42,83	-	1,18	-	1,05	1,10	0,96	-
153 (19-12-63)	69,6	271,8	172,35	44,21	-	1,17	-	1,05	1,12	0,96	-
33 (13-2-64)	73,1	273,1	173,08	41,96	-	1,18	-	1,06	1,11	0,97	-
27 (13-2-64)	73,7	267,6	175,32	40,52	-	1,20	-	1,06	1,12	0,99	+
186 (9-12-63)	71,6	251,0	181,98	41,77	-	1,16	-	1,05	1,10	0,98	-
81 (12-2-64)	71,3	256,5	183,67	40,91	-	1,15	-	1,06	1,10	0,99	-
70 (12-2-64)	73,7	252,5	180,50	38,13	-	1,17	-	1,08	1,11	1,01	-

+ Data obtained with inlet enthalpy out of range

++ Data obtained with mass velocity out of range

+++ Data obtained with both inlet enthalpy and mass velocity out of range

For $q''-\text{W}_2$ and $\Delta H-\text{W}_2$ correlations all data are out of range for equivalent diameter D_e . For Ferrel's correlation the data are out of range for equivalent diameter and length.

Table]](follows)

Pressure = 84 atm (Nominal)

Run	Mass flow rate $\frac{g}{cm^2 sec}$	Inlet temperature $^{\circ}C$	Average heat flux $\frac{W}{cm^2}$	Exit quality %	(DNBR) q^m-W_2	(DNBR) $\Delta H-W_2$	(DNBR) $W-3$	(DNBR) CISE	(DNBR) $\Delta H-FIAT$	(DNBR) Ferrel	(DNBR) Zenkovich
62 (19-12-63)	73,0	250,6	186,50	38,26	-	1,17	-	1,09	1,12	1,02	-
57 (12-2-64)	74,0	246,4	190,88	37,27	-	1,17	-	1,09	1,11	1,02	-
117 (19-12-63)	74,2	241,7	193,56	36,53	-	1,17	-	1,10	1,11	1,03	-
44 (12-2-64)	74,2	241,5	195,68	36,90	-	1,16	-	1,08	1,10	1,02	-
154 (13-2-64)	102,4	285,3	166,72	30,18	-	1,37	-	1,16	1,08	1,08	-
161 (13-2-64)	103,1	280,6	173,78	29,90	-	1,34	-	1,16	1,07	1,07	-
153 (13-2-64)	103,4	275,8	175,90	28,70	-	1,36	-	1,18	1,08	1,10	-
61 (13-2-64)	97,7	271,0	179,43	29,87	-	1,32	-	1,16	1,08	1,08	-
78 (14-2-64)	97,5	272,0	181,27	30,53	-	1,30	-	1,14	1,06	1,06	-
151 (13-2-64)	102,6	288,4	181,85	27,30	-	1,34	-	1,19	1,08	1,11	-
176 (19-12-63)	100,5	260,0	185,79	26,49	-	1,35	-	1,21	1,11	1,12	-
142 (13-2-64)	103,6	256,2	189,32	24,52	-	1,35	-	1,23	1,11	1,15	-
34 (19-12-63)	102,0	251,4	190,74	23,67	-	1,35	-	1,25	1,12	1,16	-
135 (13-2-64)	103,4	246,6	194,98	22,63	-	1,36	-	1,27	1,13	1,17	-
105 (19-12-63)	103,9	241,5	202,75	22,47	-	1,35	-	1,24	1,11	1,16	-
210 (19-12-63)	105,2	233,5	209,10	20,60	-	1,33	-	1,27	1,12	1,19	-
92 (24-6-64)	157,0	278,5	204,16	21,15	-	1,34	-	1,11	0,89	1,11	-
58 (24-6-64)	155,9	270,8	213,34	20,33	-	1,34	-	1,11	0,92	1,11	-
34 (10-6-64)	154,1	256,7	224,65	16,35	-	1,34	-	1,15	0,93	1,16	-
25 (10-6-64)	154,2	256,1	223,23	15,91	-	1,35	-	1,17	0,94	1,17	-

Table II - (follows)

Pressure = 84 atm (Nominal)

Run	Mass flow rate $\frac{\text{g}}{\text{cm}^2 \text{ sec}}$	Inlet temperature $^{\circ}\text{C}$	Average heat flux $\frac{\text{W}}{\text{cm}^2}$	Exit quality %	(DNBR) $q^* - W_2$	(DNBR) $\Delta H - W_2$	(DNBR) $W - 3$	(DNBR) CISE	(DNBR) $\Delta H - FIAT$	(DNBR) Ferrel	(DNBR) Zankiewich
300 (9-6-64)	154,8	236,2	248,67	13,20	-	1,32	0,82	1,16	0,96	1,20	-
256 (9-6-64)	153,6	216,4	269,86	10,06	-	1,30 +	0,79 +	1,18	0,98	1,24	-
214 (9-6-64)	154,1	195,4	293,88	4,69	-	1,28 +	-	1,18	0,99 +	1,26	-
167 (9-6-64)	152,4	179,0	305,18	3,70	-	1,29 +	0,79 +	1,22	1,02 +	1,31	-
176 (8-6-64)	151,2	160,4	327,79	1,61	-	1,26 +	0,78 +	1,20	1,01 +	1,31	-
158 (8-6-64)	153,0	141,0	350,39	-1,54	1,03 +	-	0,79 +	-	-	1,32	-
111 (25-11-64)	154,0	125,4	382,89	-2,30	1,03 +	-	0,75 +	-	-	1,27	-
98 (25-11-64)	154,5	112,7	401,26	-3,33	1,02 +	-	0,74 +	-	-	1,26	-
108 (24-6-64)	200,3	279,5	203,45	15,36	-	1,46	-	1,16	0,84	1,23	-
72 (24-6-64)	200,2	270,8	210,52	13,00	-	1,48	0,87	1,20	0,88	1,27	-
41 (10-6-64)	197,9	257,8	240,89	11,76	-	1,38	0,78	1,13	0,86	1,21	-
86 (10-6-64)	197,5	238,5	255,73	7,52	-	1,42	0,82	1,20	0,93	1,29	-
70 (10-6-64)	196,0	219,0	281,16	3,92	-	1,40	0,83	1,20	0,95	1,32	-
273 (9-6-64)	197,2	216,0	283,99	3,09	-	1,40 +	0,84 +	1,21	0,96	1,34	-
237 (9-6-64)	197,4	194,0	318,60	-0,06	1,06	-	0,82 +	-	-	1,34	-
189 (9-6-64)	196,1	177,0	343,33	-2,35	1,07	-	0,82 +	-	-	1,35	-
142 (8-6-64)	196,0	159,5	377,24	-3,93	1,04 +	+	0,79 +	-	-	1,33	-
90 (8-6-64)	195,9	140,0	394,19	-7,85	1,10 +	-	0,85 +	-	-	1,37	-
121 (25-11-64)	196,2	127,3	429,51	-8,29	1,10 +	-	0,80 +	-	-	1,32	-
76 (20-11-64)	196,6	116,0	447,88	-9,25	1,08 +	-	0,79 +	-	-	1,30	-
60 (20-11-64)	197,5	110,6	463,42	-9,36	1,05 +	-	0,77 +	-	-	1,28	-

TABLE III - DNB Data for Test Section n° 1

Pressure = 126 atm (Nominal)

Run	Mass flow rate $\frac{\text{g}}{\text{cm}^2 \text{ sec}}$	Inlet temperature $^{\circ}\text{C}$	Average heat flux $\frac{\text{W}}{\text{cm}^2}$	Exit quality %	(DNBR) $q''-W_2$	(DNBR) $\Delta H-W_2$	(DNBR) $W-3$	(DNBR) CISE	(DNBR) $\Delta H-\text{FIAT}$	(DNBR) Ferrel	(DNBR) Borkovich
88 (20-3-64)	103,8	220,0	236,65	18,38	-	1,16	-	1,12	0,92	1,11	-
75 (20-3-64)	196,8	226,5	264,91	- 1,14	1,20	-	0,92	-	-	1,35	-
25 (20-3-64)	198,7	198,0	306,71	- 6,04	1,22	-	0,97 +	-	-	1,39	-
128 (25-6-64)	49,8	304,0	107,37	44,47	-	1,20 ..	-	0,95	0,99	1,06	-
34 (25-6-64)	49,8	284,9	119,38	42,02	-	1,15 ++	-	0,97	0,97	1,05	-
122 (2-4-64)	49,1	266,5	134,22	43,79	-	1,07 ++	-	0,84	0,88	0,94	-
60 (2-4-64)	49,8	246,5	147,64	40,85	-	1,04 ++	-	0,93	0,90	1,00	-
72 (27-3-64)	48,8	234,0	139,16	32,32	-	1,11 ++	-	1,11	0,98	-	-
12 (27-3-64)	49,5	209,1	153,30	29,30	-	1,05 +++	-	1,15	0,97	1,10	-
196 (26-3-64)	50,8	182,0	175,90	28,72	-	1,02 +++	-	1,09	0,91 +	1,05	-
88 (26-3-64)	49,1	173,0	169,54	24,89	-	1,05 +++	-	1,20	0,95 +	1,09	-
121 (19-11-64)	46,7	53,0	226,06	20,85	-	0,94 +++	-	1,15	0,90 +	0,93	-
128 (19-11-64)	48,1	49,5	231,71	16,83	-	0,95 +++	-	1,23	0,90 +	0,93	-
104 (2-4-64)	74,5	266,0	150,19	23,24	-	1,22	-	1,15	0,89	1,11	-
44 (2-4-64)	75,0	242,7	172,37	21,89	-	1,17	-	1,13	0,89	-	-
64 (27-3-64)	73,9	230,4	172,37	17,80	-	1,20	-	1,26	0,93	1,14	-
258 (26-3-64)	74,0	209,1	180,85	12,31	-	1,21 +	0,87 +	1,43	0,96	1,18	-
176 (26-3-64)	74,4	183,8	200,63	9,13	-	1,16 +	0,86 +	1,46	0,99 +	1,16	-
57 (26-3-64)	74,0	168,0	212,64	8,44	-	1,14 +	0,84 +	1,44	0,94 +	1,15	-
158 (18-11-64)	73,5	128,7	241,60	4,74	-	1,08 +	0,82 +	1,42	0,91 +	1,09	-

TABLE III (follows)

Pressure = 126 atm (Nominal)

Run	Mass flow rate $\frac{\text{g}}{\text{cm}^2 \text{ sec}}$	Inlet temperature $^{\circ}\text{C}$	Average heat flux $\frac{\text{W}}{\text{cm}^2}$	Exit quality %	(DNBR) $q'' - W_2$	(DNBR) $\Delta H - W_2$	(DNBR) $W - 3$	(DNBR) CISE	(DNBR) $\Delta H - FIAT$	(DNBR) Ferrel	(DNBR) Bankovich
182 (18-11-64)	74,1	119,6	251,49	4,46	-	1,07 +	0,80 +	1,38	0,90 +	1,08	-
196 (18-11-64)	74,3	107,0	266,53	5,15	-	1,03 +	0,76 -	1,29	0,88 +	1,04	-
76 (19-11-64)	73,8	69,0	283,28	-2,43	1,35 +	-	0,83 +	-	-	0,99	-
83 (19-11-64)	74,1	60,5	285,40	-5,17	1,39 +	-	0,87 +	-	-	0,99	-
46 (3-4-64)	105,2	235,0	139,87	17,30	-	1,40	-	1,23	0,86	1,21	-
95 (2-4-64)	104,0	266,0	163,89	12,26	-	1,34	0,85	1,34	0,90	1,20	-
29 (2-4-64)	104,1	246,5	185,79	9,55	-	1,27	0,83	1,34	0,89	1,18	-
44 (27-3-64)	104,1	231,5	194,98	5,71	-	1,27	0,88	1,48	0,92	1,21	-
245 (26-3-64)	103,1	209,6	210,52	2,27	-	1,26 +	0,91 +	1,60	0,95	1,23	-
37 (26-3-64)	102,7	181,0	240,19	-1,40	1,32	-	0,89 +	-	-	1,19	-
167 (26-3-64)	105,3	177,5	248,67	-1,43	1,29	-	0,86 +	-	-	-	-
59 (18-11-64)	103,5	169,6	248,67	-3,61	1,46	-	0,90 +	-	-	1,20	-
42 (18-11-64)	103,5	160,2	261,38	-3,79	1,41 +	-	0,80 +	-	-	1,17	-
19 (18-11-64)	103,7	146,7	264,21	-8,11	1,49 +	-	0,94 +	-	-	1,2	-
50 (17-11-64)	103,8	137,6	274,80	-8,85	1,40 +	-	0,93 +	-	-	1,18	-
28 (17-11-64)	103,6	130,5	285,40	-8,57	1,39 +	-	0,90 +	-	-	1,15	-
23 (16-11-64)	103,7	123,2	295,99	-8,58	1,37 +	-	0,87 +	-	-	1,13	-
138 (25-6-64)	156,9	303,0	129,28	8,31	-	1,61	1,11	1,55	0,85	-	-
39 (3-4-64)	155,1	294,5	148,35	8,42	-	1,51	0,98	1,42	0,85	1,35	-
50 (25-6-64)	153,1	287,5	150,47	5,16	-	1,52	1,05	1,59	0,88	-	-

TABLE III (follows)

pressure = 12.5 atm (Nominal)

Run	Mass flow rate $\frac{g}{cm^2 sec}$	Inlet temperature $^{\circ}C$	Average heat flux $\frac{W}{cm^2}$	Exit quality %	(DNBR) q^n-W_2	(DNBR) $\Delta H-W_2$	(DNBR) $W-3$	(DNBR) CISE	(DNBR) $\Delta H-FIAT$	(DNBR) Ferrel	(DNBR) Rankine
74 (25-6-64)	154,5	284,7	158,24	5,78	-	1,50	1,02	1,52	0,87	-	-
86 (2-4-64)	152,6	270,8	179,01	3,70	-	1,42	0,95	1,49	0,87	1,29	-
94 (27-3-64)	152,6	253,2	204,87	-0,03	1,37	1,33	0,93	1,49	0,87	1,25	-
34 (27-3-64)	153,7	228,5	229,59	-5,11	1,42	-	0,98	-	-	-	-
235 (26-3-64)	153,2	211,5	248,67	-7,54	1,40	-	0,98 +	-	-	-	-
140 (26-3-64)	155,3	176,9	265,40	-15,30	1,45	-	-	-	-	1,31	-
70 (25-3-64)	152,1	170,5	291,05	-16,59	1,45	-	-	-	-	-	-
80 (18-11-64)	154,1	158,8	308,71	-18,29	1,50 +	-	-	-	-	1,27	-
85 (18-11-64)	154,4	149,2	316,48	-20,29	1,54 +	-	-	-	-	1,32	-
93 (18-11-64)	153,7	138,4	330,61	-21,62	1,49 +	-	-	-	-	-	-
29 (3-4-64)	200,2	292,0	166,72	4,34	-	1,49	1,01	1,44	0,78	-	-
96 (25-6-64)	199,0	283,7	178,02	1,92	-	1,48	1,01	1,49	0,81	-	-
64 (2-4-64)	196,9	267,4	204,16	-1,63	1,42	-	1,00	-	-	-	-
81 (27-3-64)	196,3	246,5	245,13	-4,32	1,34	-	0,94	-	-	-	-
24 (27-3-64)	196,5	234,0	265,62	-6,63	1,33	-	0,93	-	-	-	-
57 (27-3-64)	196,1	231,5	267,03	-6,98	1,33	-	0,94	-	-	-	-
216 (26-3-64)	196,3	211,7	294,58	-11,00	1,34	-	0,97 +	-	-	1,26	-
117 (26-3-64)	199,0	181,2	343,33	-16,59	1,32	-	-	-	-	1,24	-
49 (25-3-64)	195,8	176,2	351,81	-17,71	1,31	-	-	-	-	-	-
142 (18-11-64)	197,6	167,5	359,58	-19,74	1,36	-	-	-	-	-	-
113 (18-11-64)	197,5	160,7	366,64	-21,25	1,36 +	-	-	-	-	-	-

TABLE III DNB - Data for test section n° 1

Pressure = 140 atm (Nominal)

Run	Mass flow rate $\frac{\text{g}}{\text{cm}^2 \text{sec}}$	Inlet temperature $^{\circ}\text{C}$	Average heat flux $\frac{\text{W}}{\text{cm}^2}$	Exit quality %	(DNBR) $q^* - W_2$	(DNBR) $\Delta H - W_2$	(DNBR) $W - 3$	(DNBR) CISE	(DNBR) $\Delta H - FIAT$	(DNBR) Ferrel	(DNBR) Zenkelion
78 (11-3-64)	50,5	319,6	74,17	31,58	-	1,51 ++	-	1,13	1,10	-	-
97 (11-3-64)	49,6	312,0	78,41	30,61	-	1,47 ++	-	1,17	1,11	-	-
120 (11-3-64)	50,0	291,4	92,54	27,94	-	1,36 ++	-	1,19	1,06	1,26	-
217 (12-3-64)	49,4	274,6	99,80	24,22	-	1,32 ++	-	1,26	1,04	1,25	-
192 (12-3-64)	49,6	252,4	113,03	21,82	-	1,25 ++	-	1,31	1,01	1,22	-
178 (12-3-64)	49,9	234,5	131,39	23,90	-	1,13 ++	-	1,16	0,92	1,12	-
119 (12-3-64)	49,0	225,3	135,05	22,40	-	-	-	1,13	0,90	1,09	-
103 (12-3-64)	49,3	221,8	137,04	21,95	-	1,09 ++	-	1,15	0,90	1,10	-
186 (13-3-64)	51,3	191,0	164,60	22,89	-	1,03 +++	-	1,12	0,87 +	1,06	-
99 (13-3-64)	51,3	172,5	175,19	20,39	-	1,00 +++	-	1,10	0,85 +	1,02	-
56 (10-11-64)	49,4	105,9	206,99	16,91	-	0,94 +++	-	1,11	0,83 +	0,95	-
139 (27-21-64)	49,4	106,8	209,10	17,48	-	0,92 +++	-	1,04	0,80 +	0,92	-
50 (30-11-64)	49,3	91,7	223,23	20,74	-	0,89 +++	-	0,96	0,79 +	0,89	-
46 (30-11-64)	49,5	85,1	226,06	16,99	-	0,89 +++	-	0,91	0,78 +	0,88	-
31 (30-11-64)	50,8	64,1	240,19	15,94	-	0,89 +++	-	1,01	0,78 +	0,85	-
21 (30-11-64)	49,2	53,0	248,56	20,80	-	0,85 +++	-	0,91	0,76 +	0,80	-
13 (30-11-64)	50,5	47,8	255,02	18,56	-	0,86 +++	-	0,92	0,76 +	0,80	-
58 (11-3-64)	75,9	317,2	82,65	19,77	-	1,71	-	1,38	1,03	1,50	-
50 (11-3-64)	74,4	312,5	86,89	18,82	-	1,63	-	1,36	1,01	1,44	-
25 (11-3-64)	73,5	294,8	104,55	16,79	-	1,47	-	1,34	0,90	1,31	-

TABLE III - (Follows)

Pressure = 140 atm (Nominal)

Run	Mass Flow rate $\frac{\text{g}}{\text{cm}^2 \text{ sec}}$	Inlet temperature $^{\circ}\text{C}$	Average heat flux $\frac{\text{W}}{\text{cm}^2}$	Exit quality %	(DNBR) $q^* - W_2$	(DNBR) $\Delta H - W_2$	(DNBR) W_3	(DNBR) CISE	(DNBR) $\Delta H - FIAT$	(DNBR) Ferrel	(DNBR) Zenkovich
36 (11-3-64)	75,3	268,1	115,85	16,76	-	1,37	-	1,27	0,91	1,23	-
24 (11-3-64)	74,9	270,8	129,27	14,6	-	1,33	0,89	1,35	0,91	1,21	-
19 (11-3-64)	76,2	265,5	131,39	12,62	-	1,36	0,96	1,45	0,93	1,24	-
9 (11-3-64)	75,0	251,0	144,82	11,59	-	1,27	0,90	1,41	0,91	1,19	-
4 (11-3-64)	72,2	242,2	144,11	10,12	-	1,30	0,97	1,55	0,94	1,23	-
33 (12-3-64)	73,6	214,5	169,54	6,39	-	1,20 +	0,92 +	1,56	0,90	1,17	-
179 (13-3-64)	74,8	197,0	194,27	7,17	-	1,10 +	0,82 +	1,34	0,85 +	1,09	-
79 (13-3-64)	74,2	187,0	203,45	7,31	-	1,08 +	0,76 +	1,30	0,84 +	1,07	-
51 (27-11-64)	74,3	135,1	241,60	0,72	-	1,02 +	0,79 +	1,35	0,82 +	1,01	-
50 (27-11-64)	74,9	117,9	248,66	-4,06	1,49 +	-	0,84 +	-	-	1,01	-
47 (27-11-64)	74,8	109,9	252,90	-4,78	1,49 +	-	0,84 +	-	-	0,99	-
15 (27-11-64)	74,4	106,3	264,21	-1,47	1,46 +	-	0,77 +	-	-	0,97	-
37 (27-11-64)	74,0	91,0	269,15	-5,57	1,43 +	-	0,82 +	-	-	0,95	-
22 (27-11-64)	73,9	81,0	292,46	-0,23	1,43 +	-	0,69 +	-	-	0,88	-
26 (27-11-64)	74,3	71,3	299,53	-2,09	1,34 +	-	0,70 +	-	-	0,86	-
260 (12-3-64)	103,9	324,5	74,88	13,04	-	1,98	1,44	1,66	1,02	1,80	-
270 (12-3-64)	104,1	324,2	77,00	13,42	-	1,94	1,43	1,60	0,99	-	-
255 (12-3-64)	102,8	317,2	84,06	11,78	-	1,87	1,34	1,66	1,01	1,67	-
248 (12-3-64)	103,4	315,0	96,18	10,96	-	1,86	1,35	1,70	1,02	1,66	-
245 (12-3-64)	101,9	297,6	109,49	9,01	-	1,62	1,16	1,64	0,96	1,44	-

TABLE III - (Follows)

Pressure = 140 ata (Nominal)

Run	Mass flow rate $\frac{\text{g}}{\text{cm}^2 \text{sec}}$	Inlet temperature $^{\circ}\text{C}$	Average heat flux $\frac{\text{W}}{\text{cm}^2}$	Exit quality %	(DNBR) $q''-W_2$	(DNBR) $\Delta H-W_2$	(DNBR) $W-3$	(DNBR) CISE	(DNBR) $\Delta H-\text{FIAT}$	(DNBR) Ferrel	(DNBR) Zenkovich
232 (12-3-64)	103,4	275,0	134,22	4,35	-	1,48	1,10	1,76	0,95	1,34	-
208 (12-3-64)	103,9	251,2	155,41	-0,75	1,71	-	1,11	-	-	1,32	-
151 (12-3-64)	103,5	237,7	173,78	-2,33	1,53	-	1,03	-	-	1,25	-
44 (12-3-64)	102,9	216,0	197,80	-3,87	1,54	-	0,99 +	-	-	1,21	-
168 (12-3-64)	105,1	195,0	216,17	-7,87	1,54	-	1,02 +	-	-	1,22	-
112 (26-11-64)	103,7	187,6	231,00	-7,53	1,57	-	0,94 +	-	-	1,44	-
105 (26-11-64)	104,1	174,8	238,77	-40,64	1,57	-	0,98 +	-	-	1,16	-
93 (26-11-64)	103,7	168,3	245,84	-10,77	1,56	-	0,96 +	-	-	1,14	-
75 (26-11-64)	103,6	160,2	249,57	-13,44	1,54 +	-	0,99 +	-	-	1,15	-
61 (26-11-64)	103,3	151,5	251,49	-14,96	1,63 +	-	1,03 +	-	-	1,17	-
138 (26-6-64)	152,9	326,0	94,66	11,19	-	1,67	1,22	1,42	0,71	-	-
120 (26-6-64)	154,2	315,2	110,91	7,81	-	1,60	1,17	1,52	0,78	-	-
114 (26-6-64)	152,9	297,6	157,05	3,61	-	1,48	1,11	1,62	0,83	-	-
106 (26-6-64)	154,7	273,7	173,78	-1,03	1,55	-	1,01	-	-	1,28	-
91 (26-6-64)	153,3	260,5	187,20	-5,41	1,60	-	1,07	-	-	-	-
80 (26-6-64)	155,0	236,5	223,23	-8,52	1,50	-	1,00	-	-	1,23	-
48 (26-6-64)	153,8	217,4	247,25	-11,83	1,47	-	1,00	-	-	1,21	-
33 (26-6-64)	152,3	200,2	267,03	-14,76	1,46	-	1,01 +	-	-	1,20	-
16 (26-5-64)	153,0	179,0	288,22	-20,69	1,50	-	-	-	-	1,20	-
125 (26-11-64)	153,4	170,2	304,47	-21,13	1,44	-	-	-	-	1,17	-

TABLE III (Follows)

Pressure = 14L ata (Nominal)

TABLE IV DNB Data for test section n° 1 B

Pressure = 126 atm (Nominal)

Run	Mass flow rate ² g / cm sec	Inlet temperature °C	Average heat flux ² W/cm	Exit quality %	(DNBR) $q^* - W_2$	(DNBR) $\Delta H - W_2$	(DNBR) W_3	(DNBR) CISE	(DNBR) $\Delta H - FIAT$	(DNBR) Ferrel	(DNBR) Zenkevich
134 (13-10-64)	155,6	313,5	146,06	17,07	-	1,33	-	1,20	1,05	1,21	-
120 (13-10-64)	155,5	293,0	164,94	13,24	-	1,32	1,05	1,27	1,08	1,18	-
99 (13-10-64)	151,4	268,0	182,82	12,03	-	1,26	1,00	1,25	1,03	1,14	-
79 (13-10-64)	156,0	267,5	215,61	7,54	-	1,21	0,99	1,29	1,05	1,11	-
53 (13-10-64)	156,7	245,7	244,48	3,65	-	1,19	1,01	1,37	1,07	1,12	-
27 (13-10-64)	156,9	227,4	266,29	-0,34	1,17	-	1,05	-	-	1,13	1,32
81 (12-10-64)	156,1	173,7	344,78	-7,32	1,11	-	1,03 +	-	-	1,10	1,37 +
54 (12-10-64)	157,3	126,0	403,41	-15,32	1,13 +	-	-	-	-	1,07	1,53 +
18E (14-10-64)	202,3	315,5	166,93	15,24	-	1,22	-	1,10	0,95	1,17	-
95 (14-10-64)	202,3	304,5	184,81	11,95	-	1,23	0,95	1,14	0,99	1,14	-
77 (14-10-64)	195,8	295,0	202,70	10,68	-	1,19	0,91	1,13	0,99	1,10	-
51 (14-10-64)	202,6	276,5	238,47	5,82	-	1,16	0,93	1,16	1,01	1,08	-
47 (14-10-64)	189,7	227,5	311,99	-1,68	1,00	-	0,96	-	-	1,07	1,25
59 (14-10-64)	201,7	175,3	509,50	-14,02	1,16	-	1,13 +	-	-	1,15	1,71 +
19 (14-10-64)	195,5	127,5	439,18	-23,17	1,21 +	-	-	-	-	1,13	1,97 +

+ Data obtained with inlet enthalpy out of range

For Ferrel's correlation all data are out of range for lenght

TABLE IV - (Follows)

Pressure = 126 atm (Nominal)

TABLE V - DNB data for test section n° 1 C

Pressure = 132 atm (Nominal)

Run	Mass flow rate $\frac{\text{g}}{\text{cm}^2 \text{ sec}}$	Inlet temperature $^{\circ}\text{C}$	Average heat flux $\frac{\text{W}}{\text{cm}^2}$	Exit quality %	(DNBR) q^n-W_2	(DNBR) $\Delta H-W_2$	(DNBR) $W-3$	(DNBR) CISE	(DNBR) $\Delta H-\text{FIAT}$	(DNBR) Ferrel	(DNBR) Zenkewitch
17 (3-3-65)	92,9	322,3	100,87	34,38	-	1,24	-	0,96	0,93	1,17	-
67 (2-3-65)	93,8	311,8	105,5	29,46	-	1,25	-	1,02	0,97	1,19	-
237 (1-3-65)	92,6	284,5	134,49	28,05	-	1,11	-	0,99	0,92	1,08	-
130 (1-3-65)	94,1	233,1	176,23	21,26	-	1,03	-	1,07	0,93	1,06	-
62 (26-2-65)	90,7	188,3	206,37	17,93	-	0,98 +	-	1,09	0,93 +	1,04	-
46 (16-2-65)	94,9	146,8	236,52	10,09	-	0,97 +	1,05 +	1,22	0,95 +	1,04	-
106 (3-3-65)	94,6	85,8	278,84	3,83	-	0,93 +	0,93 +	1,27	0,94 +	0,96	-
31 (3-3-65)	139,8	321,8	105,5	22,13	-	1,34	-	1,14	0,98	1,34	-
80 (2-3-65)	136,8	315,5	109,56	19,78	-	1,34	-	1,18	1,01	1,32	-
93 (2-3-65)	140,3	309,5	120,58	19,12	-	1,29	-	1,17	0,99	1,26	-
11 (2-3-65)	136,5	288,0	153,04	18,57	-	1,16	-	1,10	0,95	1,13	-
145 (1-3-65)	139,9	234,4	208,11	7,98	-	1,08	0,96	1,25	0,98	1,11	-
15 (1-3-65)	137,7	185,9	253,91	1,58	-	1,03 +	0,99 +	1,35	0,99 +	1,09	-
93 (26-2-65)	139,1	134,6	310,72	-3,78	1,24 +	-	0,97 +	-	-	1,03	1,18 +
146 (3-3-65)	142,8	84,5	377,39	-7,54	1,13 +	-	0,91 +	-	-	0,93	1,12 +

+ Data obtained with inlet enthalpy out of range

For Ferrel's correlation all data are out of range for equivalent diameter and lenght

TABLE V -(Follows)

Pressure = 132 atm (Nominal)

Run	Mass flow rate $\frac{\text{g}}{\text{cm}^2 \text{sec}}$	Inlet temperature $^{\circ}\text{C}$	Average heat flux $\frac{\text{W}}{\text{cm}^2}$	Exit quality %	(DNBR) $q^n - W_2$	(DNBR) $\Delta H - W_2$	(DNBR) W_3	(DNBR) CISE	(DNBR) $\Delta H - FIAT$	(DNBR) Ferrel	(DNBR) Zenkevitch
45 (3-3-65)	181,2	323,2	108,98	17,47	-	1,36	-	1,21	1,00	1,43	-
110 (2-3-65)	185,6	309,5	132,17	13,85	-	1,29	1,09	1,22	1,00	1,30	-
22 (2-3-65)	183,9	282,8	177,39	10,39	-	1,15	0,97	1,18	0,98	1,15	-
159 (1-3-65)	175,6	233,1	240,00	3,34	-	1,06	0,96	1,22	0,99	1,10	-
31 (1-3-65)	185,4	181,1	314,20	-5,11	1,17	-	1,00 +	-	-	1,08	1,39 +
104 (26-2-65)	185,1	131,9	385,51	610,45	1,12 +	-	0,96 +	-	-	1,00	1,38 +
166 (3-3-65)	189,4	84,8	466,66	-13,80	1,02 +	-	0,91 +	-	-	0,91	1,28 +
61 (3-3-65)	224,1	323,5	113,62	14,25	-	1,38	1,23	1,26	1,01	1,05	-
131 (2-3-65)	229,0	307,8	146,09	10,49	-	1,28	1,11	1,23	1,00	1,31	-
34 (2-3-65)	229,2	279,8	204,06	6,16	-	1,14	0,97	1,44	0,96	1,13	-
175 (1-3-65)	227,3	231,0	280,58	-2,22	1,19	-	1,00	-	-	1,09	1,44
57 (1-3-65)	229,1	186,4	353,62	-6,30	1,11	-	1,02 +	-	-	1,07	1,57 +
119 (26-2-65)	232,8	127,8	451,59	-16,59	1,07 +	-	-	-	-	1,00	1,64 +
176 (3-3-65)	230,5	88,8	522,90	-19,34	1,01 +	-	-	-	-	0,92	1,52 +
80 (3-3-65)	303,7	326,2	131,01	13,17	-	1,31	1,19	1,19	0,95	1,48	-
141 (2-3-65)	314,2	300,0	174,49	7,98	-	1,25	1,02	1,08	0,94	1,24	-
47 (2-3-65)	301,0	287,5	227,82	4,67	-	1,13	0,92	1,00	0,94	1,09	-
215 (1-3-65)	312,6	236,2	347,24	-4,80	1,10	-	0,94	-	-	1,02	1,42
110 (1-3-65)	316,7	183,0	459,13	-13,59	1,06	-	1,01 +	-	-	1,01	1,69 +
155 (26-2-65)	316,2	133,2	557,10	-21,08	1,00 +	-	-	-	-	0,98	1,81 +
191 (3-3-65)	315,4	104,9	627,82	-23,37	0,98 +	-	-	-	-	0,92	1,68 +
209 (3-3-65)	316,4	89,3	664,92	-25,14	0,94 +	-	-	-	-	0,88	1,67 +

TABLE VI

DNB QUALITY < - 15%

RUN N°	PRESSURE ata	MASS FLOW RATE g/cm sec	INLET SUBCOO- LING °C	EXIT QUALITY %	DNB-FIELD (Z/L) MEASURED	(Z/L) DNB PREDICTED	PREDICTED q''_{DNB} W/cm²	MEASURED q''_{DNB} W/cm²	R DNB	DNB QUALITY %	CORRELATION	XIAL FLUX DISTRIBUTION
52(7-10-64)	126,2	152,9	83,7	- 6,5	0,61 - 0,65	0,56	370,62	307,29	1,20	- 19,3	Ferrel	Symmetrical
						0,55	442,16	317,32	1,39	- 20,5	$q''(W-2)$	Cosine
												Test Section n° 2
117(6-10-64)	126,2	152,7	106,0	- 11,5	0,61 - 0,65	0,56	423,16	343,37	1,23	- 26,1	Ferrel	Symmetrical
						0,55	514,47	354,57	1,45	- 27,4	$q''(W-2)$	Cosine
												Test Section n° 2
106(6-10-64)	126,2	153,5	145,0	- 22,0	0,61 - 0,63	0,56	512,24	385,42	1,32	- 38,4	Ferrel	Symmetrical
						0,55	644,65	399,04	1,61	- 39,9	$q''(W-2)$	Cosine
												Test Section n° 2
96(6-10-64)	126,2	148,4	167,0	- 21,7	0,61 - 0,65	0,56	545,85	456,85	1,21	- 41,4	Ferrel	Symmetrical
						0,55	887,12	466,35	1,47	- 43,2	$q''(W-2)$ +	Cosine
												Test Section n° 2
103(7-10-64)	127,7	198,0	69,4	- 7,0	0,61 - 0,68	0,56	388,83	324,09	1,19	- 17,9	Ferrel	Symmetrical
						0,55	442,40	331,88	1,33	- 18,5	$q''(W-2)$	Cosine
												Test section n° 2
73(7-10-64)	126,2	197,7	87,0	- 12,1	0,61 - 0,65	0,56	434,17	344,54	1,26	- 23,3	Ferrel	Symmetrical
						0,55	508,34	355,76	1,43	- 24,3	$q''(W-2)$	Cosine
												Test Section n° 2

+ Data obtained with inlet enthalpy out of range

For Ferrel's correlation the data are out of range for equivalent diameter and length

For $q''(W-2)$ correlation all data related to symmetrical cosine heat flux distribution are out of range for equivalent diameter.

TABLE VI - (follows) DNB QUALITY < - 15%

RUN Nº	PRESSURE ata	MASS FLOW RATE $\frac{g}{cm^2 sec}$	INLET SUB- COOLING $^{\circ}C$	EXIT QUALITY %	DNB-FIELD (Z/L)DNB MEASURED	(Z/L)DNB PREDICTED	PREDICTED q''_{DNB} $\frac{W}{cm^2}$	MEASURED q''_{DNB} $\frac{W}{cm^2}$	R_{DNB}	DNB QUALITY %	CORRELATION	AXIAL FLUX DISTRIBUTION
33(15-2-65)	139,7	95,6	143,9	- 14,5	0,53-0,62	0,56	355,61	297,95	1,19	- 35,8	Ferrel	Symmetrical
						0,55	539,37	307,69	1,75	- 37,6	$q''(W-2)$	Cosine
												Test section n° 2
38(10-12-64)	131,3	141,7	136,4	- 8,8	0,79-0,87	0,72	335,20	349,02	0,95	- 24,3	Ferrel	Upward skewed
						0,70	457,69	352,78	1,29	- 24,0	$q''(W-2)$	asymmetrical sine
												test section n° 2B
52(10-12-64)	130,3	142,4	140,5	- 10,5	0,74-0,87	0,72	343,27	349,02	0,95	- 25,0	Ferrel	Upward skewed
						0,70	471,24	352,78	1,33	- 27,1	$q''(W-2)$	asymmetrical sine
												test section n° 2B
61(10-12-64)	132,3	142,3	141,0	- 11,3	0,80-0,85	0,72	339,93	349,02	0,97	- 26,5	Ferrel	Upward skewed
						0,70	474,71	352,78	1,34	- 27,7	$q''(W-2)$	asymmetrical sine
												test section n° 2B
97(9-12-64)	131,3	142,5	141,9	- 8,2	0,82-0,87	0,72	343,37	368,51	0,93	- 24,6	Ferrel	Upward skewed
						0,70	455,55	372,49	1,25	- 25,9	$q''(W-2)$	asymmetrical sine
												test section n° 2B
26(10-12-64)	130,7	142,5	142,1	- 9,8	0,80-0,87	0,72	344,92	358,76	0,95	- 25,6	Ferrel	Upward skewed
						0,70	471,26	362,64	1,30	- 26,9	$q''(W-2)$	asymmetrical sine
												test section n° 2B
14(10-12-64)	131,3	142,3	146,7	- 12,1	0,80-0,93	0,70	354,00	359,07	0,98	- 29,2	Ferrel	Upward skewed
						0,70	485,98	359,07	1,35	- 29,2	$q''(W-2)$	asymmetrical sine
												test section n° 2B
73(9-12-64)	130,7	143,8	152,8	- 11,8	0,82-0,85	0,72	360,45	371,50	0,95	- 28,0	Ferrel	Upward skewed
						0,70	490,52	380,57	1,30	- 29,5	$q''(W-2)$	asymmetrical sine
												test section n° 2B
50(9-12-64)	131,7	142,7	177,0	- 14,8	0,79-0,84	0,72	384,57	415,28	0,92	- 33,0	Ferrel	Upward skewed
						0,70	543,47	419,79	1,29	- 34,5	$q''(W-2)^+$	asymmetrical sine
												test section n° 2B
83(9-12-64)	131,3	143,1	198,6	- 16,8	0,79-0,84	0,72	401,95	450,25	0,89	- 36,6	Ferrel	Upward skewed
						0,70	584,76	451,18	1,26	- 36,3	$q''(W-2)^+$	asymmetrical sine
												test-section n° 2B

TABLE VI - (Follows) DNB QUALITY < - 15%

RUN N°	PRESSURE ata	MASS FLOW RATE g/cm sec	INLET SUB- COOLING °C	EXIT QUALITY %	DNB-FIELD (Z/L)	(Z/L)DNB PREDICTED	PREDICTED q'' DNB W/cm ²	MEASURED q'' DNB W/cm ²	R DNB	DNB QUALITY %	CORRELATION	AXIAL FLUX DISTRIBUTION
33(9-12-64)	130,3	143,6	201,3	-16,5	0,82-0,88	0,72	412,41	452,34	0,91	- 37,8	Ferrel	Upward skewed
						0,70	597,38	457,34	1,30	- 39,5	$q''(W-2)^+$	asymmetrical sine
												test section n° 2B
29(11-12-64)	131,3	146,0	261,2	-27,6	0,76-0,85	0,72	447,89	549,83	0,81	- 50,4	Ferrel	Upward skewed
						0,80	632,55	485,20	1,30	- 41,4	$q''(W-2)^+$	asymmetrical sine
												test section n° 2B
33(21-12-64)	132,3	186,3	107,1	- 8,0	0,79-0,85	0,71	346,08	370,91	0,93	- 21,4	Ferrel	Upward skewed
						0,70	444,31	370,52	1,20	- 21,4	$q''(W-2)$	asymmetrical sine
												test section n° 2B
142(11-12-64)	131,3	183,9	136,6	-12,5	0,76-0,85	0,72	391,31	421,15	0,93	- 27,0	Ferrel	Upward skewed
						0,70	511,72	425,71	1,20	- 28,2	$q''(W-2)$	asymmetrical sine
												test section n° 2B
119(11-12-64)	129,7	185,5	142,5	-14,1	0,79-0,88	0,72	406,42	430,89	0,94	- 28,4	Ferrel	Upward skewed
						0,70	531,88	435,50	1,22	- 29,6	$q''(W-2)$	asymmetrical sine
												test-section n° 2B
155(11-12-64)	131,3	186,7	193,5	-20,6	0,76-0,85	0,72	476,41	545,92	0,87	- 38,8	Ferrel	Upward skewed
						0,70	645,84	551,64	1,17	- 40,3	$q''(W-2)^+$	asymmetrical sine
												test section n° 2B
186(11-12-64)	130,3	196,1	197,0	-25,9	0,79-0,85	0,72	498,36	534,22	0,93	- 42,8	Ferrel	Upward skewed
						0,70	587,93	540,01	1,27	- 44,2	$q''(W-2)^+$	asymmetrical sine
												test section n° 2B
213(11-12-64)	131,3	186,1	239,5	- 29,8	0,73-0,85	0,72	515,92	612,21	0,84	- 49,8	Ferrel	Upward skewed
						0,70	764,50	618,85	1,23	- 51,5	$q''(W-2)^+$	asymmetrical sine
												test section n° 2B
223(11-12-64)	131,3	186,5	242,1	-31,1	0,73-0,85	0,72	518,00	610,25	0,85	- 51,0	Ferrel	Upward skewed
						0,70	775,56	616,88	1,25	- 52,7	$q''(W-2)^+$	Asymmetrical sine
												test-section n° 2B
190(18-12-64)	132,7	229,3	95,2	- 8,4	0,79-0,85	0,71	362,39	400,20	0,90	- 20,0	Ferrel	Upward skewed
						0,70	456,87	400,10	1,14	- 20,0	$q''(W-2)$	Asymmetrical sine
												test section n° 2B

TABLE VI - (Follows)

DNB QUALITY < - 15%

RUN N°	PRESSURE ata	MASS FLOW RATE $\frac{g}{cm^2 sec}$	INLET SUB- COOLING °C	EXIT QUALITY %	DNB-FIELD (Z/L) MEASURED	(Z/L)DNB PREDICTED	PREDICTED $q'' DNB$ $\frac{W}{cm^2}$	MEASURED $q'' DNB$ $\frac{W}{cm^2}$	R DNB	DNB QUALITY %	CORRELATION	AXIAL FLUX DISTRIBUTION
185(18-12-64)	131,7	229,4	95,3	- 8,3	0,79 - 0,85	0,71	360,81	395,57	0,91	- 18,9	Ferrel	Upward skewed
						0,70	457,27	400,08	1,14	- 18,9	$q''(W-2)$	asymmetrical sine
												test section n° 2B
115(17-12-64)	131,3	229,5	145,8	- 16,7	0,79 - 0,82	0,71	452,81	497,19	0,91	- 30,8	Ferrel	Upward skewed
						0,70	581,19	502,57	1,15	- 30,8	$q''(W-2)$	asymmetrical sine
												test section n° 2B
92(17-12-64)	131,3	224,4	147,2	- 18,0	0,79 - 0,82	0,72	460,22	499,15	0,92	- 32,1	Ferrel	Upward skewed
						0,70	594,12	502,96	1,17	- 32,0	$q''(W-2)$	asymmetrical sine
												test section n° 2B
71(17-12-64)	130,3	232,5	199,9	- 26,8	0,79 - 0,82	0,72	559,29	635,62	0,88	- 43,6	Berrel	Upward skewed
						0,70	745,01	642,50	1,16	- 43,0	$q''(W-2)$ +	asymmetrical sine
												test section n° 2B
85(17-12-64)	131,3	233,0	205,2	- 28,3	0,79 - 0,82	0,72	561,25	635,62	0,88	- 45,3	Ferrel	Upward skewed
						0,70	758,06	542,50	1,18	- 45,0	$q''(W-2)$ +	asymmetrical sine
												test section n° 2B
57(17-12-64)	132,3	232,8	259,1	- 37,8	0,79 - 0,82	0,72	604,71	760,39	0,79	- 57,7	Ferrel	Upward skewed
						0,70	910,38	768,64	1,18	- 57,0	$q''(W-2)$ +	asymmetrical sine
												test section n° 2B
66(21-12-64)	131,3	311,9	102,0	- 11,3	0,79 - 0,82	0,71	450,92	538,30	0,84	- 22,9	Ferrel	Upward skewed
						0,70	551,82	538,02	1,02	- 22,9	$q''(W-2)$	asymmetrical sine
												test section n° 2B
55(21-12-64)	131,3	312,0	102,3	- 11,3	0,79 - 0,82	0,71	451,84	540,59	0,83	- 22,9	Ferrel	Upward skewed
						0,70	552,71	540,02	1,02	- 22,9	$q''(W-2)$	asymmetrical sine
												test section n° 2B
137(18-12-64)	131,3	301,4	143,8	- 20,5	0,79 - 0,82	0,72	541,30	515,15	0,88	- 33,5	Ferrel	Upward skewed
						0,70	680,07	522,80	1,09	- 33,0	$q''(W-2)$	asymmetrical sine
												test section n° 2B
74(18-12-64)	131,3	304,3	150,0	- 21,0	0,79 - 0,82	0,72	559,35	535,52	0,88	- 35,8	Ferrel	Upward skewed
						0,70	703,97	642,50	1,09	- 35,0	$q''(W-2)$	asymmetrical sine
												test section n° 2B

TABLE VI - (follows)

DNB QUALITY < - 15%

RUN N°	PRESSURE ata	MASS FLOW RATE $\text{kg}/\text{cm}^2 \cdot \text{sec}$	INLET SUB- COOLING °C	EXIT QUALITY %	EMF FIELD (Z/L) PREDICTED MEASURED	(Z/L)DNB PREDICTED	PREDICTED q'' DNB W/cm^2	MEASURED q'' DNB W/cm^2	R DNB	DNB QUALITY %	CORRELATION	AXIAL FLUX DISTRIBUTION
31(18-12-64)	130,7	316,5	201,6	- 31,5	0,79 - 0,82	0,72	682,36	805,24	0,85	- 47,3	Ferrel	Upward skewed
						0,70	684,93	813,96	1,08	- 47,0	$q''(\text{W}-2)$ +	asymmetrical sine test section n° 2B
49(18-11-64)	131,3	317,3	205,3	- 33,6	0,79 - 0,82	0,72	687,47	799,40	0,86	- 49,2	Ferrel	Upward skewed
						0,70	904,60	808,05	1,12	- 49,0	$q''(\text{W}-2)$ +	asymmetrical sine test section n° 2B
136(24-3-65)	131,4	96,5	201,9	- 2,1	0,50 - 0,59	0,41	456,44	384,72	1,18	- 42,0	Ferrel	Down skewed
						0,50	526,45	327,80	1,60	-	$q''(\text{W}-2)$ +	asymmetrical sine test section n° 2C
69(25-3-65)	132,4	94,4	241,3	- 0,02	0,58 - 0,59	0,41	476,37	451,81	1,05	- 47,7	Ferrel	Down skewed
						0,50	569,73	384,95	1,46	-	$q''(\text{W}-2)$ +	asymmetrical sine test section n° 2C
92(24-3-65)	131,7	182,8	147,3	- 8,9	0,58 - 0,64	0,50	513,56	428,37	1,20	- 29,3	Ferrel	Down skewed
						0,50	572,73	428,37	1,33	- 29,3	$q''(\text{W}-2)$	asymmetrical sine test section n° 2C
14(23-3-65)	130,3	182,2	195,2	- 17,3	0,52 - 0,58	0,41	677,66	570,86	1,18	- 48,7	Ferrel	Down skewed
						0,50	684,97	486,49	1,40	-	$q''(\text{W}-2)$ +	asymmetrical sine test section n° 2C
83(25-3-65)	132,4	182,0	248,6	- 24,7	0,50 - 0,62	0,42	721,56	669,39	1,09	- 60,1	Ferrel	Down Skewed
						0,50	815,20	580,63	1,40	-	$q''(\text{W}-2)$ +	asymmetrical sine test section n° 2C
37(24-3-65)	131,2	312,1	96,9	- 7,2	0,58 - 0,64	0,41	568,78	570,17	1,03	- 25,5	Ferrel	Down skewed
						0,50	566,95	485,62	1,16	-	$q''(\text{W}-2)$	asymmetrical sine test section n° 2C
116(24-3-65)	130,3	311,6	146,5	- 18,4	0,52 - 0,59	0,41	708,65	688,54	1,14	- 40,8	Ferrel	Down skewed
						0,50	745,08	586,68	1,27	-	$q''(\text{W}-2)$	asymmetrical sine test section n° 2C
53(25-3-65)	131,7	311,6	191,9	- 27,3	0,52 - 0,50	0,41	936,16	815,58	1,14	- 83,7	Ferrel	Down skewed
						0,50	903,42	694,94	1,30	-	$q''(\text{W}-2)$ +	asymmetrical sine test section n° 2C

TABLE VII

- 15% < DNB QUALITY < + 15%

RUN N°	PRESSURE ata	MASS FLOW RATE $\frac{g}{cm^2 sec}$	INLET SUBCOO- LING °C	EXIT QUALITY %	DNB-FIELD (Z/L) PREDICTED	(Z/L) DNB PREDICTED	$q''_{DNB,EU}$ $\frac{W}{cm^2}$	F	PREDICTED q''_{DNB} $\frac{W}{cm^2}$	MEASURED q''_{DNB} $\frac{W}{cm^2}$	R DNB	DNB QUALITY %	CORRELATION	AXIAL FLUX DISTRIBUTION
179(8-10-64)	129,7	155,8	10,1	8,0	0,77 - 1	0,62	154,56	1,02	151,77	121,99	1,24	3,3	W-3 B	Symmetrical
						0,55	-	-	217,75	134,22	1,02	1,8	Ferrel	Cosine
						1	-	-	64316	31015	2,07	0,0	CISE	Test-section
						1	-	-	84,12	80,53	1,04	8,0	ΔH(FIAT)	N° 2
89(25-9-64)	126,2	154,3	11,9	7,7	0,84 - 1	0,62	159,97	1,01	157,90	134,84	1,15	3,5	W-3 B	Symmetrical
						0,55	-	-	224,31	148,55	1,51	1,8	Ferrel	Cosine
						1	-	-	65939	33708	1,95	7,7	CISE	Test-Section
						1	-	-	92,31	89,01	1,03	7,7	ΔH (FIAT)	N° 2
74(25-9-64)	128,2	155,6	15,7	7,0	0,84 - 1	0,62	162,85	1,02	159,81	140,19	1,14	0,7	W-3 B	Symmetrical
						0,55	-	-	229,33	154,24	1,48	0,3	Ferrel	Cosine
						1	-	-	59713	29952	1,99	7,0	CISE	Test-Section
						1	-	-	95,09	92,54	1,03	7,0	ΔH (FIAT)	N° 2
63(25-9-64)	123,2	157,8	25,0	4,9	0,84 - 1	0,62	179,22	1,01	176,96	164,81	1,07	-0,5	W-3 B	Symmetrical
						0,55	-	-	251,16	181,32	1,38	-2,5	Ferrel	Cosine
						1	-	-	52156	20247	2,57	4,9	CISE	Test Section
						1	-	-	112,10	108,79	1,03	4,9	ΔH (FIAT)	N° 2
52(25-9-64)	126,2	156,0	33,4	2,9	0,77 - 1	0,63	190,49	1,02	186,25	175,41	1,06	-2,5	W-3 B	Symmetrical
						0,55	-	-	266,61	196,96	1,33	-5,2	Ferrel	Cosine
						1	-	-	42703	12995	3,28	2,9	CISE	Test-Section
						1	-	-	124,77	119,55	1,04	2,9	ΔH(FIAT)	N° 2

• CISE Correlation (W)

For Ferrel's Correlation the data are out of Range For equivalent diameter and lenght

• Data obtained with inlet enthalpy out of range.

TABLE VII (follows)

-15% < DNB QUALITY < + 15%

RUN N°	PRESSURE sta	MASS FLOW RATE $\text{g} / \text{cm sec}^2$	INLET SUBCOO LING °C	EXIT QUALITY %	DNB-FIELD (Z/L) MEASURED	(Z/L) PREDICTED	$q''_{\text{DNB,EU}}$ W/cm^2	F	PREDICTED q''_{DNB} W/cm^2	MEASURED q''_{DNB} W/cm^2	R DNB	DNB QUALITY %	CORRELATION	AXIAL FLUX DISTRIBUTION
135(7-10-64)	127,2	153,0	37,2	2,8	0,72 - 1	0,62	194,06	1,01	191,93	193,70	0,99	-3,5	W - 3 B	Symmetrical
						0,55	-	-	270,56	213,11	1,27	-5,9	Farrel	Cosine
						1	-	-	40605	12557	3,23	2,8	CISE	Test-Section
						1	-	-	128,81	127,85	1,01	2,8	$\Delta H(\text{FIAT})$	N° 2
42(25-9-64)	126,2	155,3	43,0	0,9	0,68-0,77	0,63	205,91	1,01	204,16	194,09	1,05	-5,3	W - 3 B	Symmetrical
						0,55	-	-	286,22	220,17	1,3	-8,3	Farrel	Cosine
						-	-	-	-	-	-	-	CISE	Test-Section
						1	-	-	138,84	132,10	1,05	0,9	$\Delta H(\text{FIAT})$	N° 2
112(7-10-64)	126,2	152,4	46,0	1,8	0,63-0,77	0,63	205,03	1,00	205,03	209,66	0,96	-5,0	W - 3 B	Symmetrical
						0,55	-	-	269,99	237,84	1,22	-8,3	Farrel	Cosine
						-	-	-	-	-	-	-	CISE	Test-Section
						1	-	-	142,71	142,70	0,99	1,8	$\Delta H(\text{FIAT})$	N° 2
8(25-9-64)	126,2	155,0	63,0	-4,0	0,66-0,7	0,73	225,77	1,02	221,47	163,21	1,35	-7,9	W - 3 B	Symmetrical
						0,55	-	-	329,65	255,5	1,29	-14,9	Farrel	Cosine
						-	-	-	-	-	-	-	CISE	Test-Section
						-	-	-	-	-	-	-	$\Delta H(\text{FIAT})$	N° 2
99(7-10-64)	126,2	153,7	66,0	-3,0	0,61-0,63	0,70	230,05	1,02	226,50	208,10	1,08	-8,7	W - 3 B	Symmetrical
					0,65-0,72	0,55	-	-	334,92	275,51	1,22	-14,8	Farrel	Cosine
						-	-	-	-	-	-	-	CISE	Test-Section
						-	-	-	-	-	-	-	$\Delta H(\text{FIAT})$	N° 2
83(7-10-64)	126,2	153,8	66,2	-2,9	0,63-0,68	0,68	232,21	1,02	228,43	218,46	1,03	-9,2	W - 3 B	Symmetrical
						0,55	-	-	335,45	277,87	1,21	-14,2	Farrel	Cosine
						-	-	-	-	-	-	-	CISE	Test-Section
						-	-	-	-	-	-	-	$\Delta H(\text{FIAT})$	N° 2

TABLE VII (Follows)

-15% < DNB QUALITY < + 15%

RUN NO	PRESSURE ata	MASS FLOW RATE ² g / cm sec	INLET SUBCOO- LING °C	EXIT QUALITY %	DNB-FIELD (Z/L) MEASURED	(Z/L) PREDICTED	q" DNB, EU W/cm ²	F	PREDICTED q" DNB W/cm ²	MEASURED q" DNB W/cm ²	R _{DNB}	DNB QUALITY %	CORRELATION	AXIAL FLUX DISTRIBUTION
159(B-10-64)	126,2	198,7	16,6	5,6	0,72 - 1	0,63	174,03	1,01	172,76	162,95	1,06	1,3	W - 3B	Symmetrical
						0,55	-	-	278,34	184,95	1,40	-0,6	Ferrel	Cosine
						1	-	-	57694	27561	2,09	5,6	CISE	Test-Section
						1	-	-	94,08	110,91	0,85	5,6	ΔH(FIAT)	Nº 2
149(B-10-64)	126,2	195,0	26,0	3,1	0,77 - 1	0,55	186,98	1,03	182,76	177,51	1,03	-1,2	W - 3B	Symmetrical
						0,55	-	-	278,19	208,40	1,31	-3,8	Ferrel	Cosine
						1	-	-	45379	16522	2,75	3,1	CISE	Test-Section
						1	-	-	112,29	125,04	0,90	3,1	ΔH(FIAT)	Nº 2
158(B-10-64)	126,2	195,5	33,9	1,4	0,72 - 1	0,65	202,81	1,02	199,15	199,16	1,00	-3,3	W - 3B	Symmetrical
						0,55	-	-	296,65	233,12	1,27	-6,3	Ferrel	Cosine
						-	-	-	-	-	-	-	CISE	Test-Section
						1	-	-	126,28	139,87	0,91	1,4	ΔH(FIAT)	Nº 2
103(28-9-64)	126,2	196,9	39,0	-0,4	0,72 - 0,77	0,66	213,32	1,02	209,79	196,93	1,03	-4,9	W - 3B	Symmetrical
						0,55	-	-	310,23	240,19	1,29	-8,3	Ferrel	Cosine
						-	-	-	-	-	-	-	CISE	Test-Section
						-	-	-	-	-	-	-	ΔH(FIAT)	Nº 2
117(7-10-64)	126,2	195,9	48,0	-2,0	0,72 - 0,84	0,68	226,54	1,01	223,16	211,05	1,06	-6,7	W - 3B	Symmetrical
						0,55	--	-	331,98	268,45	1,23	-10,9	Ferrel	Cosine
						-	-	-	-	-	-	-	CISE	Test Section
						-	-	-	-	-	-	-	ΔH(FIAT)	Nº 2
130(7-10-64)	126,2	196,4	49,0	-2,5	0,65 - 0,84	0,69	227,56	1,04	218,90	201,59	1,06	-6,8	W - 3B	Symmetrical
						0,55	-	-	334,95	268,45	1,25	-12,4	Ferrel	Cosine
						-	-	-	-	-	-	-	CISE	Test-Section
						-	-	-	-	-	-	-	ΔH(FIAT)	Nº 2

TABLE VII (follows)

-15% << DNB QUALITY << + 15%

RUN N°	PRESSURE ata	MASS FLOW RATE $\text{g/cm}^2 \text{ sec}$	INLET SUBCOO- LING °C	EXIT QUALITY %	DNB-FIELD (Z/L) MEASURED	(Z/L) DNB PREDICTED	$q''_{\text{DNB,EU}}$ W/cm^2	F	PREDICTED q''_{DNB} W/cm^2	MEASURED q''_{DNB} W/cm^2	R DNB	DNB QUALITY %	CORRELATION	AXIAL FLUX DISTRIBUTION
87(28-9-64)	126,2	197,4	51,0	-3,3	0,72 - 0,77	0,72	229,01	1,02	223,84	183,31	1,22	-6,9	W - 3B	Symmetrical
						0,55	-	-	340,88	270,81	1,25	-12,27	Farrel	Cosine
						-	-	-	-	-	-	-	CISE	Test Section
						-	-	-	--	-	-	-	$\Delta H(\text{FIAT})$	N° 2
95(17-2-65)	140,7	96,1	4,2	18,4	0,96 - 1 0,66 - 0,92	0,63	112,55	1,05	107,06	104,83	1,02	11,5	W - 3B	Symmetrical
						0,55	-	-	160,96	118,92	1,35	8,7	Farrel	Cosine
						1	-	-	64955	46621	1,39	18,4	CISE	Test-Section
						1	-	-	71,35	71,35	1,00	18,4	$\Delta H(\text{FIAT})$	N° 2
211(16-2-65)	139,7	98,1	8,6	17,2	0,66-0,84	0,82	118,31	1,03	114,35	116,65	0,98	10,3	W - 3B	Symmetrical
						0,55	-	-	165,38	128,34	1,29	7,7	Farrel	Cosine
						1	-	-	56806	40861	1,39	17,2	CISE	Test Section
						1	-	-	76,86	77,00	0,99	17,2	$\Delta H(\text{FIAT})$	N° 2
160(16-2-65)	141,7	95,6	24,1	11,9	0,58 - 0,84	0,60	139,33	1,03	135,14	139,62	0,97	4,0	W - 3B	Symmetrical
						0,55	-	-	182,49	149,53	1,22	1,64	Farrel	Cosine
						1	-	-	48420	29062	1,67	11,9	CISE	Test-Section
						1	-	-	90,13	89,72	1,01	11,9	$\Delta H(\text{FIAT})$	N° 2
69(16-2-65)	139,7	95,8	45,7	7,2	0,58 - 0,75	0,59	170,89	1,02	166,10	175,54	0,96	-3,4	W - 3B	Symmetrical
						0,55	-	-	213,76	183,68	1,16	-5,6	Farrel	Cosine
						1	-	-	42021	18927	2,22	7,2	CISE	Test Section
						1	-	-	112,75	110,20	1,02	7,2	$\Delta H(\text{FIAT})$	N° 2
40(17-2-65)	141,2	142,4	8,5	12,9	0,69 - 0,9	0,62	125,13	1,02	122,43	115,58	1,06	7,4	W - 3B	Symmetrical
						0,55	-	-	187,41	127,16	1,47	5,7	Farrel	Cosine
						1	-	-	62599	42742	1,46	12,9	CISE	Test Section
						1	-	-	60,95	76,29	0,80	12,9	$\Delta H(\text{FIAT})$	N° 2

TABLE VII - (Follows)

- 15% < DNB QUALITY < + 15%

RUN Nº	PRESSURE ata	MASS FLOW RATE $\frac{g}{cm^2 sec}$	INLET SUBCOOLING °C	EXIT QUALITY %	DNB-FIELD (Z/L) MEASURED	(Z/L) DNB PR DICTEC	4" DNB ED W/cm ²	F	PREDICTED 4" DNB W/cm ²	MEASURED 4" DNB W/cm ²	R DNB	DNB QUALITY %	CORRELATION	AXIAL FLUX DISTRIBUTION
188(16-2-65)	141,7	142,9	12,1	10,3	0,66 - 0,92	0,62	136,28	1,03	132,15	158,05	0,96	4,8	W - 3B	Symmetrical
						0,55	-	-	199,31	151,86	1,31	2,6	Ferrel	Cosine
						1	-	-	55385	37936	1,46	10,3	CISE	Test Section
						1	-	-	73,60	91,13	0,81	10,3	$\Delta H(FIAT)$	Nº 2
141(16-2-65)	141,7	142,6	26,5	6,3	0,56 - 0,80	0,60	159,47	1,02	156,15	174,80	0,89	-0,1	W - 3B	Symmetrical
						0,55	-	-	221,75	167,21	1,18	-2,1	Ferrel	Cosine
						1	-	-	45595	24308	1,87	6,3	CISE	Test-Section
						1	-	-	94,71	112,32	0,84	6,3	$\Delta H(FIAT)$	Nº 2
120(16-2-65)	143,0	139,8	45,5	1,4	0,62 - 0,75	0,62	186,65	1,02	182,45	203,33	0,90	-5,9	W - 3B	Symmetrical
						0,55	-	-	251,07	223,71	1,12	-9,1	Ferrel	Cosine
						-	-	-	-	-	-	-	CISE	Test Section
						1	-	-	119,06	134,22	0,89	1,4	$\Delta H(FIAT)$	Nº 2
98(16-2-55)	139,0	140,7	46,6	1,4	0,58 - 0,75	0,62	191,55	1,02	187,54	206,54	0,91	-6,1	W - 3B	Symmetrical
						0,55	-	-	259,08	227,24	1,14	-9,2	Ferrel	Cosine
						-	-	-	-	-	-	-	CISE	Test Section
						1	-	-	124,52	136,34	0,91	1,4	$\Delta H(FIAT)$	Nº 2
124(25-12-64)	131,3	85,5	61,7	20,2	0,80 - 0,88	0,61	169,47	1,02	166,33	182,07	0,91	13,1	W - 3B	UPWARD Skewed
						0,71	-	-	181,93	209,13	0,87	4,5	Ferrel	asymmetrical
						1	-	-	26143	21290	1,22	20,2	CISE	sine test
						1	-	-	134,84	122,90	1,09	20,2	$\Delta H(FIAT)$	section N° 2B
132(29-12-64)	131,7	86,5	62,4	19,6	0,8 - 0,9	0,81	170,36	1,02	16,53	182,07	0,91	2,8	W - 3B	Upward skewed
						0,71	-	-	182,28	209,13	0,87	4,1	Ferrel	asymmetrical
						1	-	-	26014	21291	1,22	19,6	CISE	sine test sec-
						1	-	-	134,42	122,90	1,09	19,6	$\Delta H(FIAT)$	tion N° 2 B

TABLE VII - (Follows)

-15% < DNB QUALITY <+ 15%

RUN Nº	PRESSURE ata	MASS FLOW RATE $\text{g}/\text{cm}^2 \cdot \text{sec}$	INLET SUBCOO- LING °C	EXIT QUALITY %	DNB-FIELD (Z/L) MEASURED	(Z/L)DNB PREDICTED	$q''_{\text{DNB,EU}}$ W/cm^2	β	PREDICTED q''_{DNB} W/cm^2	MEASURED q''_{DNB} W/cm^2	R DNB	DNB QUALITY %	CORRELATION	AXIAL FLUX DISTRIBUTION
41(22-12-64)	131,3	94,0	60,0	18,1	0,80-0,88	0,81	174,51	1,02	170,35	187,22	0,91	11,5	W - 3B	Upward skewed
						0,71	-	-	187,85	215,05	0,87	3,4	Ferrel	asymmetrical
						1	-	-	26121	20852	1,25	18,1	CISE	sine test
						1	-	-	138,66	126,42	1,09	18,1	$\Delta H(\text{FIAT})$	section N° 2B
57(22-12-64)	131,7	94,3	61,8	17,5	0,80-0,88	0,81	176,67	1,02	172,69	189,94	0,91	11	W - 3B	Upward skewed
						0,71	-	-	189,59	217,02	0,87	2,7	Ferrel	asymmetrical
						1	-	-	26016	20731	1,25	17,5	CISE	sine test
						1	-	-	139,18	127,53	1,09	17,5	$\Delta H(\text{FIAT})$	section N° 2B
172(18-12-64)	131,7	95,2	105,6	10,1	0,80-0,85	0,81	231,09	1,03	223,23	233,59	0,95	1,4	W - 3B	Upward skewed
						0,71	-	-	236,81	268,32	0,88	-8,6	Ferrel	asymmetrical
						4	-	-	19621	10844	1,81	10,1	CISE	sine test
						1	-	-	172,87	157,68	1,09	10,1	$\Delta H(\text{FIAT})$	Section N° 2B
159(18-12-64)	133,0	95,0	109,5	8,2	0,73-0,85	0,81	239,24	1,04	230,98	233,59	0,99	-0,5	W - 3B	Upward skewed
						0,71	-	-	239,69	268,32	0,89	-0,1	Ferrel	asymmetrical
						1	-	-	17998	8854	2,03	8,2	CISE	sine test
						1	-	-	175,19	157,68	1,11	8,2	$\Delta H(\text{FIAT})$	section N° 2B
115(29-12-64)	132,3	98,7	60,6	15,4	0,80-0,90	0,81	181,98	1,03	177,11	187,82	0,95	9,3	W - 3B	Upward skewed
						0,71	-	-	192,01	215,05	0,89	1,4	Ferrel	asymmetrical
						1	-	-	25503	19189	1,33	15,4	CISE	sine test
						1	-	-	141,42	126,38	1,12	15,4	$\Delta H(\text{FIAT})$	section N° 2B
105(29-12-64)	132,3	98,8	60,9	15,2	0,80-0,90	0,81	182,72	1,03	177,54	187,22	0,95	9,1	W - 3B	Upward skewed
						0,71	-	-	192,39	215,05	0,89	1,3	Ferrel	asymmetrical
						1	-	-	25507	19060	1,33	16,2	CISE	SINE TEST
						1	-	-	140,91	126,38	1,11	15,2	$\Delta H(\text{FIAT})$	Section n° 2B

TABLE VII - (Follows)

- 15% < DNB QUALITY < + 15%

RUN N°	PRESSURE ata	MASS FLOW RATE $\frac{g}{cm^2 sec}$	INLET SUB- COOLING °C	EXIT QUALITY %	DNB-FIELD (Z/L) MEASURED	(Z/L)DNB PREDICTED	$Q''_{DNB,EU}$ $\frac{cm^2}{cm}$	F	PREDICTED q''_{DNB} $\frac{cm^2}{cm}$	MEASURED q''_{DNB} $\frac{cm^2}{cm}$	R R_{DNB}	DNB QUALITY %	CORRELATION	AXIAL FLUX DISTRIBUTION
95(23-12-64)	132,3	113,5	58,5	11,7	0,76 - 0,90	0,81	194,33	1,02	189,51	194,09	0,98	6,3	W - 38	Upward skewed
						0,71	-	-	203,54	222,94	0,91	-0,7	Ferrel	asymmetrical
						1	-	-	24809	17101	1,45	11,7	CISE	sine test
						1	-	-	148,20	131,01	1,13	11,7	ΔH (FIAT)	section N° 2B
83(23-12-64)	131,3	113,8	59,2	11,5	0,80 - 0,90	0,81	197,50	1,03	192,08	194,09	0,99	5,9	W - 38	Upward skewed
						0,71	-	-	205,70	222,94	0,92	1,1	Ferrel	asymmetrical
						1	-	-	24399	15745	1,55	11,5	CISE	sine test
						1	-	-	149,81	131,01	1,14	11,5	ΔH (FIAT)	section n° 2B
59(29-12-64)	131,3	126,4	59,0	10,4	0,75 - 0,88	0,81	202,50	1,03	197,25	209,55	0,94	5,0	W - 38	Upward skewed
						0,71	-	-	216,45	240,70	0,90	1,7	Ferrel	asymmetrical
						1	-	-	24663	16997	1,45	10,4	CISE	sine test
						1	-	-	157,38	141,45	1,11	10,4	ΔH (FIAT)	section n° 2B
74(23-12-64)	131,3	126,6	50,0	9,9	0,76 - 0,90	0,81	205,35	1,02	200,79	209,55	0,96	4,5	W - 38	Upward skewed
						0,71	-	-	217,98	240,70	0,90	-2,3	Ferrel	asymmetrical
						1	-	-	23865	15574	1,53	9,9	CISE	sine test
						1	-	-	158,59	141,45	1,12	9,9	ΔH (FIAT)	section n° 2B
64(11-12-64)	131,7	142,6	5,9	17,4	0,82 - 1	0,81	144,55	0,99	145,72	123,57	1,18	13,5	W - 38	Upward skewed
						0,71	-	-	161,94	142,05	1,14	10,8	Ferrel	asymmetrical
						1	-	-	37340	28604	1,32	17,4	CISE	sine test
						1	-	-	101,65	83,48	1,22	17,4	ΔH (FIAT)	section n° 2B
48(11-12-64)	131,7	139,2	8,8	17,2	0,84 - 1	0,81	146,44	0,99	146,74	128,82	1,14	13,4	W - 38	Upward skewed
						0,71	-	-	163,45	147,97	1,10	9,5	Ferrel	asymmetrical
						1	-	-	36354	27856	1,30	17,2	CISE	sine test
						1	-	-	103,16	86,95	1,19	17,2	ΔH (FIAT)	section n° 2B

TABLE VII - (Follows)

- 15% < DNB QUALITY < + 15%

RUN N°	PRESSURE ata	MASS FLOW RATE $\text{kg}/\text{cm}^2 \cdot \text{sec}$	INLET SUBCOO- LING °C	EXIT QUALITY %	DNB-FIELD (Z/L) MEASURED	(Z/L)DNB PREDICTED	$q''_{\text{DNB,EU}}$ W/cm^2	F	PREDICTED q''_{DNB} W/cm^2	MEASURED q''_{DNB} W/cm^2	R DNB	DNB QUALITY %	CORRELATION	AXIAL FLUX DISTRIBUTION
149(9-12-64)	130,3	141,5	12,9	16,1	0,80 - 0,99	0,81	135,75	1,00	153,75	139,13	1,10	12,5	W - 3B	Upward skewed
						0,71	-	-	170,27	159,81	1,06	8,6	Ferrel	asymmetrical
						1	-	-	35653	27292	1,31	16,1	CISE	sine test
						1	-	-	111,80	93,94	1,19	16,1	$\Delta H(\text{FIAT})$	section n° 2B
167(10-12-64)	131,3	141,4	13,4	15,7	0,80 - 1	0,81	154,27	1,01	153,36	137,38	1,12	12,1	W - 3B	Upward skewed
						0,71	-	-	139,90	157,84	1,06	8,2	Ferrel	asymmetrical
						1	-	-	34455	26172	1,32	15,7	CISE	sine test
						1	-	-	112,76	92,75	1,19	15,7	$\Delta H(\text{FIAT})$	section n° 2B
156(9-12-64)	131,3	141,6	13,7	16,1	0,80 - 0,97	0,81	152,91	1,00	152,91	140,85	1,08	12,5	W - 3B	Upward skewed
						0,71	-	-	170,33	161,78	1,05	8,4	Ferrel	asymmetrical
						1	-	-	34777	27077	1,28	16,1	CISE	sine test
						1	-	-	111,80	95,07	1,17	16,1	$\Delta H(\text{FIAT})$	section n° 2B
36(11-12-64)	131,3	143,7	16,1	15,0	0,80 - 1	0,81	157,98	1,00	157,98	144,26	1,09	11,5	W - 3B	Upward skewed
						0,71	-	-	174,25	165,73	1,05	7,4	Ferrel	asymmetrical
						1	-	-	34077	26057	1,31	16,1	CISE	sine test
						1	-	-	115,37	97,39	1,18	16,1	$\Delta H(\text{FIAT})$	section n° 2B
31(11-12-64)	130,3	141,6	18,8	14,7	0,80 - 0,97	0,81	161,75	1,01	160,46	149,43	1,07	11,2	W - 3B	Upward skewed
						0,71	-	-	177,39	171,35	1,03	6,9	Ferrel	asymmetrical
						1	-	-	33541	25343	1,32	14,7	CISE	sine test
						1	-	-	119,57	100,67	1,18	14,7	$\Delta H(\text{FIAT})$	section n° 2B
34(7-12-64)	129,7	140,4	21,4	13,9	0,80 - 0,90	0,81	166,01	1,01	163,88	152,87	1,07	10,6	W - 3B	Upward skewed
						0,71	-	-	180,39	175,59	1,02	6,2	Ferrel	asymmetrical
						1	-	-	32811	24417	1,34	13,9	CISE	sine test
						1	-	-	123,06	103,22	1,19	13,9	$\Delta H(\text{FIAT})$	section n° 2B

TABLE VII - (Follows)

- 15% < DNB QUALITY <+ 15%

RUN N°	PRESSURE ata	MASS FLOW RATE $\frac{\text{g}}{\text{cm sec}}$	INLET SUB- COOLING °C	EXIT QUALITY %	DNB-FIELD (Z/L) MEASURED	(Z/L) DNB PREDICTED	$q''_{\text{DNB, EU}}$ $\frac{\text{W}}{\text{cm}^2}$	F	PREDICTED q''_{DNB} $\frac{\text{W}}{\text{cm}^2}$	MEASURED q''_{DNB} $\frac{\text{W}}{\text{cm}^2}$	R q''_{DNB}	DNB QUALITY %	CORRELATION	AXIAL FLUX DISTRIBUTION
61(7-12-64)	132,3	140,7	32,8	10,6	0,80 - 0,90	0,81	183,37	1,03	178,77	164,89	1,08	6,9	W - 3B	Upward skewed
						0,71	-	-	192,21	189,40	1,01	2,1	Ferrel	asymmetrical
						1	-	-	27576	18093	1,52	10,6	CISE	sine test
						1	-	-	134,26	11,34	1,20	10,6	$\Delta H(\text{FIAT})$	section n° 2B
56(7-12-64)	135,0	139,2	41,1	9,5	0,80 - 0,90	0,81	193,01	1,03	188,05	178,63	1,05	5,3	W - 3B	Upward skewed
						0,71	-	-	201,79	205,19	0,98	0,1	Ferrel	asymmetrical
						1	-	-	25899	17022	1,52	9,5	CISE	sine test
						1	+	-	142,88	120,58	1,18	9,5	$\Delta H(\text{FIAT})$	section n° 2B
162(10-12-64)	131,3	139,0	43,4	9,9	0,80 - 0,94	0,81	195,32	1,02	190,91	187,22	1,02	5,5	W - 3B	Upward skewed
						0,71	-	-	203,22	215,05	0,96	0,0	Ferrel	asymmetrical
						1	-	-	26429	17840	1,48	9,9	CISE	sine test
						1	-	-	147,32	126,38	1,16	9,9	$\Delta H(\text{FIAT})$	section n° 2B
49(7-12-64)	131,3	140,1	50,2	7,2	0,80 - 0,90	0,81	211,57	1,02	207,39	190,65	1,09	2,7	W - 3B	Upward skewed
						0,71	-	-	215,97	218,99	0,99	-2,8	Ferrel	asymmetrical
						1	-	-	22749	12359	1,84	7,2	CISE	sine test
						1	-	-	155,68	128,39	1,20	7,2	$\Delta H(\text{FIAT})$	section n° 2B
147(10-12-64)	131,3	140,2	50,7	7,2	0,80 - 0,93	0,81	211,82	1,02	207,63	192,37	1,08	2,7	W - 3B	Upward skewed
						0,71	-	-	216,78	220,97	0,98	-2,8	Ferrel	asymmetrical
						1	-	-	22749	12472	1,82	7,2	CISE	sine test
						1	-	-	156,36	129,85	1,20	7,2	$\Delta H(\text{FIAT})$	section n° 2B
130(10-12-64)	132,3	140,0	54,7	6,5	0,80 - 0,93	0,81	215,54	1,02	211,99	199,24	1,06	2,0	W - 3B	Upward skewed
						0,71	-	-	220,61	228,86	0,96	-3,8	Ferrel	asymmetrical
						1	-	-	21147	11062	1,91	6,5	CISE	sine test
						1	-	-	159,76	134,49	1,18	5,5	$\Delta H(\text{FIAT})$	section n° 2B

TABLE VII (Follows) - 15% < DNB QUALITY <+ 15%

RUN N°	PRESSURE ata	MASS FLOW RATE $\text{g}^2/\text{cm sec}$	INLET SUBCOO- LING °C	EXIT QUALITY %	DNB-FIELD (Z/L) MEASURED	(Z/L)DNB PREDICTED	$q''_{\text{DNB,EU}}/ \text{cm}^2$	F	PREDICTED $q''_{\text{DNB}}/ \text{cm}^2$	MEASURED $q''_{\text{DNB}}/ \text{cm}^2$	R q''_{DNB}	DNB QUALITY %	CORRELATION	AXIAL FLUX DISTRIBUTION
48(4-12-64)	130,2	141,3	60,4	4,4	0,82 - 0,90	0,81	232,42	1,01	229,09	202,67	1,13	- 0,2	W - 38	Upward skewed
						0,71	-	-	232,18	282,18	1,00	- 6,1	Farrel	asymmetrical
						1	-	-	18837	8218	2,3	4,4	CISE	sine test
						1	-	-	159,07	136,81	1,23	4,4	ΔH(FIAT)	section N° 28
121(10-12-64)	131,3	141,3	61,3	4,9	0,80 - 0,93	0,81	229,83	1,03	223,27	207,83	1,07	0,1	W - 38	Upward skewed
						0,71	-	-	232,07	238,73	0,97	- 6,0	Farrel	asymmetrical
						1	-	-	19957	8920	2,2	4,9	CISE	sine test
						1	-	-	169,11	140,29	1,20	4,9	ΔH(FIAT)	section n° 28
36(4-12-64)	131,3	141,4	61,5	3,5	0,82 - 0,90	0,81	235,71	1,01	233,86	200,96	1,16	- 1,0	W - 38	Upward skewed
						0,71	-	-	232,40	230,83	1,01	- 6,9	Farrel	symmetrical
						1	-	-	17017	6750	2,58	3,6	CISE	sine test
						1	-	-	159,37	135,65	1,25	3,5	ΔH(FIAT)	section n° 28
107(10-12-64)	132,3	139,2	54,7	5,3	0,74 - 0,93	0,81	228,28	1,03	221,89	216,42	1,02	0,3	W - 38	Upward skewed
						0,71	-	-	233,60	248,60	0,94	- 6,1	Farrel	asymmetrical
						1	-	-	19740	9628	2,0	5,3	CISE	sine test
						1	-	-	170,51	146,1	1,17	5,3	ΔH(FIAT)	section n° 28
94(10-12-64)	132,3	142,2	74,9	2,2	0,80 - 0,93	0,81	251,30	1,00	251,30	228,44	1,1	- 3,1	W - 38	Upward skewed
						0,71	-	-	250,56	262,40	0,95	- 9,7	Farrel	asymmetrical
						1	-	-	14687	4413	3,3	2,2	CISE	sine test
						1	-	-	184,05	154,25	1,19	2,2	ΔH(FIAT)	section n° 28
39(4-12-64)	131,3	142,9	77,0	0,6	0,60 - 0,90	0,81	262,17	1,00	262,17	225,00	1,16	- 4,5	W - 38	Upward skewed
						0,71	-	-	255,72	258,45	0,99	- 11,1	Farrel	symmetrical
						-	-	-	-	-	-	-	CISE	sine test
						-	-	-	-	-	-	-	ΔH(FIAT)	section n° 28

TABLE VII - (Follows) -15% < DNB QUALITY < +15%

RUN N°	PRESSURE ata	MASS FLOW RATE $\frac{g}{cm \text{ sec}^2}$	INLET SUBCOO- LING °C	EXIT QUALITY %	DNB-FIELD (Z/L) PREDICTED MEASURED	(Z/L)DNB PREDICTED	$q^*_{\text{BNB,EU}}$ $\frac{\text{W}}{\text{cm}^2}$	F	PREDICTED q^*_{DNB} $\frac{\text{W}}{\text{cm}^2}$	MEASURED q^*_{DNB} $\frac{\text{W}}{\text{cm}^2}$	R_{DNB}	DNB QUALITY %	CORRELATION	AXIAL FLUX DISTRIBUTION
79(7-12-64)	131,3	142,8	81,0	-0,06	0,80 - 0,93	0,81	269,6	1,05	256,75	230,16	1,11	- 5,6	W - 38	Upward skewed
						0,71	-	-	261,63	264,37	0,99	-12,2	Farrel	asymmetrical
						-	-	-	-	-	-	-	CISE	sine test
						-	-	-	-	-	-	-	$\Delta H(\text{FIAT})$	section n° 2B
2847(7-12-64)	130,7	142,0	82,4	0,8	0,82 - 0,90	0,81	265,47	1,01	263,41	235,31	1,12	- 4,8	W - 38	Upward skewed
						0,71	-	-	262,14	270,29	0,97	-11,5	Farrel	asymmetrical
						-	-	-	-	-	-	-	CISE	sine test
						-	-	-	-	-	-	-	$\Delta H(\text{FIAT})$	section n° 2B
15(9-12-64)	131,7	142,9	94,1	-2,4	0,79 - 0,84	0,81	291,07	1,05	277,21	249,05	1,11	- 8,5	W - 38	Upward skewed
						0,71	-	-	279,92	286,08	0,98	-15,6	Farrel	asymmetrical
						-	-	-	-	-	-	-	CISE	sine test
						-	-	-	-	-	-	-	$\Delta H(\text{FIAT})$	section n° 2B
140(9-12-64)	130,3	136,3	101,8	-0,5	0,79 - 0,84	0,81	288,30	1,02	283,77	264,52	1,07	-7,5	W - 38	Upward skewed
						0,71	-	-	286,94	303,83	0,94	-15,4	Farrel	asymmetrical
						-	-	-	-	-	-	-	CISE	sine test
						-	-	-	-	-	-	-	$\Delta H(\text{FIAT})$	section n° 2B
131(9-12-64)	131,3	141,8	111,8	-3,6	0,80 - 0,85	0,81	314,04	1,05	299,08	281,69	1,06	-10,8	W - 38	Upward skewed
						0,71	-	-	305,59	323,56	0,94	-18,9	Farrel	asymmetrical
						-	-	-	-	-	-	-	CISE	sine test
						-	-	-	-	-	-	-	$\Delta H(\text{FIAT})$	section n° 2B
122(9-12-64)	132,8	141,4	121,1	-5,3	0,79 - 0,84	0,81	328,73	1,04	316,08	293,71	1,07	-12,8	W - 38 @	Upward skewed
						0,71	-	-	316,26	337,38	0,94	-21,3	Farrel	asymmetrical
						-	-	-	-	-	-	-	CISE	sine test
						-	-	-	-	-	-	-	$\Delta H(\text{FIAT})$	section n° 2B

TABLE VII - (Follows) - $15\% < \text{DNB QUALITY} < + 15\%$

RUN N°	PRESSURE ata	MASS FLOW RATE $\frac{\text{g}}{\text{cm sec}}$	INLET SUB- COOLING °C	EXIT QUALITY %	DNB-FIELD (Z/L) PREDICTED	(Z/L)DNB MEASURED	$q''_{\text{DNB,EU}}$ $\frac{\text{W}}{\text{cm}^2}$	F	PREDICTED q''_{DNB} $\frac{\text{W}}{\text{cm}^2}$	MEASURED q''_{DNB} $\frac{\text{W}}{\text{cm}^2}$	R_{DNB}	DNB QUALITY	CORRELATION	AXIAL FLUX DISTRIBUTION
110(9-12-64)	131,3	142,1	132,1	-6,1	0,79 - 0,84	0,85	326,15	1,21	269,72	252,74	1,07	-11,2	W - 3B	Upward skewed
						0,72	-	-	330,03	356,81	0,92	-21,9	Farrel	asymmetrical
						-	-	-	-	-	-	-	CISE	sine test
						-	-	-	-	-	-	-	$\Delta H(\text{FIAT})$	section n° 2B
78(11-12-64)	130,3	185,0	8,3	13,4	0,86 - 1	0,81	161,78	0,99	162,43	140,84	1,16	10,1	W - 3B	Upward skewed
						0,71	-	-	184,81	161,78	1,14	7,1	Farrel	asymmetrical
						1	-	-	37905	15049	2,52	13,4	CISE	sine test
						1	-	-	113,68	95,07	1,18	13,4	$\Delta H(\text{FIAT})$	section n° 2B
77(11-12-64)	129,3	185,9	9,0	12,9	0,79 - 1	0,81	165,62	0,99	166,54	140,84	1,18	9,7	W - 3B	Upward skewed
						0,71	-	-	187,04	161,78	1,16	6,7	Farrel	asymmetrical
						1	-	-	37986	27914	1,36	12,9	CISE	sine test
						1	-	-	115,16	95,07	1,22	12,9	$\Delta H(\text{FIAT})$	section n° 2B
113(11-12-64)	131,3	179,9	51,6	4,3	0,79 - 1	0,81	232,88	1,02	228,16	228,16	1,00	0,2	W - 3B	Upward skewed
						0,71	-	-	246,06	252,40	0,94	-5,1	Farrel	asymmetrical
						1	-	-	19731	10606	1,86	4,3	CISE	sine test
						1	-	-	178,28	154,20	1,15	4,3	$\Delta H(\text{FIAT})$	section n° 2B
88(11-12-64)	131,3	184,0	61,8	1,3	0,73 - 0,91	0,81	258,78	1,01	257,11	245,62	1,05	-3,1	W - 3B	Upward skewed
						0,71	-	-	266,06	282,13	0,94	-8,5	Farrel	asymmetrical
						-	-	-	-	-	-	-	CISE	sine test
						1	-	-	195,67	165,80	1,18	1,3	$\Delta H(\text{FIAT})$	section n° 2B
89(11-12-64)	132,3	185,5	64,2	0,6	0,79 - 0,88	0,81	262,88	0,99	264,22	250,77	1,05	-3,7	W - 3B	Upward skewed
						0,71	-	-	269,14	288,05	0,93	-9,3	Farrel	asymmetrical
						-	-	-	-	-	-	-	CISE	sine test
						1	-	-	198,61	169,87	1,14	0,6	$\Delta H(\text{FIAT})$	section n° 2B

TABLE VII - (Follows) - 15% < DNB QUALITY < + 15%

RUN N°	PRESSURE ata	MASS FLOW RATE $\frac{g}{cm^2 sec}$	INLET SUBCOOL LING $^{\circ}C$	EXIT QUALITY %	DNB -FIELD (Z/L) MEASURED	(Z/L)DNB PREDICTED	$q''_{DNB, EU}$ $^2/cm$	F	PREDICTED q''_{DNB} $^2 w/cm$	MEASURED q''_{DNB} $^2 w/cm$	R DNB	DNB QUALITY	CORRELATION	AXIAL FLUX DISTRIBUTION
22(21-12-64)	131,3	185,9	105,2	-6,9	0,79 - 0,85	0,81	352,23	1,12	314,49	322,90	0,97	-13,3	W - 3B	Upward skewed
						0,71	-	-	344,32	370,91	0,93	-20,4	Ferrel	asymmetrical
						-	-	-	-	-	-	-	CISE	sine test
						-	-	-	-	-	-	-	ΔH (FIAT)	section n° 2B
13(29-12-64)	131,3	230,1	4,1	11,8	0,88 - 1	0,81	166,57	0,98	170,59	135,69	1,26	8,7	W - 3B	Upward skewed
						0,71	-	-	194,96	155,86	1,25	6,3	Ferrel	asymmetrical
						1	-	-	40632	29670	1,37	11,8	CISE	sine test
						1	-	-	110,54	91,59	1,21	11,8	ΔH (FIAT)	section n° 2B
6(23-12-64)	131,3	230,4	4,4	11,6	0,88 - 1	0,81	167,69	0,98	171,03	135,69	1,26	8,6	W - 3B	Upward skewed
						0,71	-	-	195,51	155,86	1,25	6,2	Ferrel	asymmetrical
						1	-	-	40161	29670	1,35	11,6	CISE	sine test
						1	-	-	111,20	91,59	1,21	11,6	ΔH (FIAT)	section n° 2B
86(22-12-64)	132,3	228,6	7,4	11,0	0,85 - 1	0,81	169,92	0,98	172,99	145,99	1,18	8,2	W - 3B	Upward skewed
						0,71	-	-	198,11	157,70	1,18	5,6	Ferrel	asymmetrical
						1	-	-	37637	28685	1,31	11,0	CISE	sine test
						1	-	-	115,60	98,55	1,17	11,0	ΔH (FIAT)	section n° 2B
99(22-12-64)	131,3	229,0	7,5	11,0	0,88 - 1	0,81	172,10	0,98	174,94	146,00	1,20	8,1	W - 3B	Upward skewed
						0,71	-	-	199,59	167,70	1,19	5,5	Ferrel	asymmetrical
						1	-	-	38103	28408	1,34	11,0	CISE	sine test
						1	-	-	117,40	98,55	1,19	11,0	ΔH (FIAT)	section n° 2B
111(21-12-64)	130,3	231,0	63,5	-1,0	0,82 - 0,88	0,81	290,34	0,95	304,29	291,99	1,04	-5,1	W - 3B	Upward skewed
						0,71	-	-	302,87	335,39	0,90	-10,3	Ferrel	asymmetrical
						-	-	-	-	-	-	-	CISE	sine test
						-	-	-	-	-	-	-	ΔH (FIAT)	section n° 2B

TABLE VII - (Follows)

- 15% < DNB QUALITY < + 15%

RUN N°	PRESSURE ata	MASS FLOW RATE $\frac{kg}{cm^2 \cdot sec}$	INLET SUB- COOLING °C	EXIT QUALITY %	DNB -FIELD (Z/L) MEASURED	(Z/L)DNB PREDICTED	$q''_{DNB, EU}$ W/cm^2	F	PREDICTED q''_{DNB} W/cm^2	MEASURED q''_{DNB} W/cm^2	R DNB	DNB QUALITY %	CORRELATION	AXIAL FLUX DISTRIBUTION
17(22-12-64)	132,3	231,2	65	-1,9	0,79 - 0,88	0,81	294,22	0,94	312,96	291,99	1,07	-5,9	W - 3B	Upward skewed
						0,71	-	-	302,41	335,39	0,90	-11,1	Ferrel	asymmetrical
						-	-	-	-	-	-	-	CISE	sine test
						-	-	-	-	-	-	-	$\Delta H(FIAT)$	section n° 28
148(22-12-64)	131,3	308,6	1,2	10,5	0,88 - 1	0,81	176,11	0,94	186,32	140,84	1,32	7,4	W - 3B	Upward skewed
						0,71	-	-	214,85	161,80	1,32	5,6	Ferrel	asymmetrical
						1	-	-	43421	33919	1,28	10,5	CISE	sine test
						1	-	-	110,73	95,07	1,16	10,5	$\Delta H(FIAT)$	section n° 28
136(22-12-64)	131,7	306,1	1,6	10,5	0,88 - 1	0,81	174,64	0,94	185,40	144,28	1,28	7,5	W - 3B	Upward skewed
						0,71	-	-	214,29	165,73	1,29	5,7	Ferrel	asymmetrical
						1	-	-	43477	34229	1,27	10,5	CISE	sine test
						1	-	-	110,85	97,39	1,14	10,5	$\Delta H(FIAT)$	section n° 28
162(22-12-64)	131,7	309,1	1,6	10,4	0,88 - 1	0,81	175,46	0,94	186,24	144,28	1,29	7,5	W - 3B	Upward skewed
						0,71	-	-	215,15	165,72	1,30	5,6	Ferrel	asymmetrical
						1	-	-	43509	34154	1,27	10,4	CISE	sine test
						1	-	-	111,07	97,39	1,14	10,4	$\Delta H(FIAT)$	section n° 28
79(22-12-64)	131,7	312,2	8,8	8,3	0,85 - 1	0,81	191,16	0,95	200,85	175,20	1,15	5,8	W - 3B	Upward skewed
						0,71	-	-	228,59	201,24	1,14	3,6	Ferrel	asymmetrical
						1	-	-	35568	293,33	1,21	8,3	CISE	sine test
						1	-	-	131,00	118,25	1,11	8,3	$\Delta H(FIAT)$	section n° 28
72(22-12-64)	132,7	313,0	9,8	7,9	0,85 - 1	0,81	193,22	0,96	201,51	176,91	1,14	5,5	W - 3B	Upward skewed
						0,71	-	-	229,43	203,22	1,13	3,2	Ferrel	asymmetrical
						1	-	-	33849	27951	1,21	7,9	CISE	sine test
						1	-	-	131,96	119,42	1,10	7,9	$\Delta H(FIAT)$	section n° 28

TABLE VII - (Follows)

- 15% < DNB QUALITY < + 15%

RUN N°	PRESSURE ata	MASS FLOW RATE $\text{g}/\text{cm}^2 \text{sec}$	INLET SUBCOO- LING °C	EXIT QUALITY X	DNB-FIELD (Z/L) PREDICTED MEASURED	(Z/L)DNB PREDICTED	$q''_{\text{DNB,EU}}$ W/cm^3	F	PREDICTED q''_{DNB} W/cm^2	MEASURED q''_{DNB} W/cm^2	R _{DNB}	DNB QUALITY %	CORRELATION	AXIAL FLUX DISTRIBUTION
99(21-12-64)	131,3	315,4	64,2	-4,0	0,79 - 0,82	0,87	322,74	1,22	264,05	250,34	1,02	- 5,7	W - 3B	Upward skewed
						0,71	-	-	353,02	414,33	0,85	-12,6	Ferrel	asymmetrical
						-	-	-	-	-	-	-	CISE	sine test
						-	-	-	-	-	-	-	$\Delta H(\text{FIAT})$	section n° 2B
89(21-12-64)	131,3	314,2	63,3	-4,7	0,79 - 0,82	0,87	330,38	1,17	281,38	257,11	1,09	- 6,3	W - 3B	Upward skewed
						0,71	-	-	356,24	412,35	0,86	-13,3	Ferrel	asymmetrical
						-	-	-	-	-	-	-	CISE	sine test
						-	-	-	-	-	-	-	$\Delta H(\text{FIAT})$	section N°2B
180(23-3-65)	132,3	95,6	11,5	28,5	0,52 - 0,76	0,59	122,50	1,06	115,70	120,32	0,96	20,8	W - 3B	Down skewed
						0,41	-	-	177,85	159,80	1,11	11,5	Ferrel	asymmetrical
						1	-	-	35299	32313	1,09	28,5	CISE	sine test
						1	-	-	97,40	93,91	1,04	28,5	$\Delta H(\text{FIAT})$	section n° 2C
103(23-3-65)	132,3	94,9	19,3	27,5	0,52 - 0,73	0,59	129,17	1,07	120,77	130,72	0,92	19,7	W - 3B	Down skewed
						0,41	-	-	187,15	173,63	1,08	9,5	Ferrel	asymmetrical
						1	-	-	34505	31519	1,09	27,6	CISE	sine test
						1	-	-	104,76	102,062	1,05	27,6	$\Delta H(\text{FIAT})$	section n° 2C
57(23-3-65)	132,3	93,3	45,0	22,6	0,50 - 0,67	0,59	161,43	1,10	146,59	153,59	0,95	13,3	W - 3B	Down skewed
						0,41	-	-	221,77	203,99	1,09	1,1	Ferrel	asymmetrical
						1	-	-	32360	25257	1,28	22,6	CISE	sine test
						1	-	-	125,84	119,92	1,05	22,6	$\Delta H(\text{FIAT})$	section n° 2C
70(24-3-65)	131,7	94,8	146,3	9,1	0,50 - 0,59	0,59	264,30	1,04	273,36	251,64	1,08	-7,0	W - 3B Ⓛ	Down skewed
						0,41	-	-	382,30	334,19	1,14	-26,3	Ferrel	asymmetrical
						1	-	-	25545	10101	2,53	9,1	CISE	sine test
						1	-	-	200,79	195,48	1,02	9,1	$\Delta H(\text{FIAT})$ Ⓛ	section n° 2C

TABLE VII - (Follows) - 15% < DNB QUALITY < + 15%

RUN N°	PRESSURE ata	MASS FLOW rate $\frac{g}{cm \cdot sec}$	INLET SUBCOO LING °C	EXIT QUALITY %	DNB-FIELD (Z/L) PREDICTED	(Z/L)DNB MEASURED	$q^*_{DNB,EU}$ $\frac{W}{cm^2}$	F	PREDICTED q^*_{DNB} $\frac{W}{cm^2}$	MEASURED q^*_{DNB} $\frac{W}{cm^2}$	R DNB	DNB QUALITY %	CORRELATION	AXIAL FLUX DISTRIBUTION
271(23-3-65)	132,6	182,7	4,7	18,1	0,88 - 0,92	0,59	143,74	1,05	137,38	136,66	1,01	12,8	W - 3B	Down skewed
						0,41	-	-	220,67	181,51	1,21	7,4	Ferrel	asymmetrical
					0,52 - 0,79	1	-	-	44301	37945	1,16	18,1	CISE	sine test
						1	-	-	101,43	106,66	0,95	18,1	ΔH (FIAT)	section n° 2C
201(23-3-65)	132,3	181,3	9,1	15,9	0,52 - 0,79	0,57	157,51	1,07	147,26	141,38	1,04	10,5	W - 3B	Down skewed
						0,41	-	-	228,35	183,48	1,24	5,3	Ferrel	asymmetrical
						1	-	-	43037	33597	1,28	15,9	CISE	sine test
						1	-	-	109,81	107,82	1,02	15,9	ΔH (FIAT)	section n° 2C
134(23-3-65)	132,3	180,5	15,9	14,1	0,52 - 0,76	0,57	169,29	1,08	157,06	153,55	1,02	8,7	W - 3B	Down skewed
						0,41	-	-	240,49	139,26	1,21	3,0	Ferrel	asymmetrical
						1	-	-	41042	30414	1,35	14,1	CISE	sine test
						1	+	-	122,47	117,10	1,04	14,1	ΔH (FIAT)	section n° 2C
57(23-3-65)	131,7	178,7	42,3	8,7	0,52 - 0,67	0,59	214,22	1,09	196,85	197,58	0,99	2,5	W - 3B	Down skewed
						0,41	-	-	296,73	262,39	1,13	-5,6	Ferrel	asymmetrical
						1	-	-	34757	19613	1,77	8,7	CISE	sine test
						1	-	-	163,48	154,20	1,06	8,7	ΔH (FIAT)	section n° 2C
182(22-3-65)	131,7	182,1	98,5	-1,2	0,55 - 0,64	0,51	361,94	1,12	323,17	328,58	0,98	-15,6	W - 3B	Down skewed
						0,41	-	-	441,43	390,62	1,13	-22,7	Ferrel	asymmetrical
						-	-	-	-	-	-	-	CISE	sine test
						-	-	-	-	-	-	-	ΔH (FIAT)	section n° 2C
291(23-3-65)	132,3	312,6	4,8	11,0	0,88 - 0,91	0,59	177,83	1,04	171,49	156,89	1,10	7,3	W - 3B	Down skewed
						0,41	-	-	275,72	207,15	1,33	3,6	Ferrel	asymmetrical
					0,52 - 0,79	1	-	-	47341	38417	1,24	11,0	CISE	sine test
						1	-	-	118,99	121,74	0,98	11,0	ΔH (FIAT)	section n° 2C

Table VII - follows

- 15% < DNB QUALITY < + 15%

TABLE VII -Bis.

RUN N°	PRESSURE ata	MASS FLOW RATE $\frac{2}{g/cm \text{ sec}}$	INLET SUBCOO- LING $^{\circ}\text{C}$	EXIT QUALITY %	DNB-FIELD (Z/L) PREDICTED	(Z/L)DNB MEASURED	$q''_{\text{DNB,EU}} \frac{W}{cm^2}$	F	PREDICTED $q''_{\text{DNB}} \frac{W}{cm^2}$	MEASURED $q''_{\text{DNB}} \frac{W}{cm^2}$	R DNB	DNB QUALI- TY	CORRELATION	AXIAL FLUX DISTRIBUTION
79(7-12-64)	131,3	142,8	81,0	- 0,05	0,80 - 0,93	0,81	269,60	0,99	271,58	230,15	1,18	-5,5	W - 3B ++	Upward skewed
						0,81	269,60	1,05	256,76	230,16	1,11	-5,6	W-3B +++	asymmetrical
														sine test
														section n° 2B
15(7-12-54)	131,7	142,9	94,1	- 2,4	0,79 - 0,84	0,81	291,07	0,93	313,58	249,06	1,20	-8,5	W - 3B ++	Upward skewed
						0,81	291,07	1,05	277,21	249,06	1,11	-8,5	W - 3B +++	asymmetrical
														sine test
														section n° 2B
131(9-12-54)	131,3	141,8	111,8	- 3,5	0,80 - 0,85	0,85	298,27	1,05	210,32	220,49	1,24	-8,1	W - 3B ++	Upward skewed
						0,81	314,04	1,05	299,08	281,59	1,05	-10,8	W - 3B +++	asymmetrical
														sine test
														section n° 2B
122(9-12-64)	132,3	141,4	121,1	- 5,2	0,79 - 0,84	0,85	311,58	1,06	294,55	230,15	1,24	-10,0	W - 3B ++	Upward skewed
						0,81	328,73	1,04	310,08	293,72	1,07	-12,8	W - 3B +++	asymmetrical
														sine test
														section n° 2B
182(22-5-55)	131,7	182,1	98,5	-1,2	0,55 - 0,64	0,65	306,90	1,15	257,11	222,89	1,19	-7,8	W - 3B ++	Down skewed
						0,51	361,94	1,12	323,16	328,56	0,96	-15,0	W - 3B +++	asymmetrical
														sine test
														section n° 2C

++ MIT (Bubble detachment point)

+++ Bowring (Bubble detachment point)

TABLE VIII - DNB Quality > 15%

RUN No	Pressure ata	Mass flow rate $\text{g/cm}^2 \text{sec}$	Inlet Subcooling °C	Exit quality %	DNB-Field (Z/L) predicted	(Z/L) DNB predicted	Predicted q''_{DNB} W/cm^2	Measured q''_{DNB} W/cm^2	R R_{DNB}	DNB quality %	Correlation	Axial flux distribution
170 (B-10-64)	127,2	50,2	12,0	35,3	0,84 - 1	0,55	139,50	134,20	1,04	17,5	Ferrel	Symmetrical
						1	55220	47060	1,17	35,3	CISE	Cosine
						1	99,71	80,53	1,23	35,3	ΔH (FIAT)	Test Section
						1	181,24	118,16	1,53	35,3	ΔH (W-2)	n° 2
171 (B-10-64)	124,2	51,4	32,0	34,3	0,84 - 1	0,55	160,93	155,01	0,97	13,5	Ferrel	Symmetrical
						1	55669	46520	1,15	34,3	CISE	Cosine
						1	114,42	99,31	1,15	34,3	ΔH (FIAT)	Test Section
						1	197,20	142,85	1,38	34,3	ΔH (W-2)	n° 2
127 (B-10-64)	125,2	51,3	15,5	36,4	0,94 - 1	0,55	173,00	193,10	0,89	12,0	Ferrel	Symmetrical
					0,63 - 0,65	1	53091	54460	1,05	36,3	CISE	Cosine
						1	118,92	115,82	1,02	36,3	ΔH (FIAT)	Test section
						1	205,02	150,33	1,23	36,3	ΔH (W-2)	n° 2
135 (B-10-64)	125,2	51,8	45,9	35,3	0,94 - 1	0,55	174,20	191,91	0,91	11,27	Ferrel	Symmetrical
					0,33 - 0,35	1	53264	49399	1,08	35,3	CISE	Cosine
						1	119,18	115,15	1,03	35,3	ΔH (FIAT)	Test Section
						1	204,54	153,59	1,25	35,3	ΔH (W-2)	n° 2
120 (17-2-65)	140,2	16,1	2,7	38,0	0,7 - 1	0,55	118,55	107,14	1,11	20,3	Ferrel	Symmetrical
						1	45730	42355	1,08	38,0	CISE	Cosine
						1	77,28	54,28	1,20	38,0	ΔH (FIAT)	Test Section
						1	159,89	102,90	1,55	38,0	ΔH (W-2)	n° 2

+ For CISE Correlation (W)

+ For ΔH (W-2) Correlation (kcal/kg)For ΔH (W-2) correlation all data related to symmetrical cosine heat flux distribution are out of range for equivalent diameter.

For Ferrel's correlation the data are out of range for equivalent diameter and lenght.

TABLE VIII (Follows)

DNB quality > 15%

RUN no	Pressure ata	Mass flow rate $\frac{kg}{cm^2 \cdot sec}$	Inlet Subcooling °C	Exit quality %	DNB-Field (Z/L) predicted	(Z/L) DNB predicted	Predicted q''_{DNB} $\frac{W}{cm^2}$	Measured q''_{DNB} $\frac{W}{cm^2}$	R R_{DNB}	DNB quality %	Correlation	Axial flux distribution
16 (17-2-65)	140,7	46,7	9,3	34,11	0,7 - 0,97	0,55	122,68	113,03	1,08	18,1	Ferrel	Symmetrical
						1	44148	38252	1,15	34,1	CISE	Cosine
						1	85,18	67,82	1,25	34,1	ΔH (FIAT)	Test Section
						1	165,96	107,05	1,55	34,1	ΔH (W-2)	n° 2
176 (16-2-65)	144,7	44,3	29,2	37,65	0,86 - 0,92	0,55	131,35	141,29	0,93	15,7	Ferrel	Symmetrical
						1	38677	41640	0,93	37,6	CISE	Cosine
						1	84,03	84,77	0,99	37,6	ΔH (FIAT)	Test Section
						1	177,79	140,91	1,26	37,6	ΔH (W-2)	n° 2
156 (23-12-64)	131,3	76,0	57,2	27,02	0,8 - 0,9	0,71	165,60	199,26	0,83	9,9	Ferrel	Upward skewed asymmetrical sine
						1	26710	24721	1,08	27,0	CISE	metrical sine
						1	124,79	117,10	1,06	27,0	ΔH (FIAT)	test section
						1	183,36	151,91	1,21	27,0	ΔH (W-2)	n° 2 B
143 (23-12-64)	131,7	73,5	59,8	27,03	0,78 - 0,9	0,71	165,62	199,26	0,83	9,7	Ferrel	Upward skewed
						1	26051	24244	1,07	27,0	CISE	asymmetrical sine
						1	124,79	117,10	1,06	27,0	ΔH (FIAT)	test section
						1	186,42	155,14	1,20	27,0	ΔH (W-2)	n° 2 B
28 (23-12-64)	131,3	94,1	3,8	27,02	0,94 - 1	0,71	134,99	130,22	1,03	16,8	Ferrel	Upward skewed
						1	34888	29430	1,18	27,0	CISE	asymmetrical sine
						1	90,01	76,52	1,17	27,0	ΔH (FIAT)	test section
						1	126,31	79,18	1,59	27,0	ΔH (W-2)	n° 2 B
40 (23-12-64)	132,3	92,7	3,8	27,3	0,85 - 1	0,71	133,53	130,22	1,02	17,1	Ferrel	Upward skewed
						1	34165	29374	1,16	27,3	CISE	asymmetrical sine
						1	90,75	76,52	1,18	27,3	ΔH (FIAT)	test section
						1	126,78	80,4	1,57	27,3	ΔH (W-2)	n° 2 B

TABLE VIII (Follows) DNB Quality > 15%

RUN Nº	Pressure ata	Mass Flow rate $\frac{g}{cm^2 sec}$	Inlet Subcooling °C	Exit quality %	DNB-Field (Z/L) measured	(Z/L) DNB predicted	Predicted q" DNB W/cm^2	Measured q" DNB W/cm^2	R _{DNB}	DNB quality x	Correlation	Axial flux distribution
111(22 12-54)	131,5	94,1	8,4	25,0	0,8 - 1	0,71	138,90	138,0	1,01	15,0	Ferrel	Upward skewed
						1	33488	28884	1,16	26,0	CISE	asymmetrical sine
						1	94,81	81,16	1,16	26,0	ΔH (FIAT)	test section
						1	130,53	84,01	1,55	26,0	ΔH (W-2)	nº 2 B
122 (22-12-54)	132,3	94,0	8,6	25,4	0,8 - 1	0,71	138,20	136,12	1,01	15,3	Ferrel	Upward skewed
						1	33008	28081	1,17	25,4	CISE	asymmetrical sine
						1	95,15	82,02	1,18	25,4	ΔH (FIAT)	test section
						1	129,30	82,85	1,55	25,4	ΔH (W-2)	nº 2 B
72 (11-12-54)	131,3	140,8	3,2	18,2	0,82 - 1	0,71	158,34	134,14	1,16	10,8	Ferrel	Upward skewed
						1	39145	29012	1,35	18,2	CISE	asymmetrical sine
						1	96,07	78,84	1,21	18,2	ΔH (FIAT)	test section
						1	93,93	54,51	1,72	18,2	ΔH (W-2)	nº 2 B
348 (29-3-55)	133,4	93,7	3,8	33,0	0,94 - 1	0,41	155,30	145,70	1,05	15,3	Ferrel	Down skewed
					0,52-0,86	1	35484	30231	0,98	33,0	CISE	asymmetrical sine
						1	88,40	91,59	0,93	33,0	ΔH (FIAT)	test section
						1	124,54	95,22	1,31	33,0	ΔH (W-2)	nº 2 C
241(23-3-55)	132,3	94,5	4,8	31,6	0,52 - 0,91	0,41	169,02	154,60	1,09	14,4	Ferrel	Down skewed
						1	35941	34804	1,03	31,6	CISE	asymmetrical sine
						1	90,56	90,90	0,99	31,6	ΔH (FIAT)	test section
						1	125,04	93,71	1,34	31,6	ΔH(W-2)	nº 2 C
320 (25-3-55)	134,5	94,4	5,8	32,7	0,91 - 1	0,41	158,10	160,59	1,05	12,8	Ferrel	Down skewed
					0,52 - 0,88	1	34777	35583	0,97	32,7	CISE	asymmetrical sine
						1	89,59	94,39	0,95	32,7	ΔH (FIAT)	test section
						1	124,48	98,01	1,27	32,7	ΔH (W-2)	nº 2 C

Table IX. - Comparison of DNB data in square annular test section with DNB correlations-
Heated lenght 560 mm - Nominal pressure 84 ata.

Run	Mass flow rate gr/cm ² sec	Inlet tempera- ture °C	Exit quality %	Measured Values			Calculated DNB Ratios						
				Power kW	Heat flux watt/cm ²	Enthalpy rise Kcal/Kg	W-2q" DNB using D _h	Modified W-2q" DNB	W-2 " DNB using D _h	Modified W-2 " DNB using D _h	"-3q" DNB using D _h	CISE: Imposed Inlet Subcooling	CISE: Imposed Saturation Length
98(10-6-65)	92,4	226,6	4,9	56,7	315,4	102,25			1,84	0,79	0,66	1,18	1,50
79(10-6-65)	153,8	227,9	-2,2	69,2	385	75	0,95	0,855			0,80		
56(10-6-65)	224,1	225,3	-7,9	78,3	435,6	58,24	1,06	0,954			0,69		
25(10-6-65)	395,6	223,1	-13,4	99,7	554,7	42	1,19	1,071			0,78		

Table X. - Comparison of DNB data in square annular test section
with DNB correlations - Heated lenght 560 mm. Nominal
pressure 126 ata.

Run	Mass flow rate gr/cm ² sec	Inlet tempera- ture °C	Exit quality %	Measured Values			Calculated DNB Ratios			
				Power kW	Heat flux watt/cm ²	Enthalpy rise Kcal/kg	W-2q" DNB using D _h	Modified W-2q" DNB	W-3q" DNB using D _h	Modified W-3q" DNB
15(10-9-64)	68,5	275	-1,1	28	156	68,17	1,79	1,611	1,07	1,57
68(15-9-64)	154,1	280,5	-5,1	46,5	259	50,3	1,31	1,179	0,78	1,12
83(15-9-64)	154,1	280,5	-4,9	47	262	50,84	1,28	1,152	0,77	1,10
13(16-9-64)	163,1	276,5	-7,4	47,5	264	48,55	1,35	1,215	0,82	1,16
54(20-5-64)	159,6	246,4	-16	56	312	58,47	1,45	1,305		
50(16-9-64)	155,8	240,6	-18,7	55	306	58,85	1,59	1,431		
65(16-9-64)	157,4	234	-21,3	55,5	309	58,79	1,64	1,476		
36(29-7-64)	156,6	177	-37,1	71	396	75,56	1,77	1,593		
28(16-9-64)	271,5	280,5	-12	50,5	281	31	1,59	1,431	0,99	1,39
35(21-5-64)	273,6	255,6	-19,4	63	354	38,39	1,62	1,458		
47(16-9-64)	271,4	241	-24,5	68,5	382	42,1	1,66	1,494		
103(30-7-64)	271,9	197	-33,4	106	590	65	1,38	1,242		
80(29-7-64)	271,1	181,3	-42,1	93	518	57,18	1,72	1,548		
100(29-7-64)	405,6	184,5	-44,7	113,5	632	46,65	1,75	1,575		

Table XI. - Comparison of DNB data in square annular test section with
DNB correlations - Heated lenght 560 mm. Nominal Pressure 132 atm.

Run	Mass flow rate gr/cm ² sec	Inlet tempera- ture °C	Exit quality %	Measured Values			Calculated DNB Ratio							
				Power kW	Heat flux watt/cm ²	Enthalpy rise Kcal/kg	W-2q" DNB using D _h	Modified W-2q" DNB using D _h	W-2 R _{DNB} using D _h	Modified W-2 R _{DNB} using D _h	W-3q" DNB using D _h	Modified W-3q" DNB using D _h	CISE: Imposed Inlet Subcooling	CISE: Imposed Saturation Length
125(1-6-65)	94,0	328,3	15,5	26,6	148	47,19			2,03	0,91	0,71	1,30	0,77	0,74
107(1-6-65)	91,9	324,4	19,1	27,7	154,1	50,27			2,04	0,91	0,72	1,30	0,82	0,79
167(3-6-65)	97,1	302,3	6,1	35,6	198	61,14			1,86	0,80	0,70	1,10	1,09	1,23
30(25-5-65)	90,7	300	8,5	37	205,8	68,03			1,79	0,78	0,66	1,06	1,02	1,06
101(3-6-65)	94,3	273,5	-1,2	43,3	240,9	76,56	1,25	1,125			0,71	1,04		
79(1-6-65)	93,9	257,2	-6,4	44,8	249,2	57	1,37	1,233			0,77			
50(4-6-65)	88,7	234,6	-9,5	50	278,2	93,92	1,36	1,224			0,76			
42(8-6-65)	93,4	197,9	-21,8	57,7	321	103	1,50	1,35						
87(7-6-65)	92,9	170,6	-30,1	60,8	339	109,07	1,64	1,476						
15(1-6-65)	156,1	328,7	9,2	26,2	145,7	27,97			2,04	0,89	0,86		0,96	0,95
100(1-6-65)	151,3	325,4	9,0	30,4	169,1	33,50			1,85	0,81	0,74		0,94	0,92
142(3-6-65)	159,1	307,1	1,2	38,4	213,6	40,23			1,81	0,77	0,75	1,12	1,26	1,79
82(26-5-65)	148,3	302,1	2,1	42,4	235,9	47,65			1,72	0,73	0,67	1,01	1,17	1,47
44(26-5-65)	156,9	281,2	-6,6	47,6	264,8	50,57	1,30	1,17			0,77	1,10		
61(3-6-65)	153,7	278,2	-6,9	48,6	270,4	52,72	1,29	1,161			0,76	1,08		
81(3-6-65)	154,5	276,1	-7,9	48,7	270,9	52,54	1,32	1,188			0,78	1,11		
54(1-6-65)	161,3	270,2	-9,9	51	283,7	52,7	1,34	1,206			0,80			
35(4-6-65)	155,4	227,9	-22,0	59,4	330,5	63,72	1,55	1,395						
36(4-6-65)	155,7	226,6	-24,7	60	333,8	64,22	1,58	1,422						
24(8-6-65)	154,9	200,3	-31,8	68	378,3	73,19	1,61	1,449						

Table XI. - Follows

Run	Mass flow rate gr/cm ² sec	Inlet tempera- ture °C	Exit quality %	Measured Values			Calculated DNB Ratio							
				Power kW	Heat flux watt/cm ²	Enthalpy Rise Kcal/kg	W-2q" DNB using D _h	Modified W-2q" DNB	W-2 E _{DNB} using D _h	Modified W-2 q ⁴ DNB using D _h	W-3q" DNB using D _h	Modified W-3q" DNB using D _h	CISE: Imposed Inlet Subcooling	CISE: Imposed Saturation Length
72(7-6-65)	153,6	174,8	-39,3	72	400,6	78,15	1,73	1,557						
114(1-6-65)	213,2	328	7,1	30,4	169,1	23,77			1,64	0,71	0,88		1	1
91(1-6-65)	221,9	321,5	3,9	34,4	191,4	25,85			1,65	0,71	0,78		1,14	1,24
121(3-6-65)	231,2	306,6	-2,7	42	233,7	30,28	1,32	1,188			0,82	1,19		
94(26-5-65)	211,8	294,5	-5,1	50,8	282,6	38,29	1,23	1,107			0,73	1,05		
39(3-6-65)	222,9	276,1	-11,8	55,9	311	41,81	1,36	1,224			0,82	1,15		
34(1-6-65)	222,5	262,6	-16,2	60,8	338,3	45,56	1,41	1,269						
21(4-6-65)	231,1	228,1	-28,8	71,3	396,7	51,42	1,60	1,44						
12(8-6-65)	224,1	197,9	-37,5	81	450,6	60,24	1,64	1,476						
62(7-6-65)	210,4	170,6	-44,8	87,1	484,6	69,01	1,69	1,521						
110(1-6-65)	394,9	327,8	4,5	33	183,6	13,93					0,89		0,99	0,98
119(26-5-65)	418,5	306,6	-5,0	56,8	316	22,63	1,31	1,179			0,79	1,13		
106(3-6-65)	410,5	306,6	-5,9	54	300,4	21,93	1,40	1,26			0,84	1,20		
107(26-5-65)	394,9	293,8	-9,1	66	367,2	27,86	1,30	1,17			0,79	1,12		
23(3-6-65)	393,7	280,5	-13,8	72,9	405,6	30,87	1,36	1,224			0,76	1,06		
15(3-6-65)	392,8	281,5	-13,4	77	428,4	32,68	1,28	1,152			0,78	1,09		
21(31-5-65)	398,3	263,3	-19,6	84,8	471,8	35,49	1,38	1,242						
12(4-6-65)	397,6	233,6	-30,7	96	534,1	40,25	1,54	1,386						
64(4-6-65)	401,9	195,5	-41,9	113	628,7	46,87	1,64	1,476						
53(7-6-65)	398,1	174,4	-49,1	127,5	709,4	53,39	1,61	1,449						

Table XII - Comparison of D NB data in square annular test section with DNB correlations - Heated lenght 1183 mm - Nominal pressure 84 ata.

Run	Mass flow rate gr/cm ² sec	Inlet temperatu re °C	Exit quality %	Measured Values			Calculated DNB Ratios						
				Power kW	Heat flux watt/cm ²	Enthalpy rise Kcal/Kg	W-2q" DNB using D _h	Modified W-2q" DNB	W-2 H DNB using D _h	Modified W-2 H DNB using D _h	W-3q" DNB using D _h	CISE: Imposed Inlet Subcooling	CISE: Imposed Saturation Lenght
193(29-7-65)	91,9	260,3	13,6	51,1	134,7	92,67			1,82	1,05	0,84	1,14	1,25
152(29-7-65)	93,2	226,6	8,5	62,8	165,5	112,3			1,68	0,95	1,23	1,23	1,64
112(29-7-65)	92,8	199,3	2,9	69	181,8	123,9						1,33	2,60
65(29-7-65)	92,5	171,8	-0,3	79,2	208,7	142,6	0,86	0,774					
184(29-7-65)	154,2	259,5	8,0	68,5	180,5	74,05			1,61	0,91	1,07	1,19	1,39
144(29-7-65)	153,1	231	2,1	79,6	209,8	86,68			1,58	0,87	1,06	1,32	2,20
101(29-7-65)	154,9	197,2	-3,9	95,2	250,9	102,48	0,80	0,72					
63(29-7-65)	155,5	171,3	-8,4	106,5	280,7	114,2	0,83	0,747					
175(29-7-65)	222,3	260	5,4	85,5	225,3	64,12			1,43	0,80	0,92	1,17	1,34
133(29-7-65)	222,1	232	0,3	106	279,3	79,57			1,36	0,75	0,82	1,24	1,85
89(29-7-65)	227,0	202	-6,7	119,3	-314,4	87,6	0,76	0,684					
58(29-7-65)	222,5	172,5	-11,4	137,1	-361,3	102,7	0,77	0,693					
163(29-7-65)	397,1	261,5	2,1	121,1	-319,1	50,8					0,78	1,07	1,15
121(29-7-65)	394,3	234,9	-4,6	139,9	-368,7	59,15	0,70	0,63				0,83	
73(29-7-65)	399,8	199,8	-13,0	164,4	433,3	68,57	0,79	0,711					
49(29-7-65)	397,4	173,4	-18,3	186	492,3	78,37	0,81	0,729					

Table XIII-Comparison of DNB data in square annular test section with DNB Correlations - Heated Length 1183 mm - Nominal Pressure 132 atu.

Run	Mass flow rate gr/cm ² sec	Inlet Temperature °C	Exit Quality %	Measured Values			Calculated DNB Ratio							
				Power kW	Heat flux watt/cm ²	Enthalpy rise Kcal/kg using D _h	W-2q" DNB	Modified W-2q" DNB	W-2 R _{DNB} using D _h	Modified W-2 R _{DNB}	W-3q" DNB using D _h	Modified W-3q" DNB	CISE: Imposed Inlet Subcooling	CISE: Imposed Saturation Length
171(28-7-65)	91,8	321,5	21,1	39,4	103,8	71,54			1,46	0,87			0,70	0,63
145(28-7-65)	91,9	289,7	14,8	54,8	144,4	99,41			1,28	0,74	0,82	1,49	0,90	0,79
159(13-7-65)	93,6	257,7	3,5	59,4	156,5	105,78			1,39	0,77	1,04		1,29	4,21
104(28-7-65)	92,4	231,5	1,0	70,8	186,6	127,80			1,28	0,70	0,95		1,17	2,42
113(13-7-65)	92,9	227,4	-0,5	71,9	189,5		0,90	0,81			1,05			
100(28-7-65)	93,4	223,5	-2,5	72,2	190,3		0,92	0,828			1			
76(28-7-65)	93,3	198,6	-3,8	84,6	222,9		0,85	0,765						
36(29-7-65)	92,7	172,3	-5,5	96,2	253,5		0,80	0,72						
163(28-7-65)	152,0	323,2	15,1	47,5	125,2	52,09			1,23	0,71	0,85		0,75	0,69
123(28-7-65)	152,5	294,5	5,3	62	163,4	67,8			1,25	0,70	0,91	1,41	1,09	1,26
147(15-7-65)	154,0	263,3	-4,3	72,1	190		0,92	0,828			1,05			
101(13-7-65)	155,2	229,5	-12,4	87,8	231,4		0,94	0,846			1,08			
64(28-7-65)	155,7	196,2	-17,4	109	287,2		0,87	0,783						
13(29-7-65)	154,7	173,2	-26,1	109,8	289,4		1	0,9						
154(28-7-65)	222,6	320,8	8,7	53,4	140,7	40			1,08	0,61	0,91		0,92	0,88
111(28-7-65)	219,0	297,1	1,1	70	184,5	53,29			1,15	0,63	0,94	1,40	1,19	1,75
128(13-7-65)	222,7	263,8	-8,3	89,3	235,3		0,88	0,792			1,02			
88(13-7-65)	224,7	227,9	-16,2	107,6	283,6		0,94	0,846						
50(28-7-65)	224,4	199,8	-23,8	126,8	334,17		0,91	0,819						
186(28-7-65)	222,9	174,8	-36,3	119,3	314,4		1,15	1,035						
149(28-7-65)	395,1	321,8	4,9	63,1	166,3						0,95		0,99	0,98
108(28-7-65)	387,9	300	-2,2	92,1	242,7		0,82	0,738			0,92	1,34		
124(13-7-65)	403,0	257,7	-15,7	127,1	334,9		0,91	0,819						
92(28-7-65)	396,9	234,9	-21,9	146,3	385,5		0,92	0,828						
76(13-7-65)	397,9	233,1	-24,1	144,2	380		0,96	0,864						
25(13-7-65)	399,8	199,6	-34,4	160,6	423,2		1,05	0,945						
182(28-7-65)	397,9	174,8	-40,8	179,8	473,8		1,05	0,945						

TABLE XIV - GENERAL DATA OF THE NORMAL UNIT CELL.
DNB RATIOS CALCULATED BY q'' (W-2) AND W-3 CORRELATIONS
WITH MEMORY EFFECT METHOD.

Correlation	-	q'' (W-2)	q'' (W-3)
Pressure	ata	131,70	131,70
Coolant mass velocity	$g/sec.cm^2$	150,70	150,70
Inlet enthalpy	Kcal/Kg	310,20	310,20
Equivalent diameter	mm	11,58	11,58
Flow area	mm^2	94,60	94,60
DNB Position	Z/L	0,71	0,81
Critical enthalpy	Kcal/Kg	347,40	355,20
DNB ratio	-	1,75	1,35

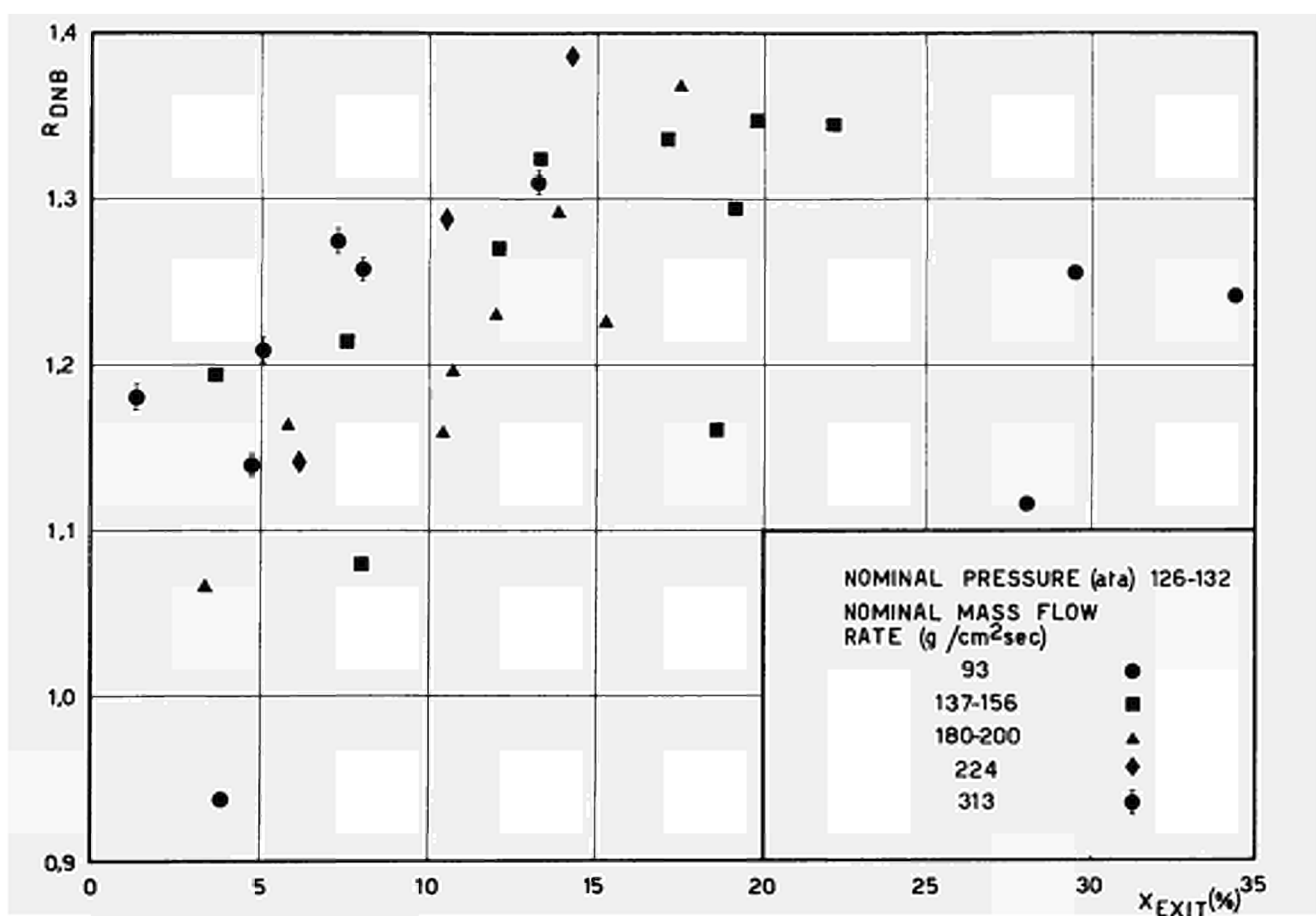
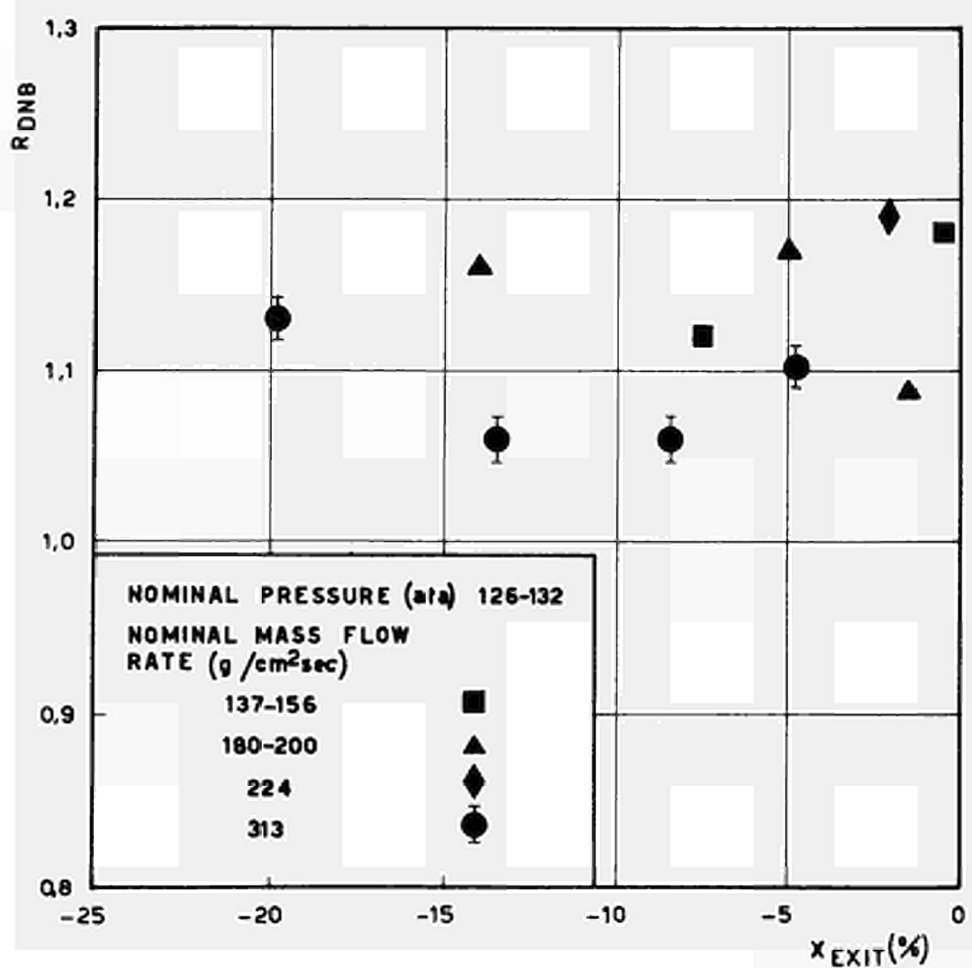


Fig. 1 and 2



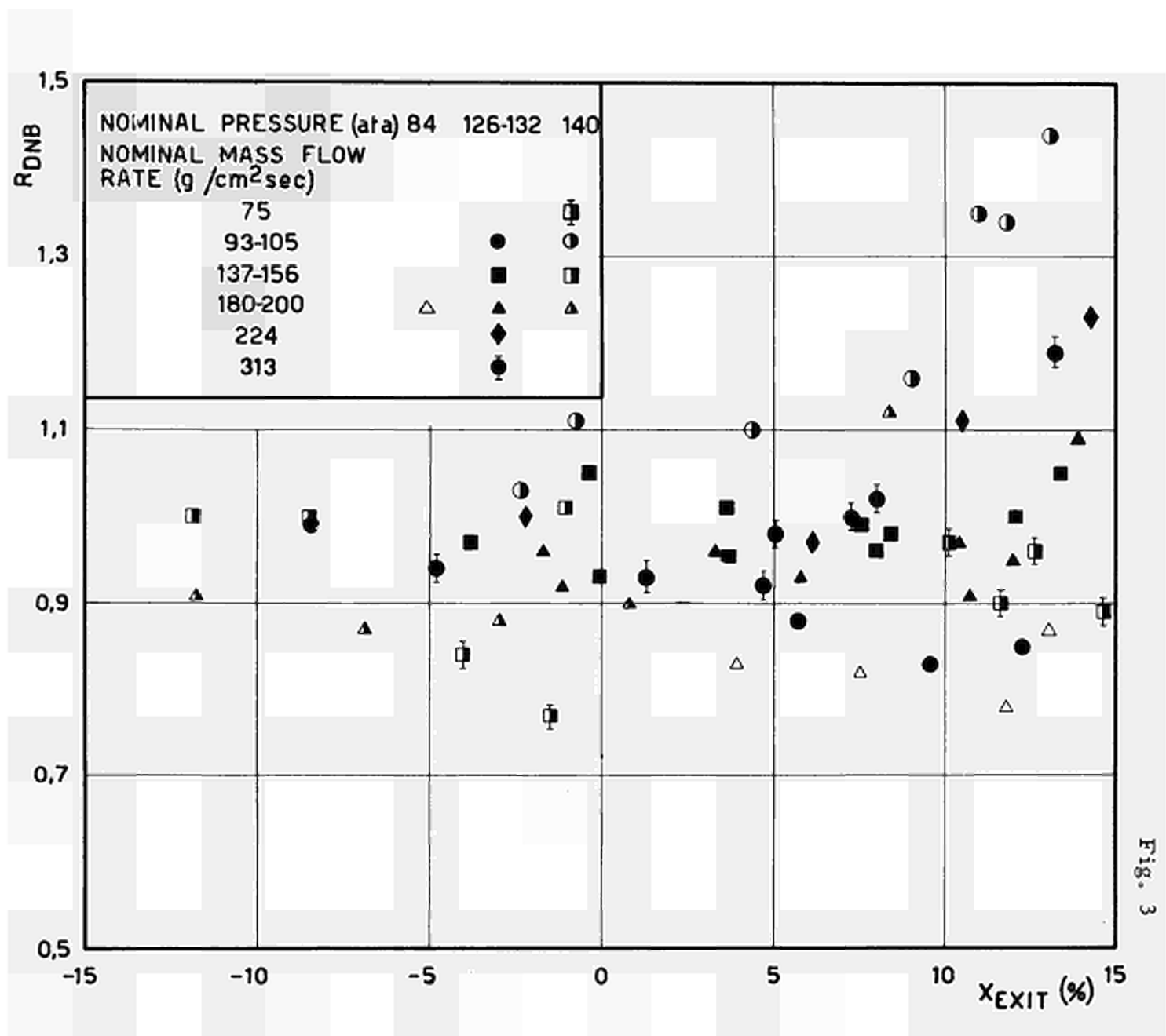
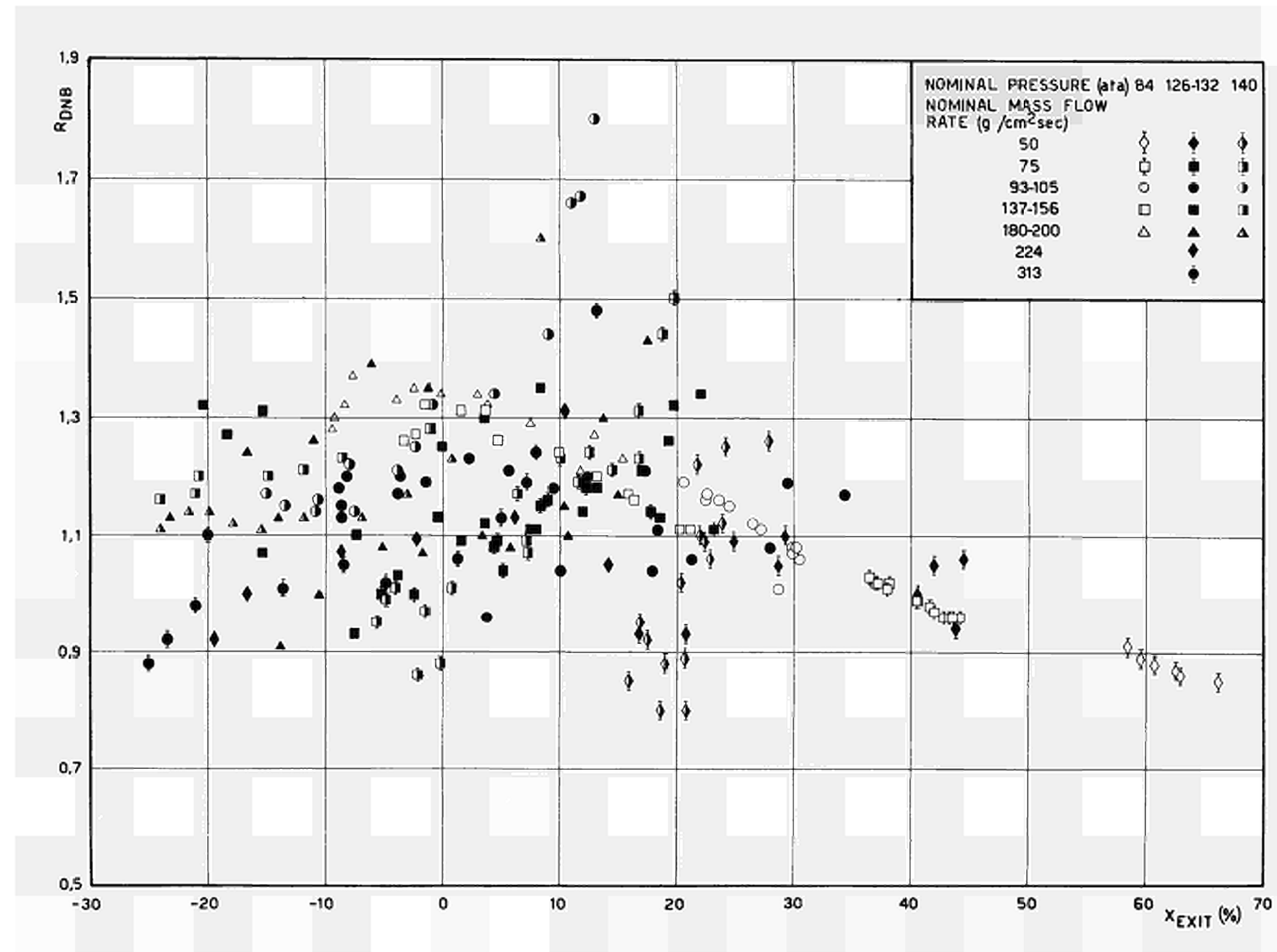


Fig. 4



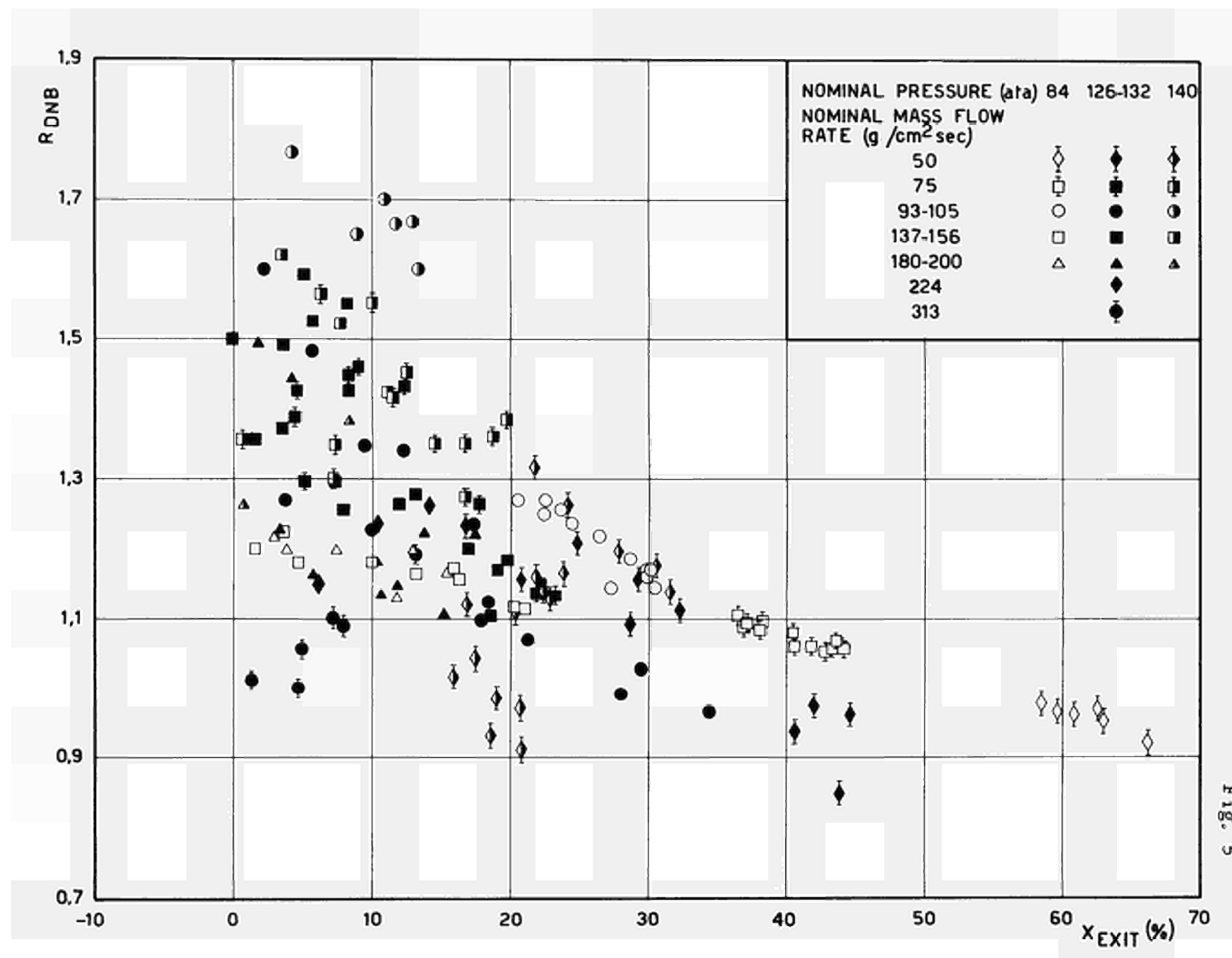


Fig. 6

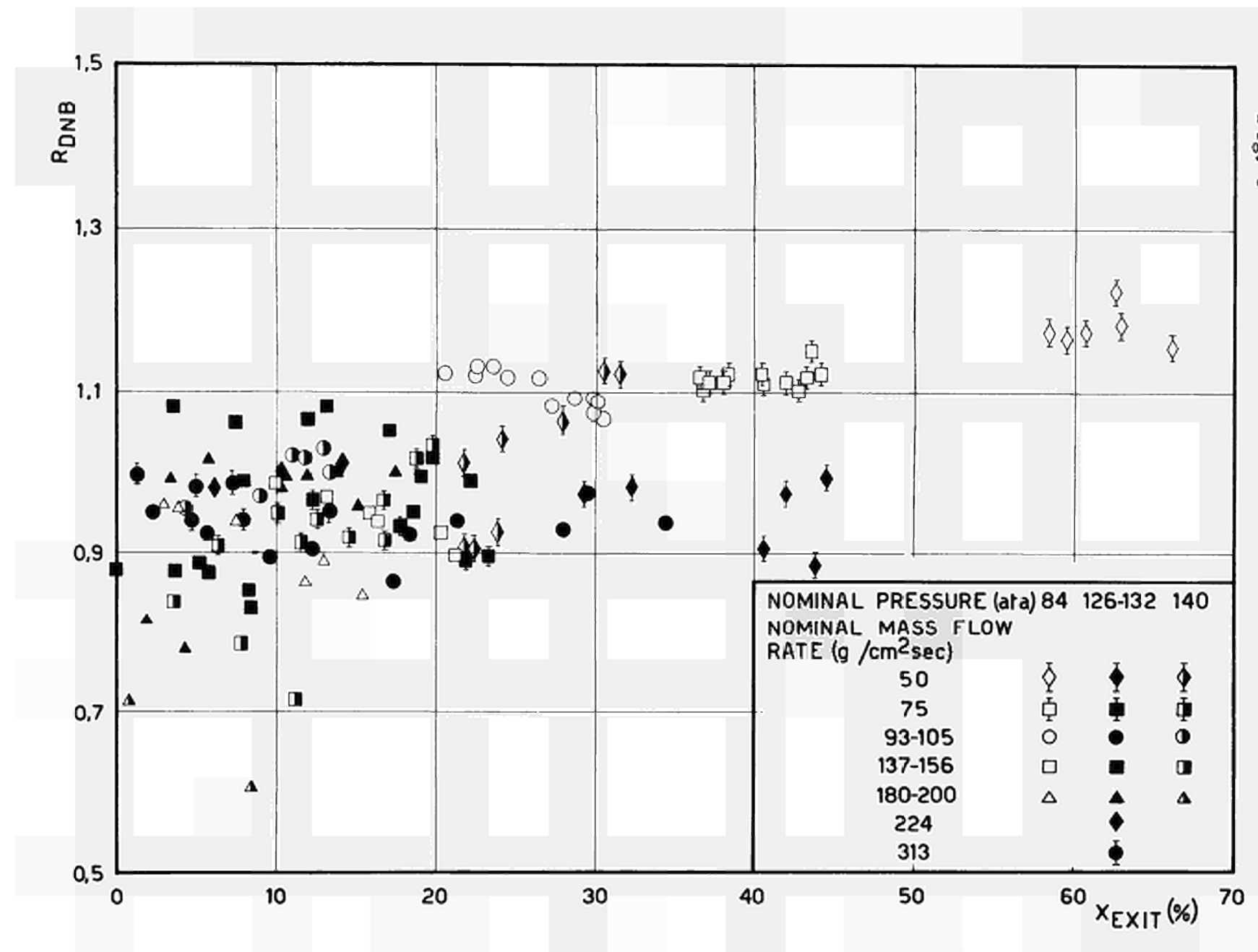


Fig. 7

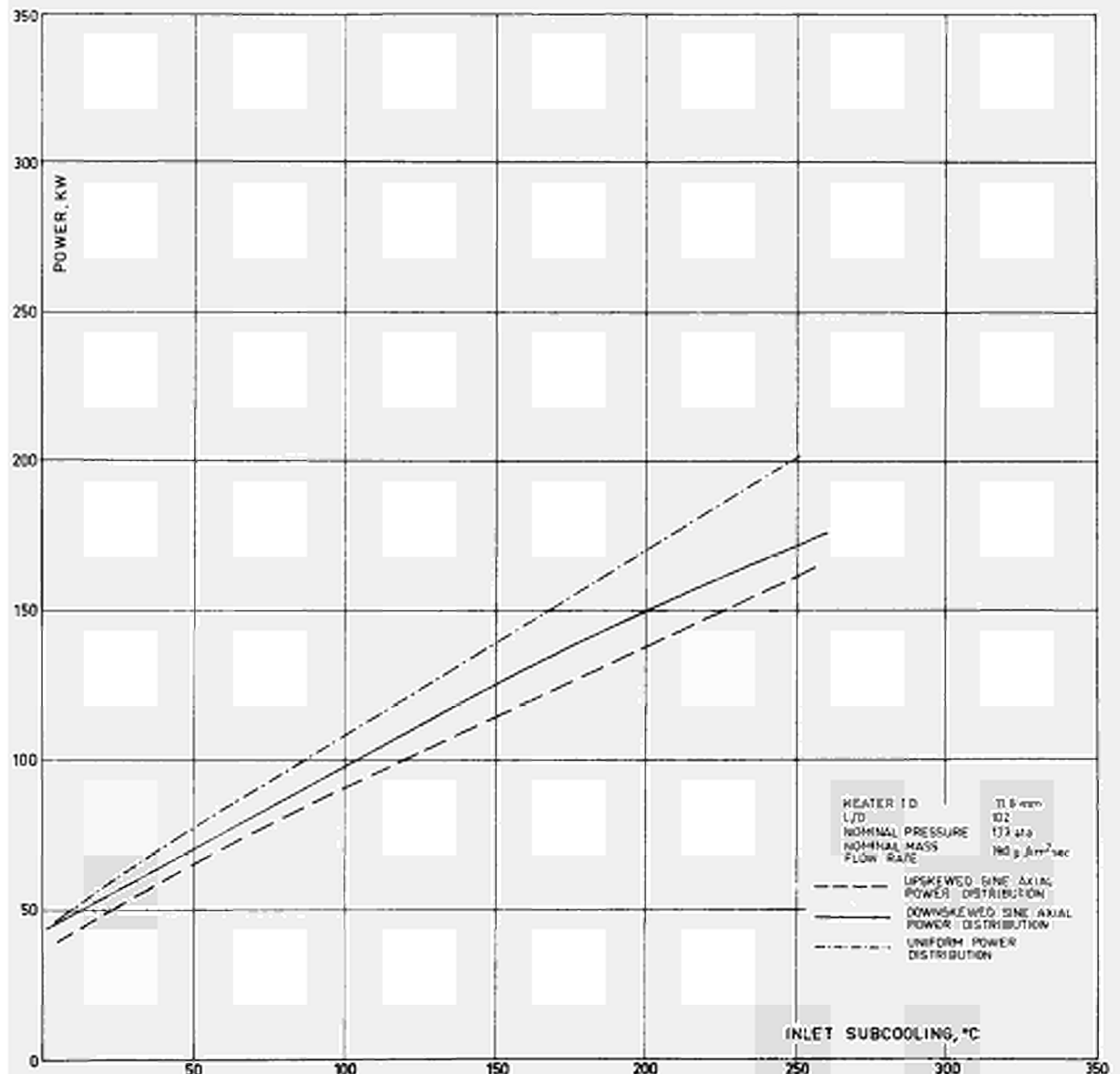


Fig. 8

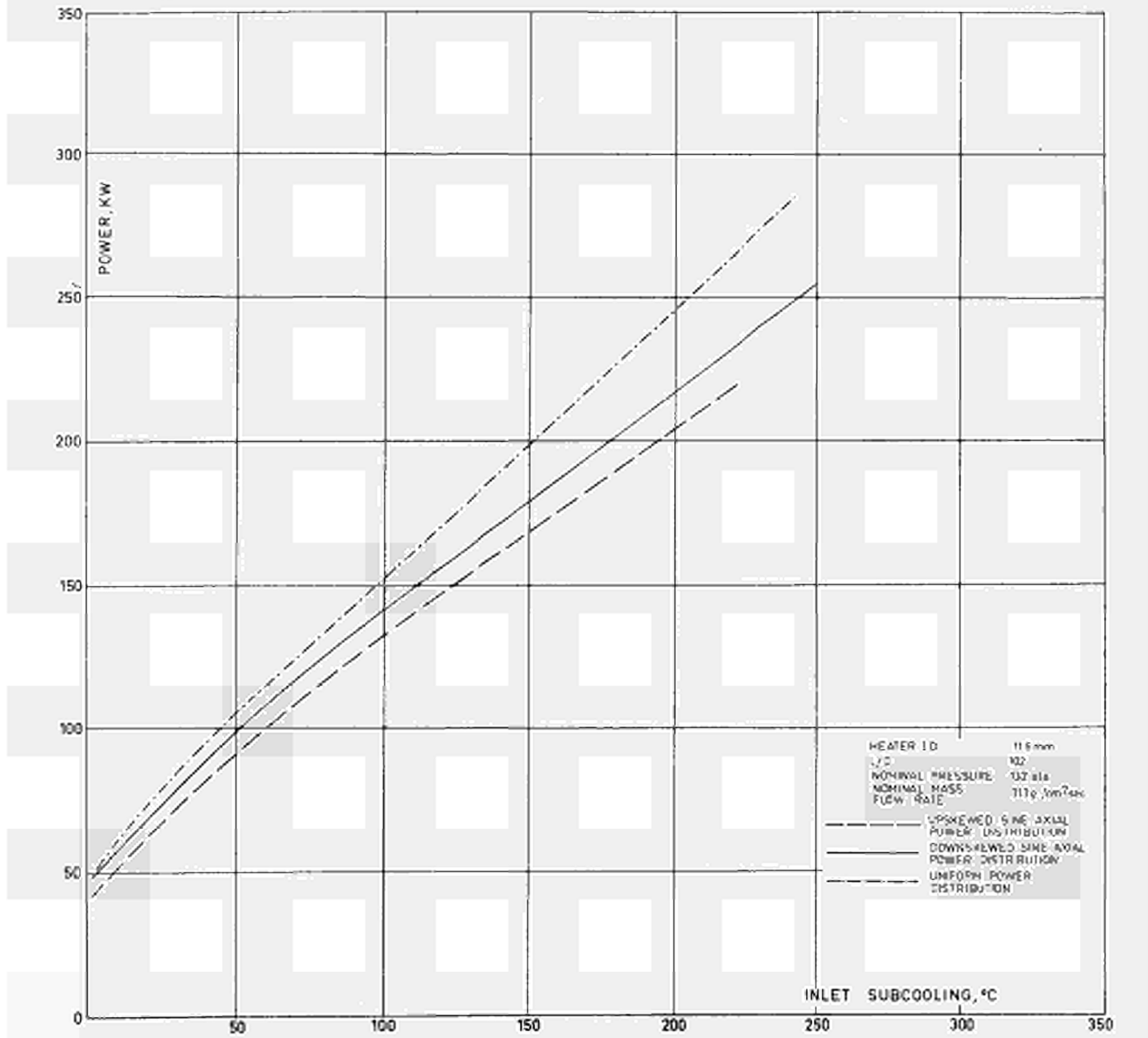
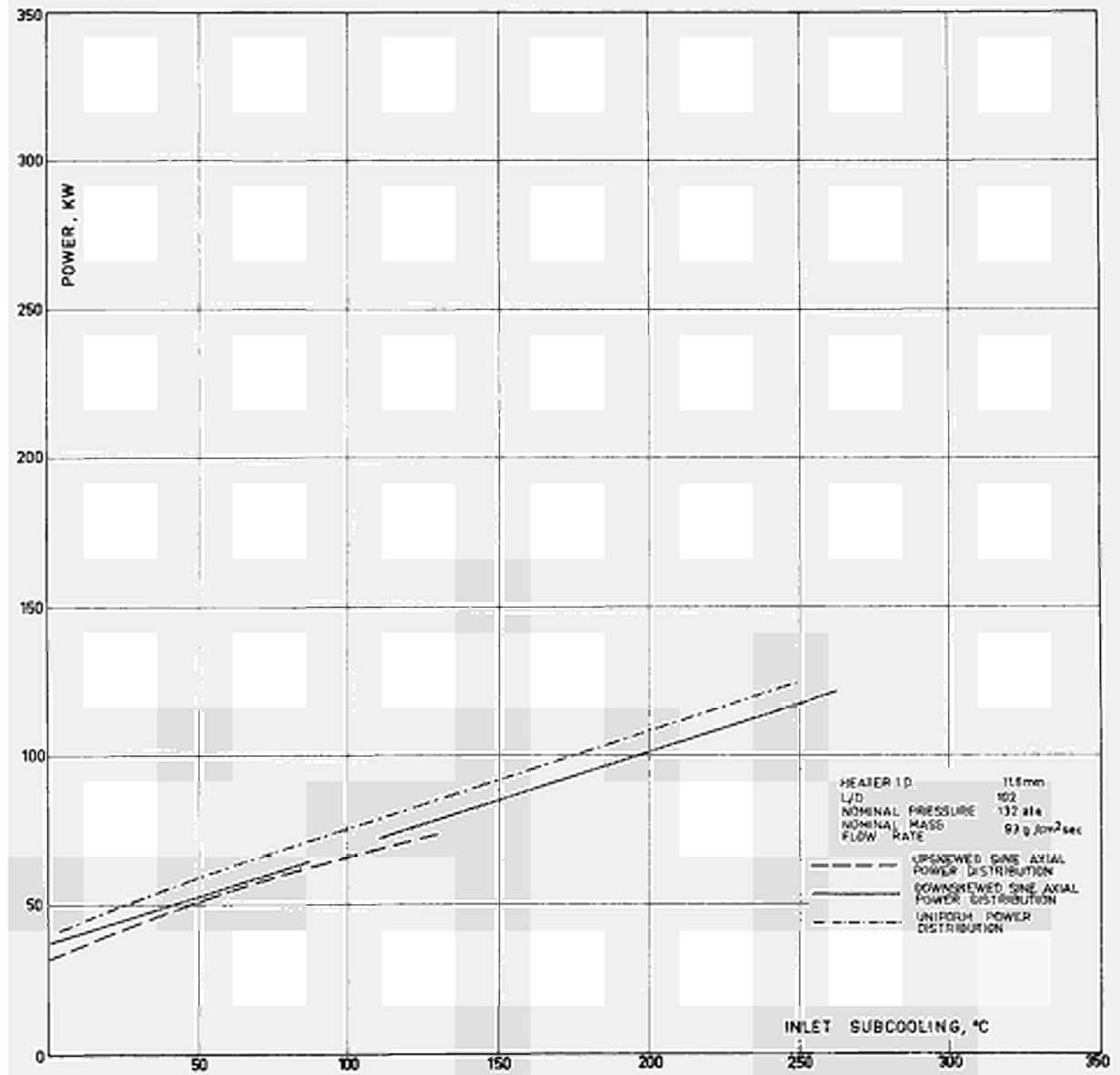


Fig. 9



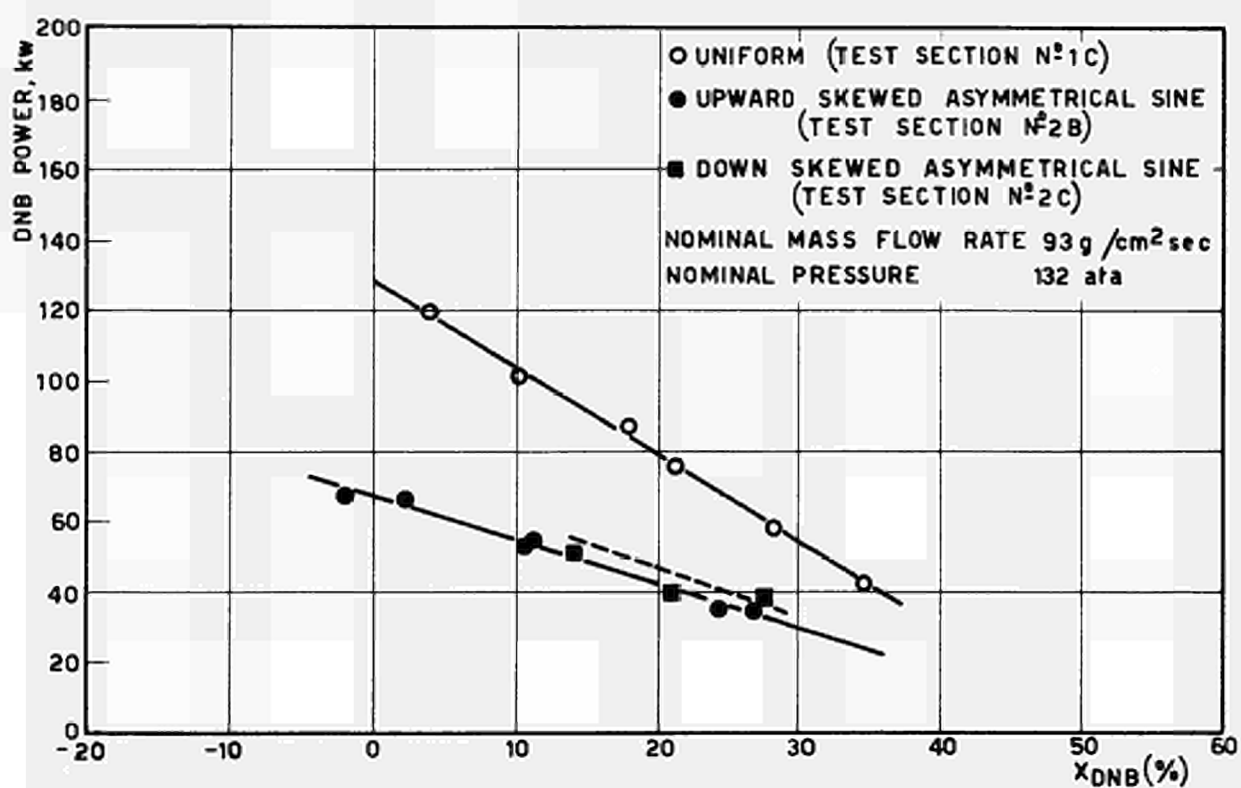


Fig. 10

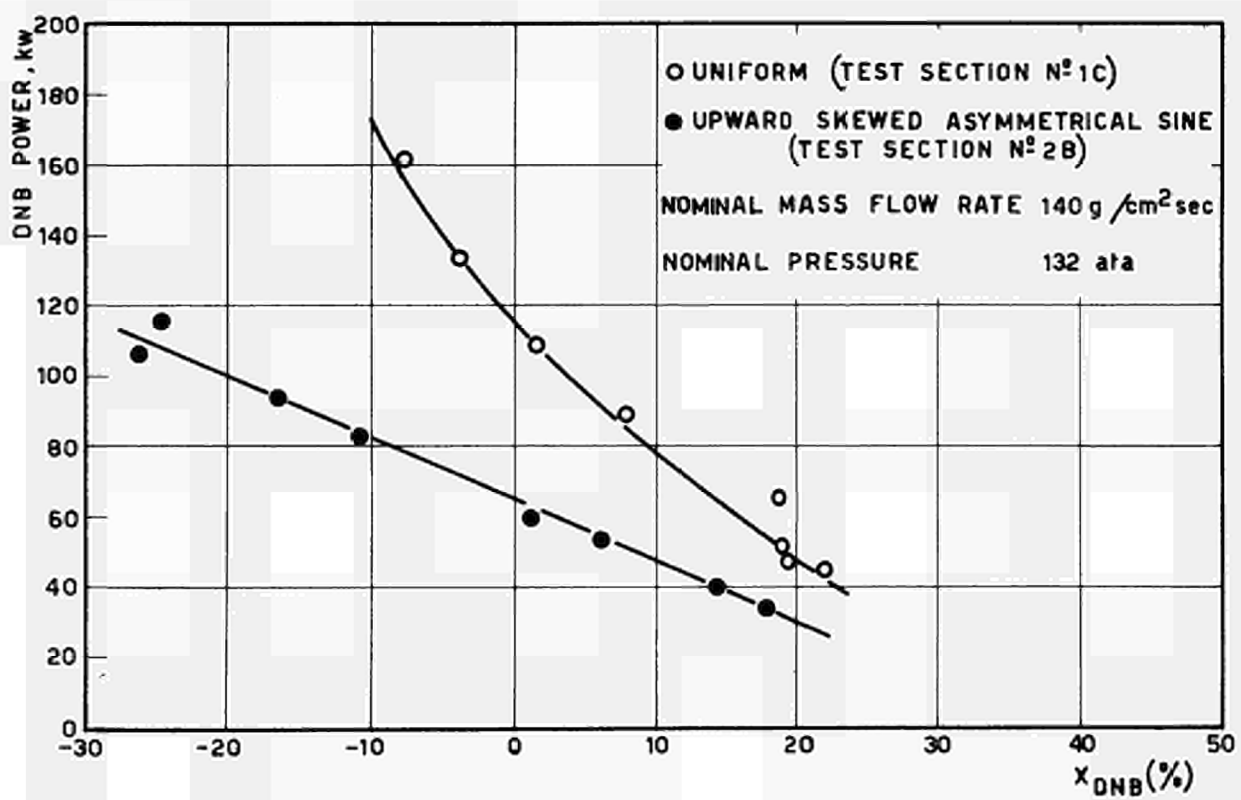
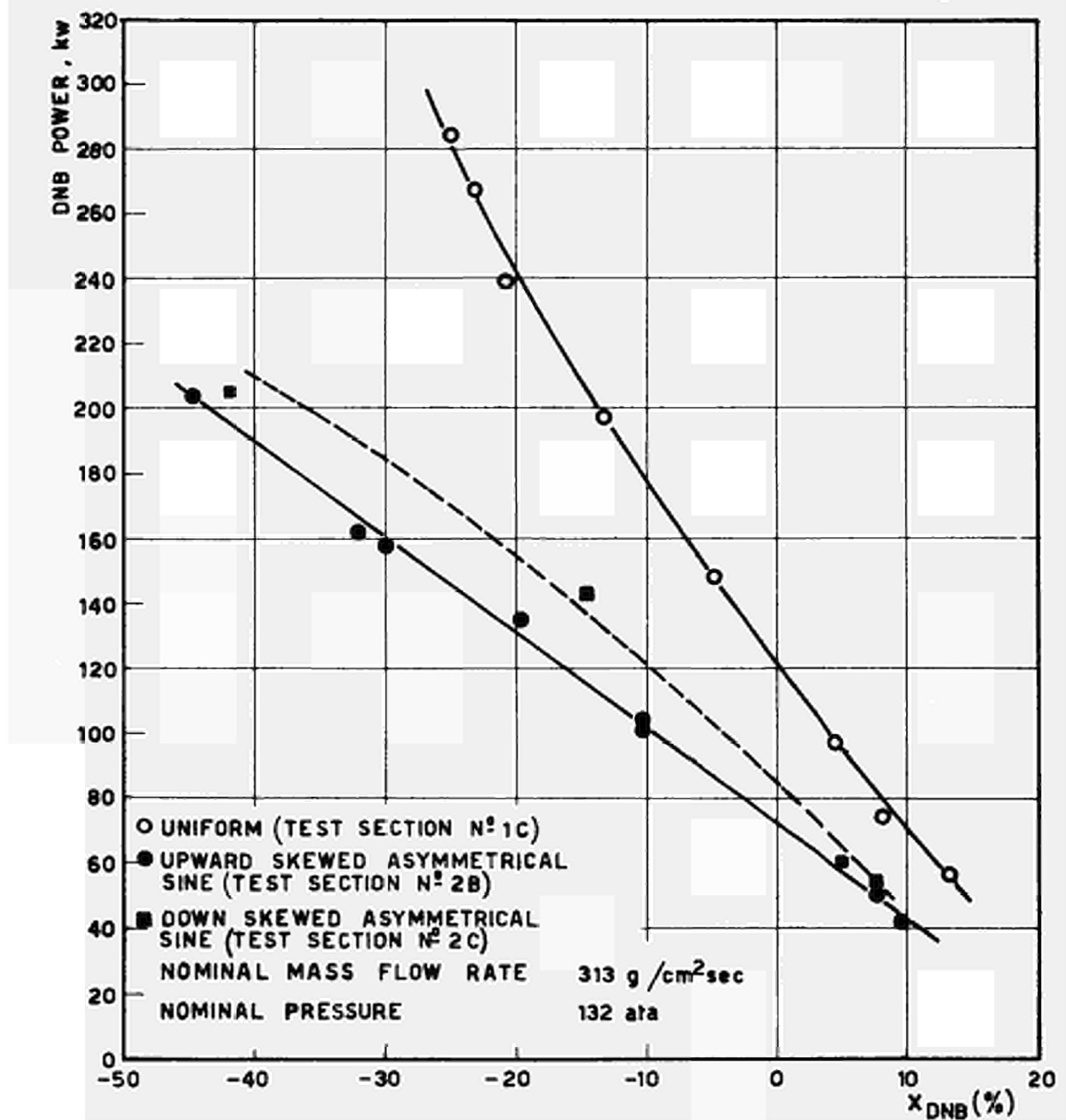


Fig. 11



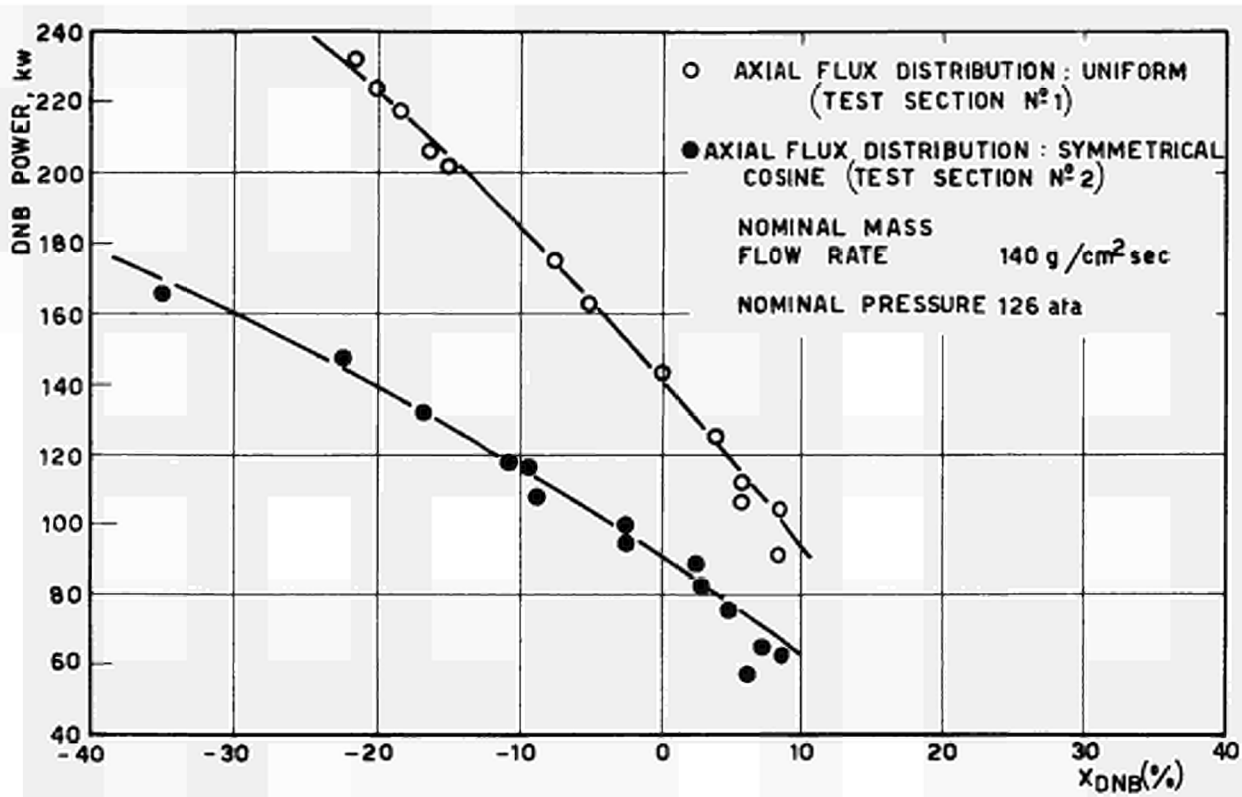
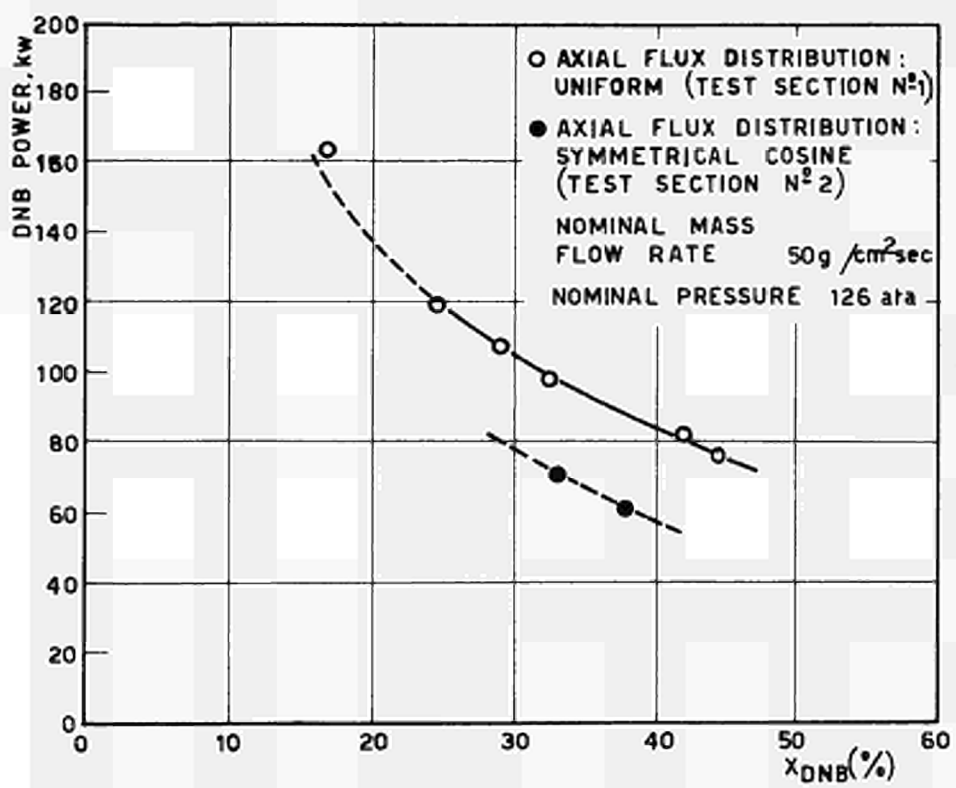


Fig. 12



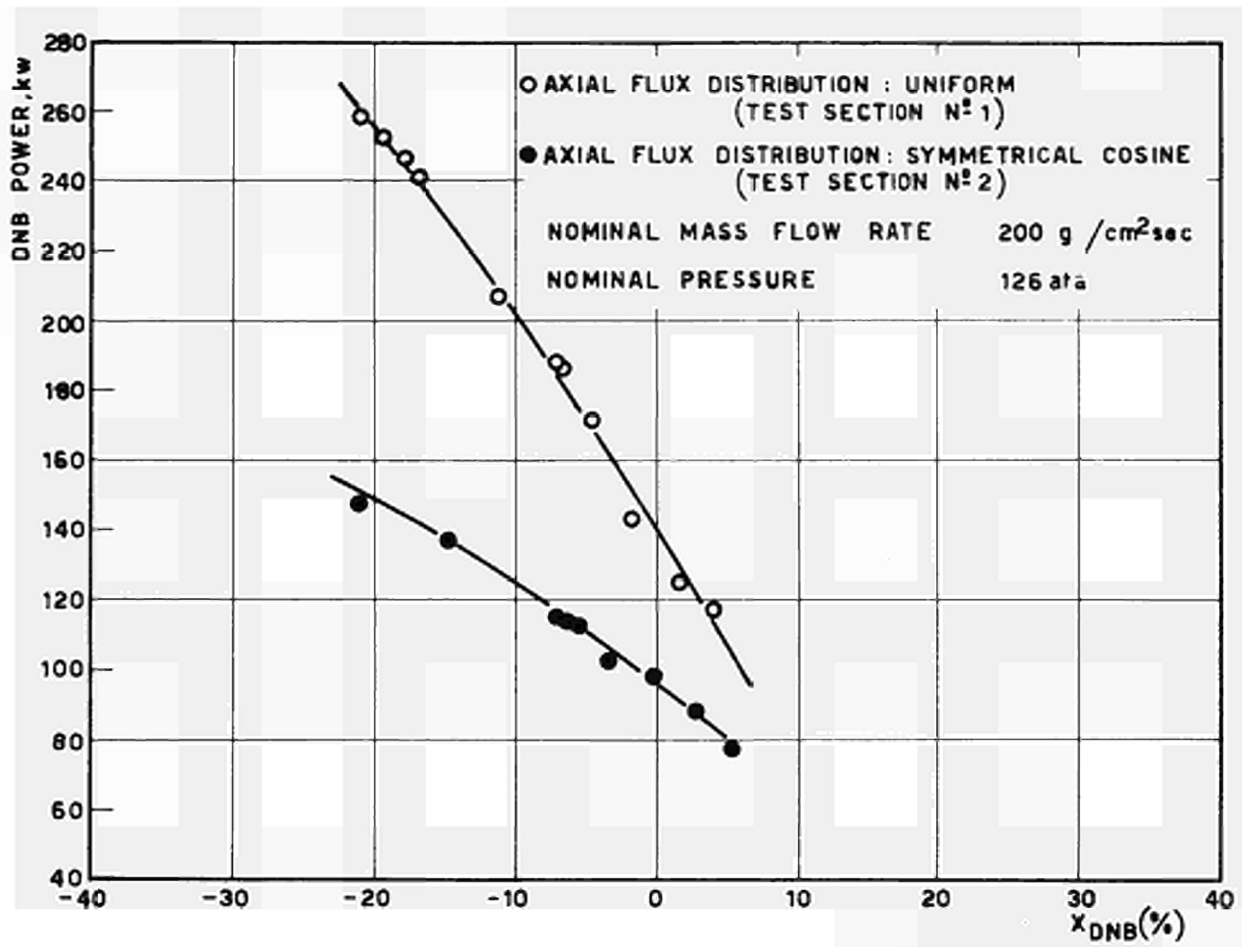
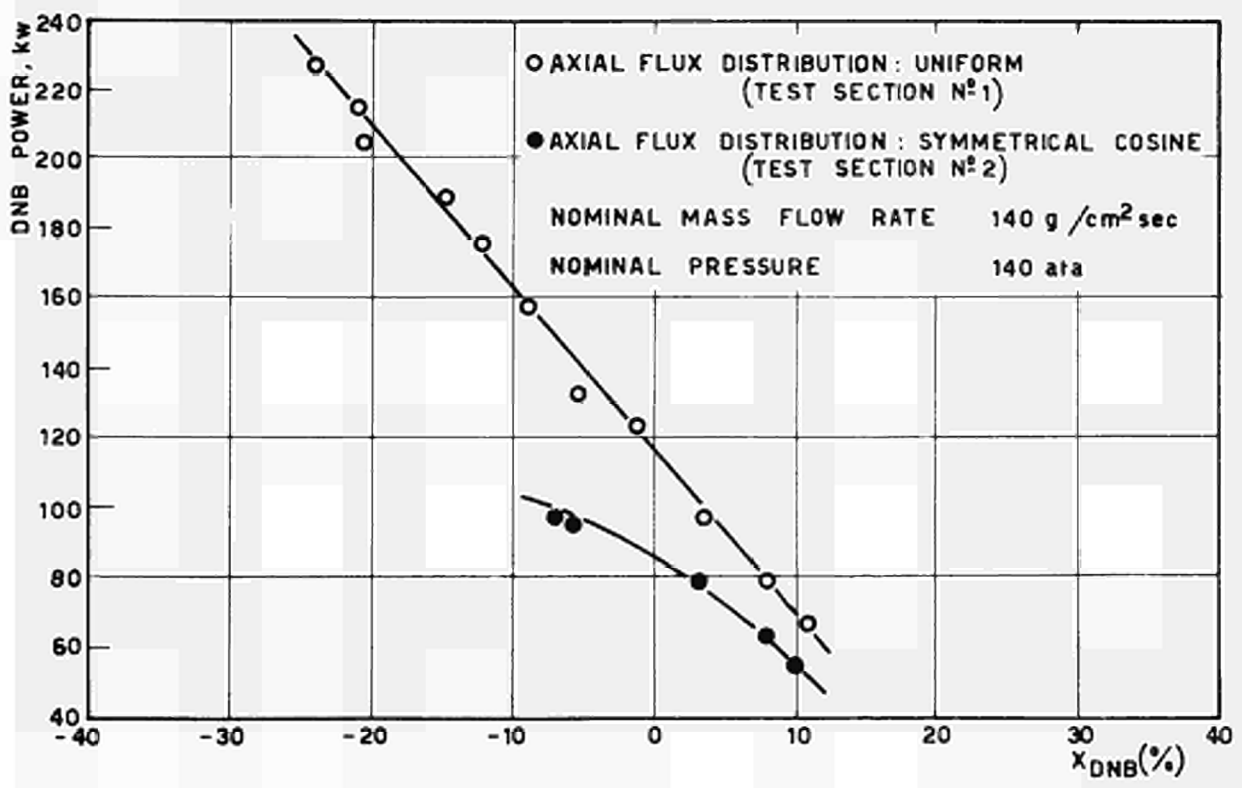


Fig. 13



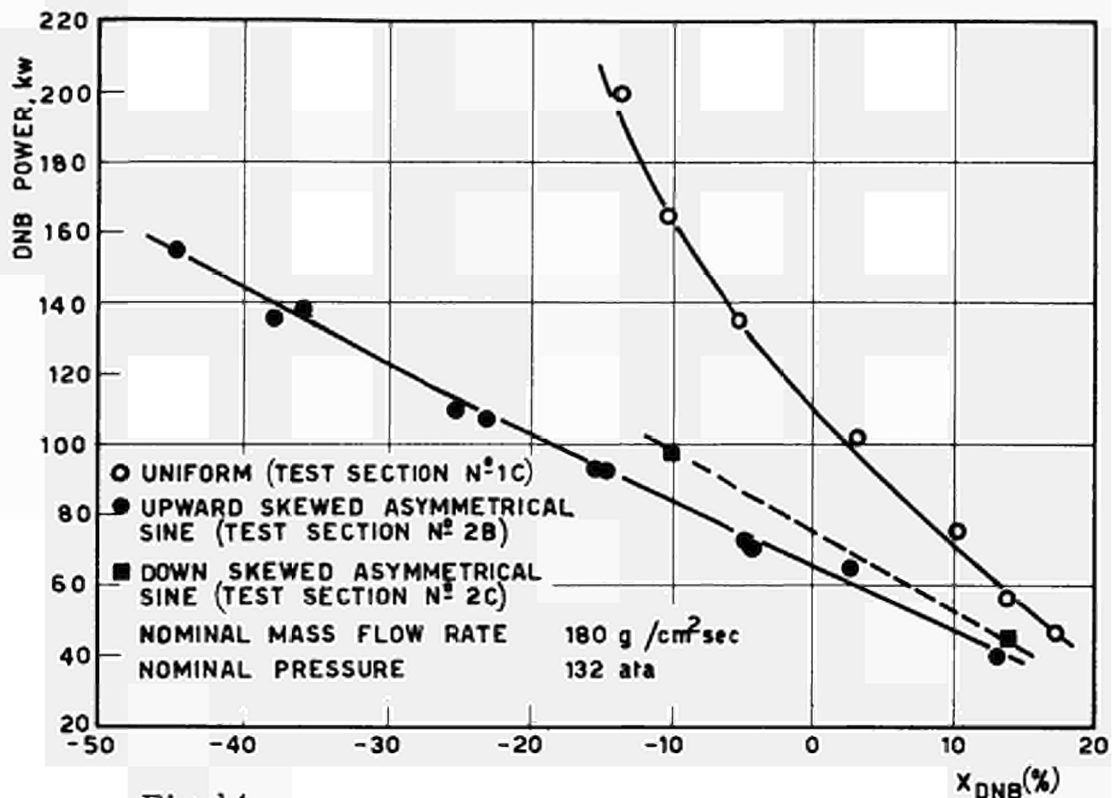
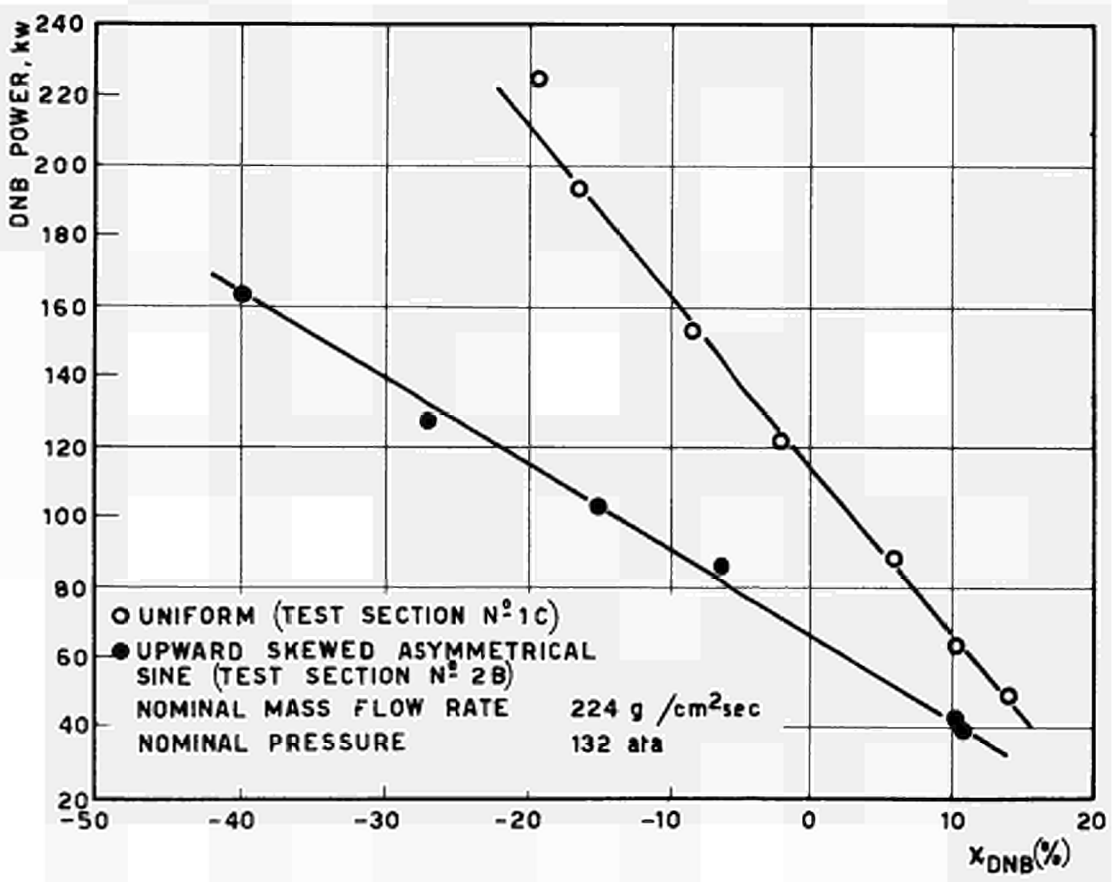


Fig. 14



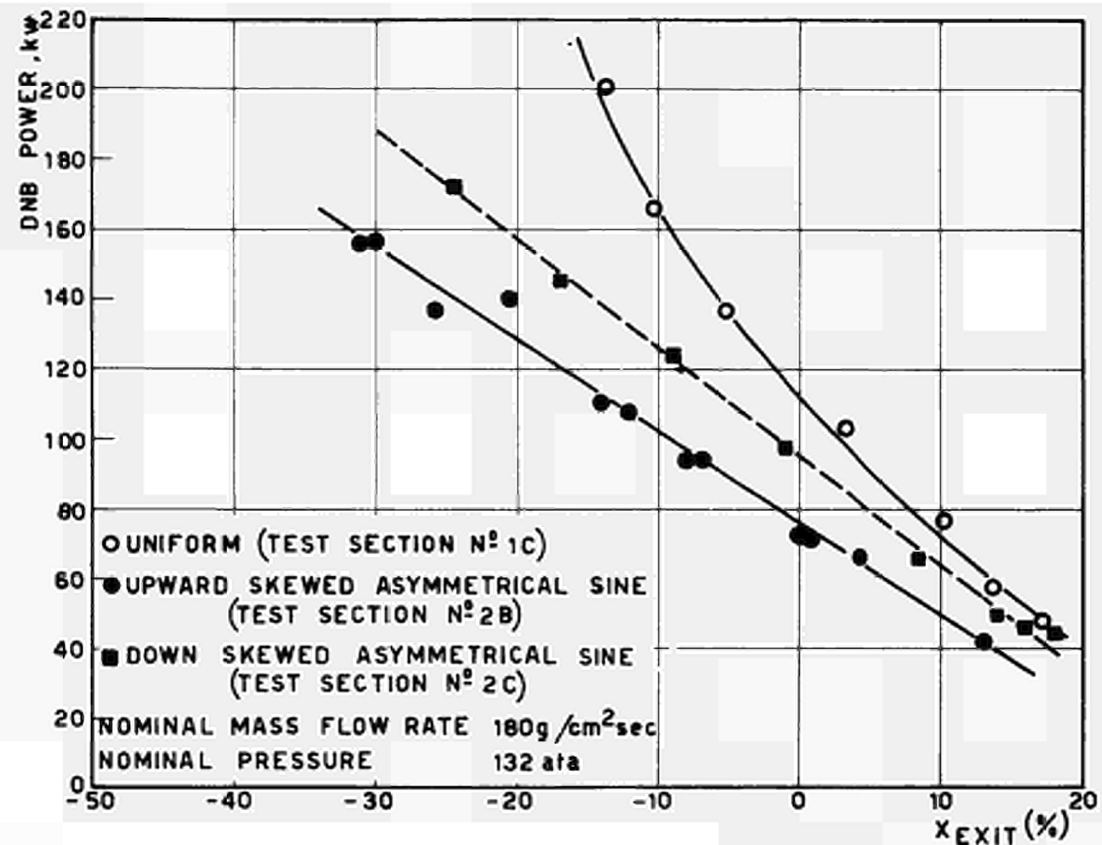


Fig. 15

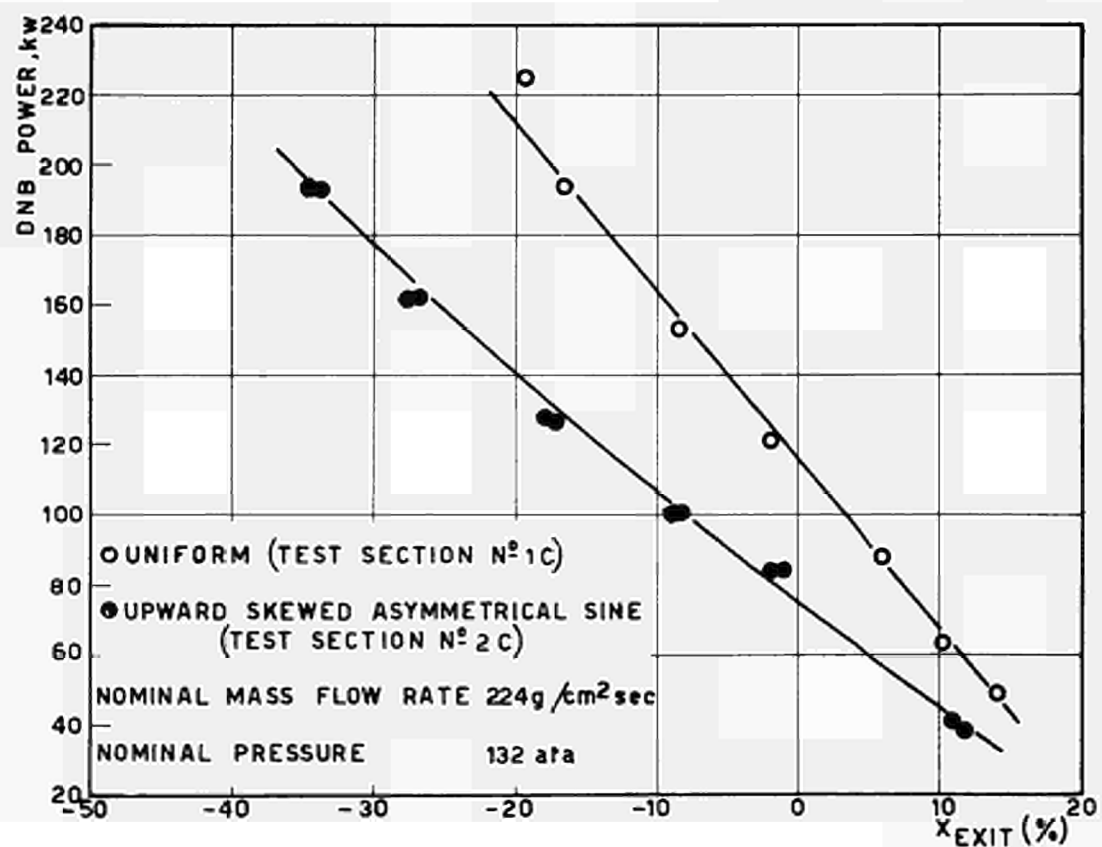
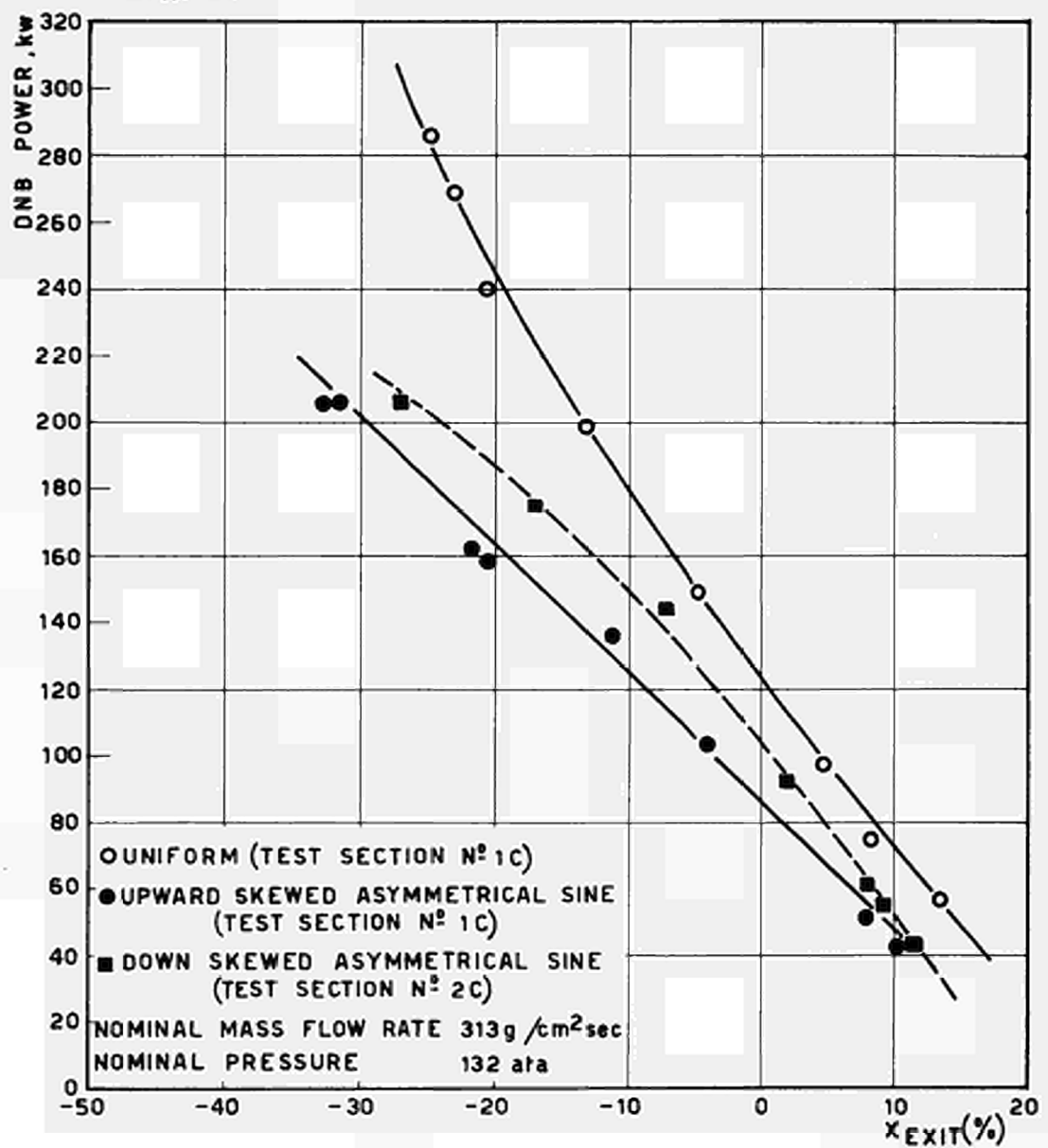


Fig. 16



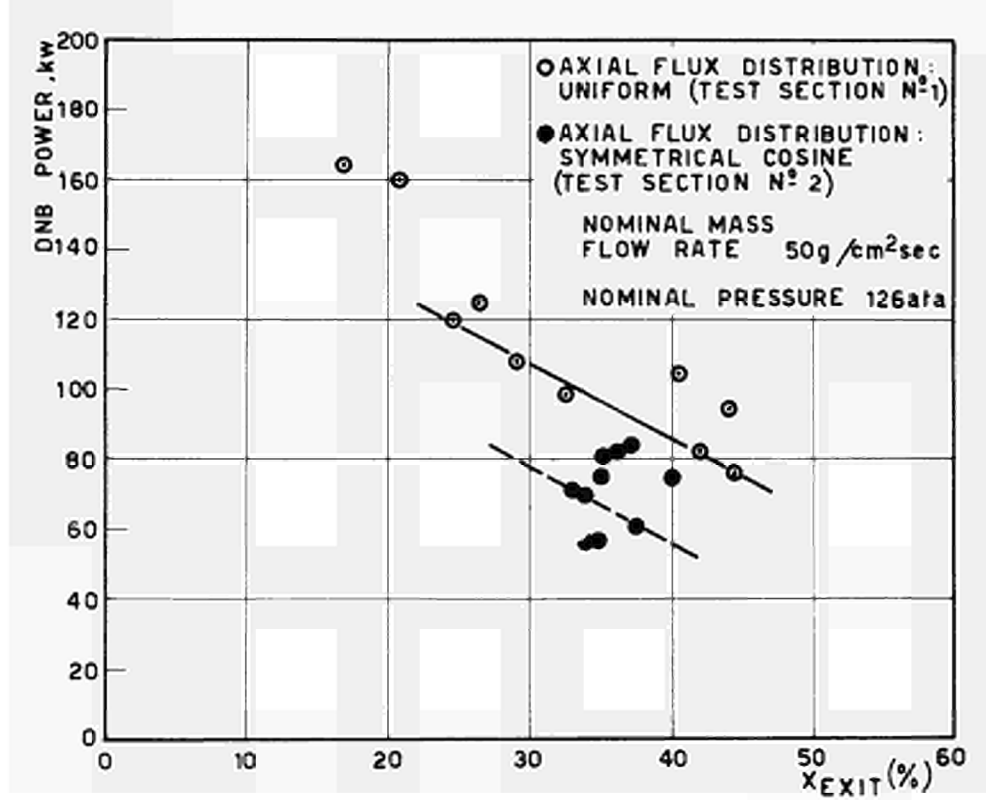
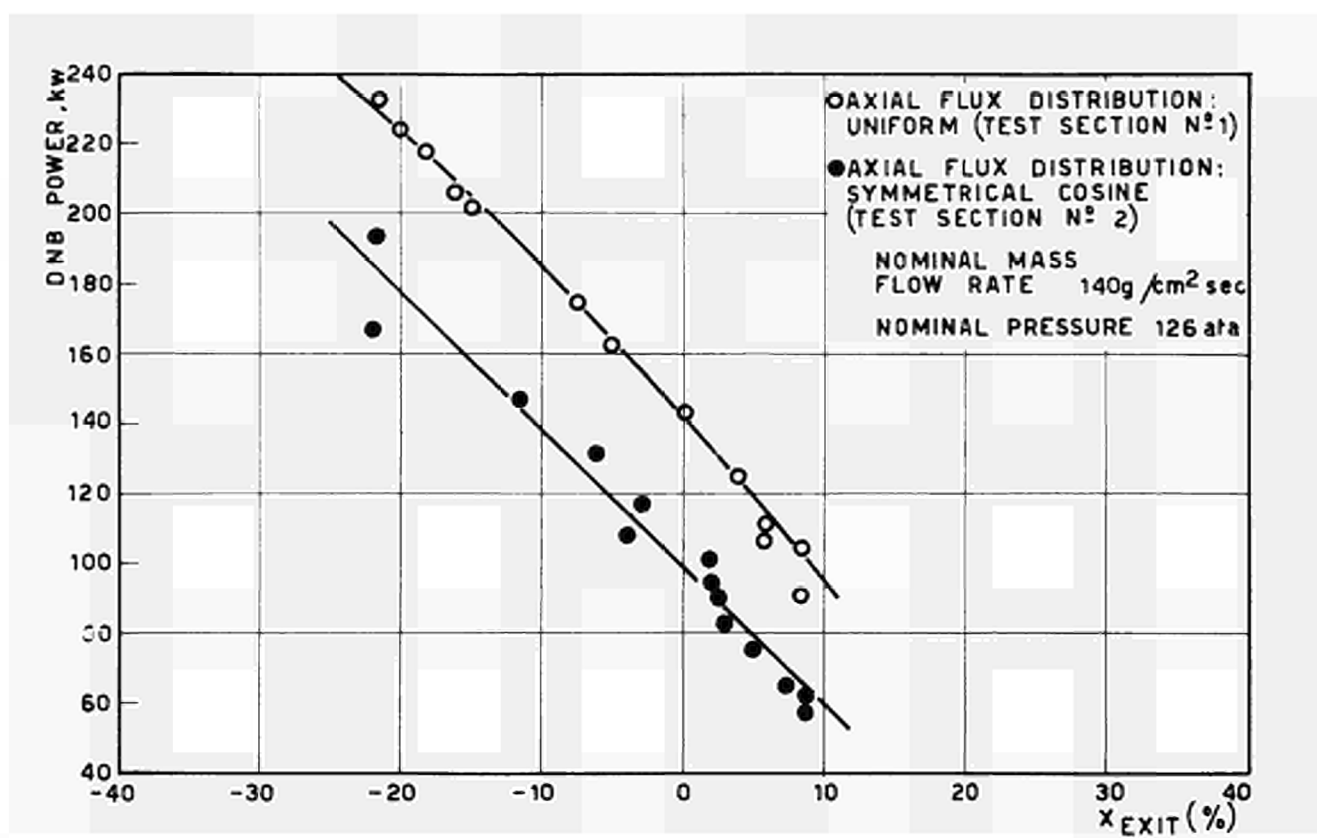


Fig. 17

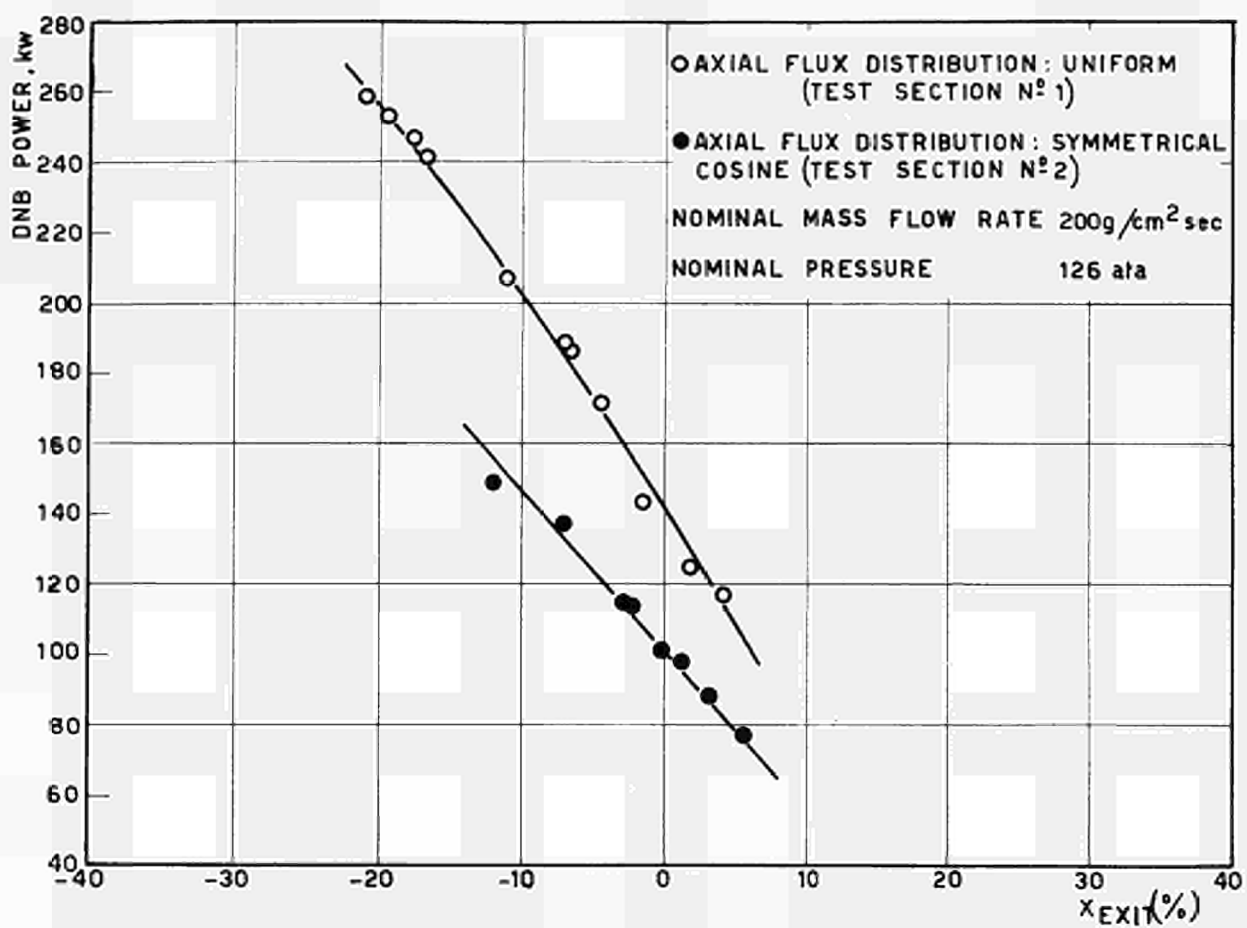
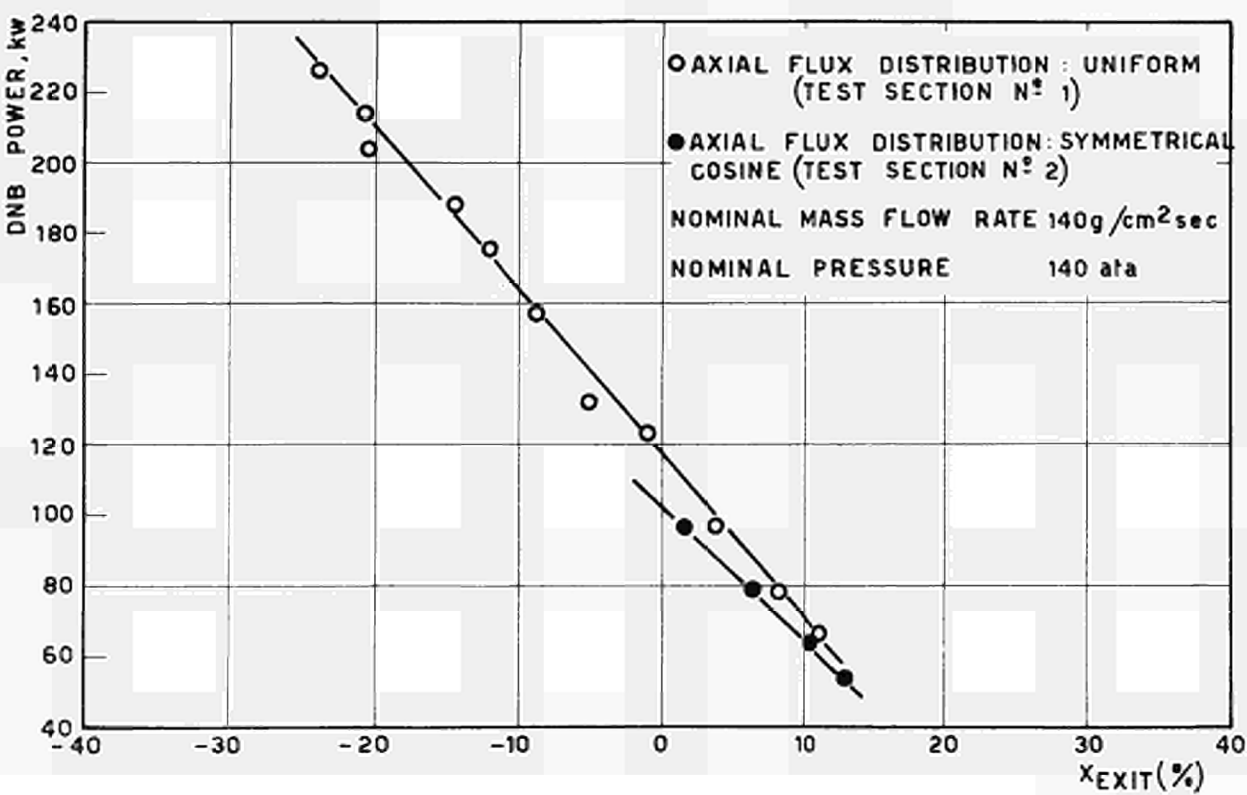


Fig. 18



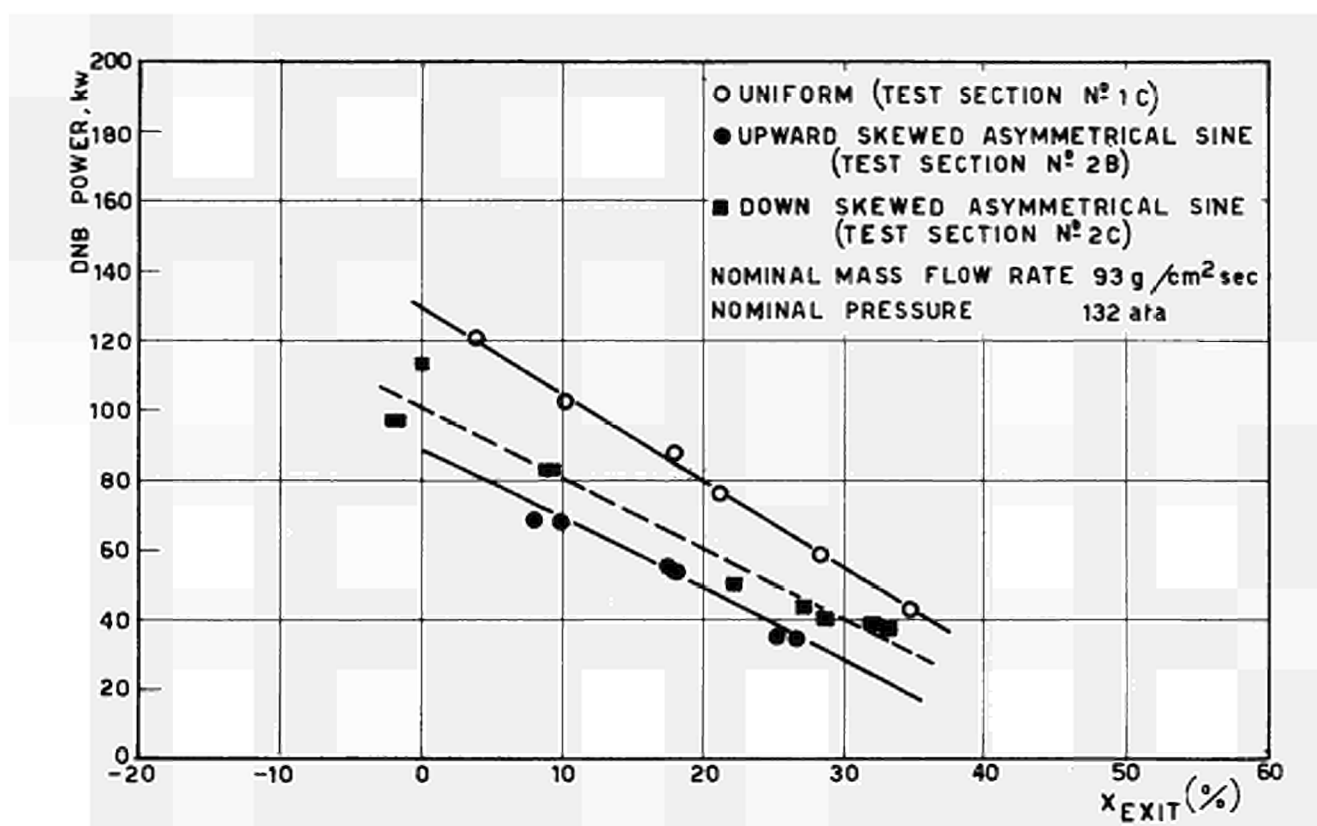


Fig. 19

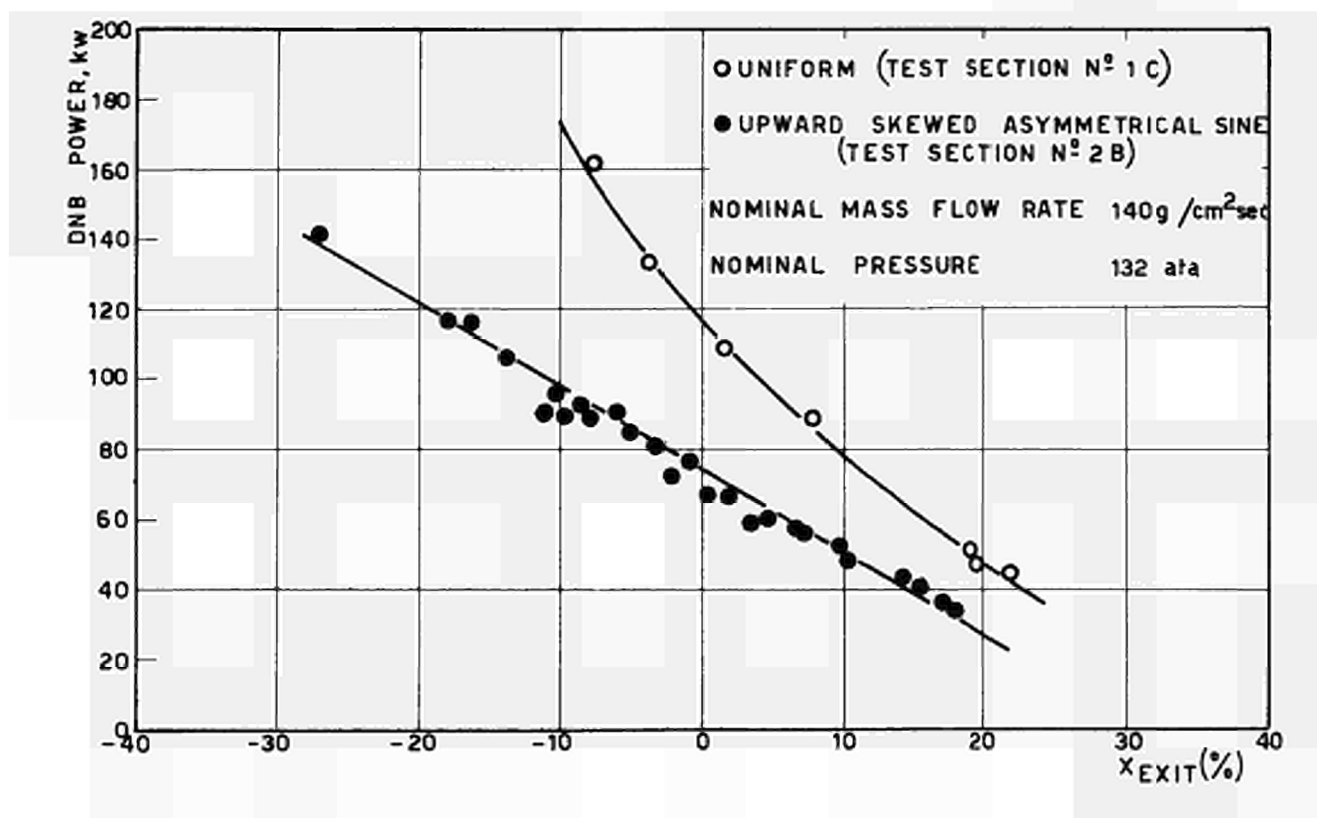
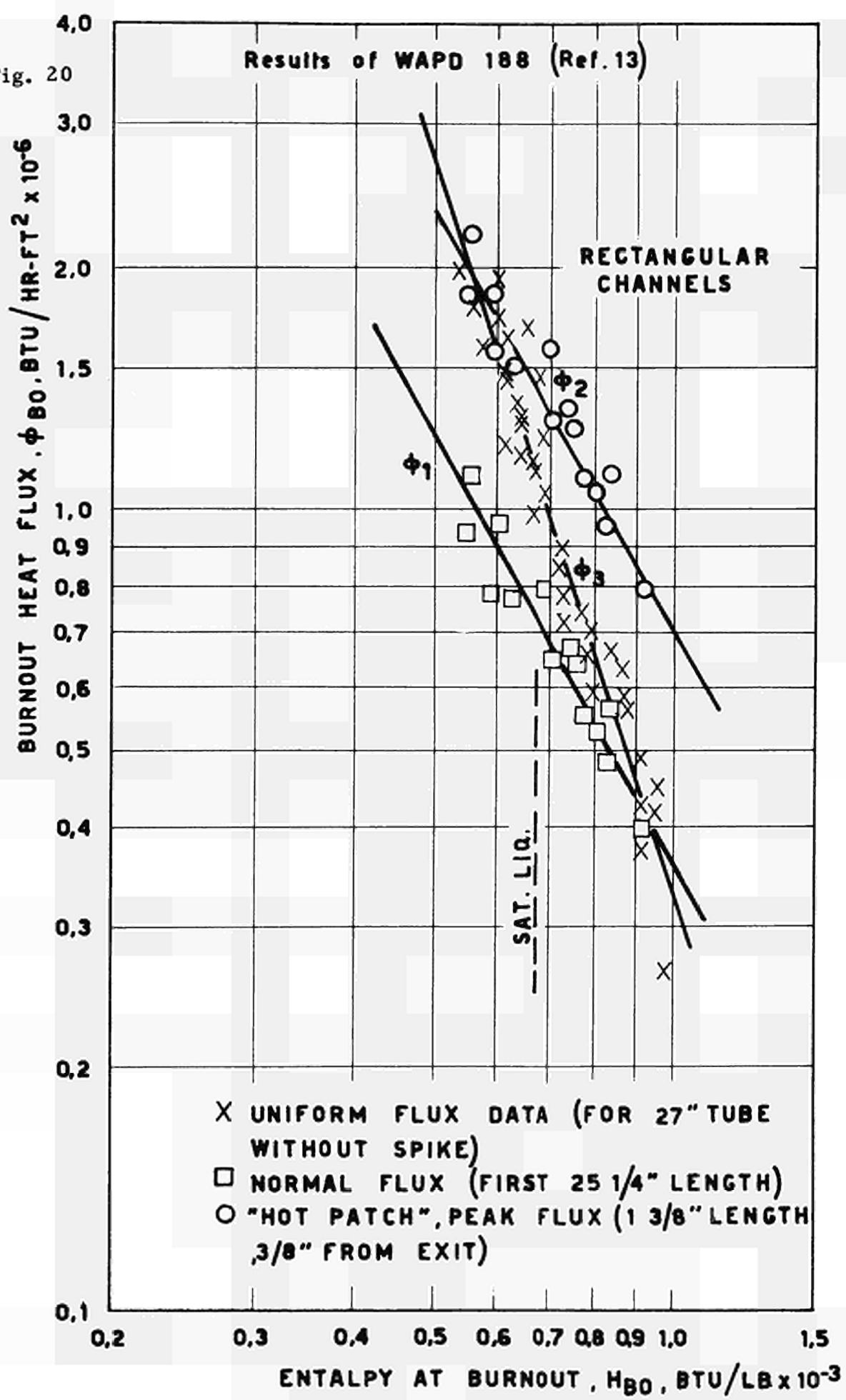


Fig. 20

Results of WAPD 188 (Ref. 13)



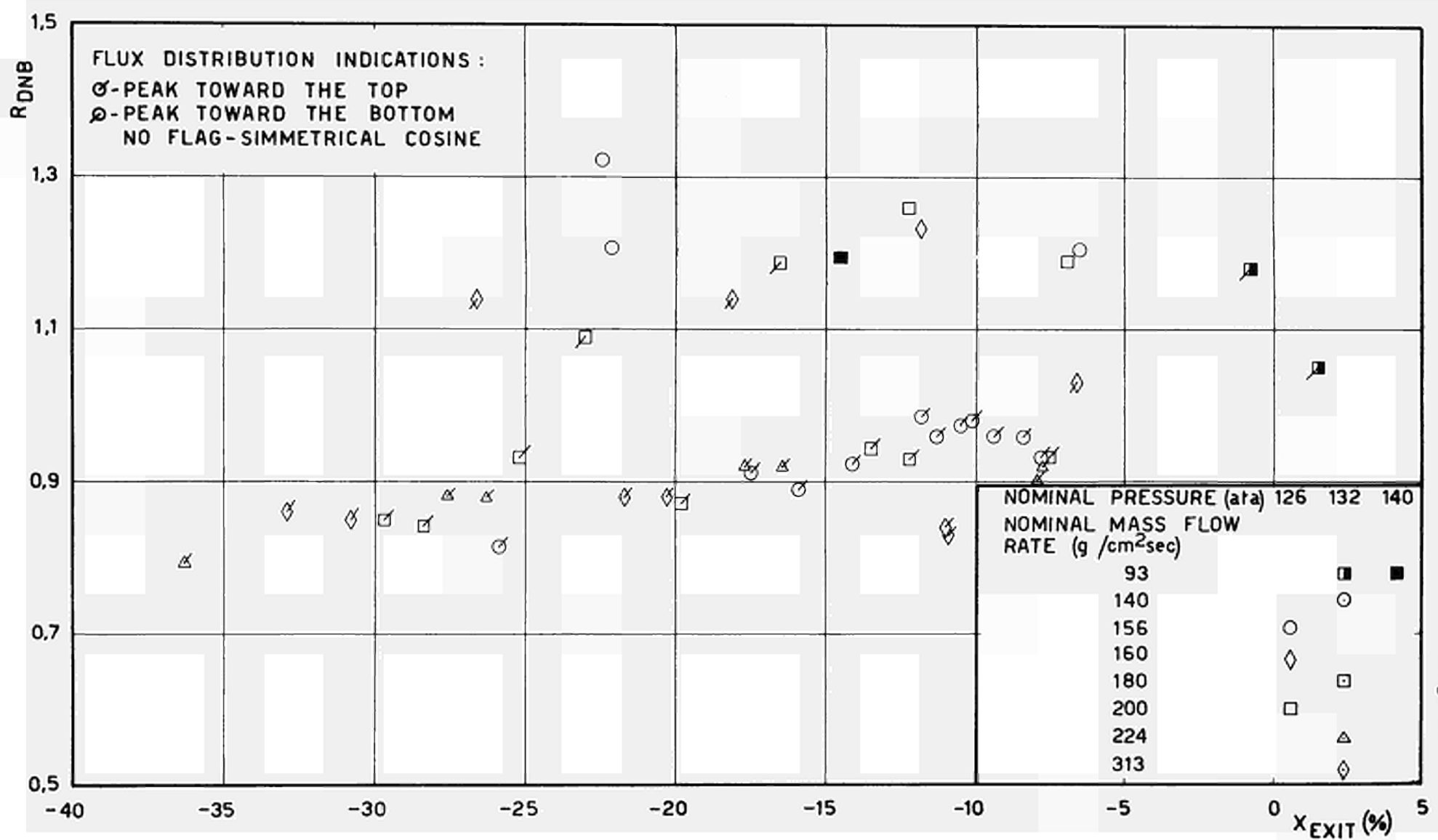


Fig. 21

Fig. 22

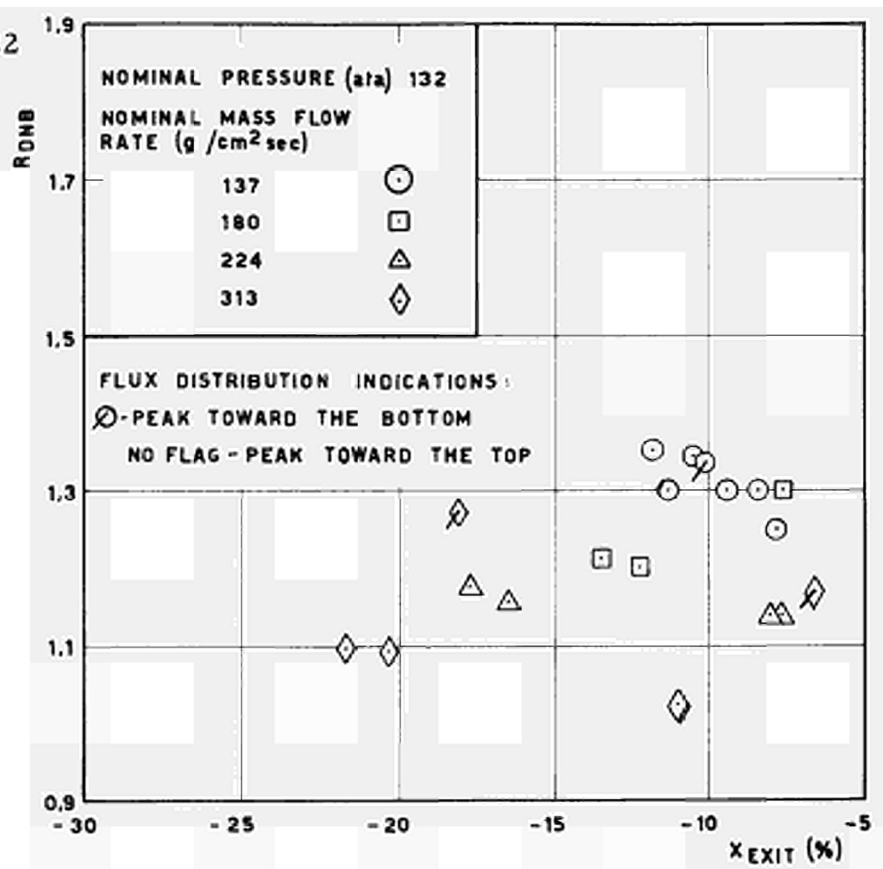
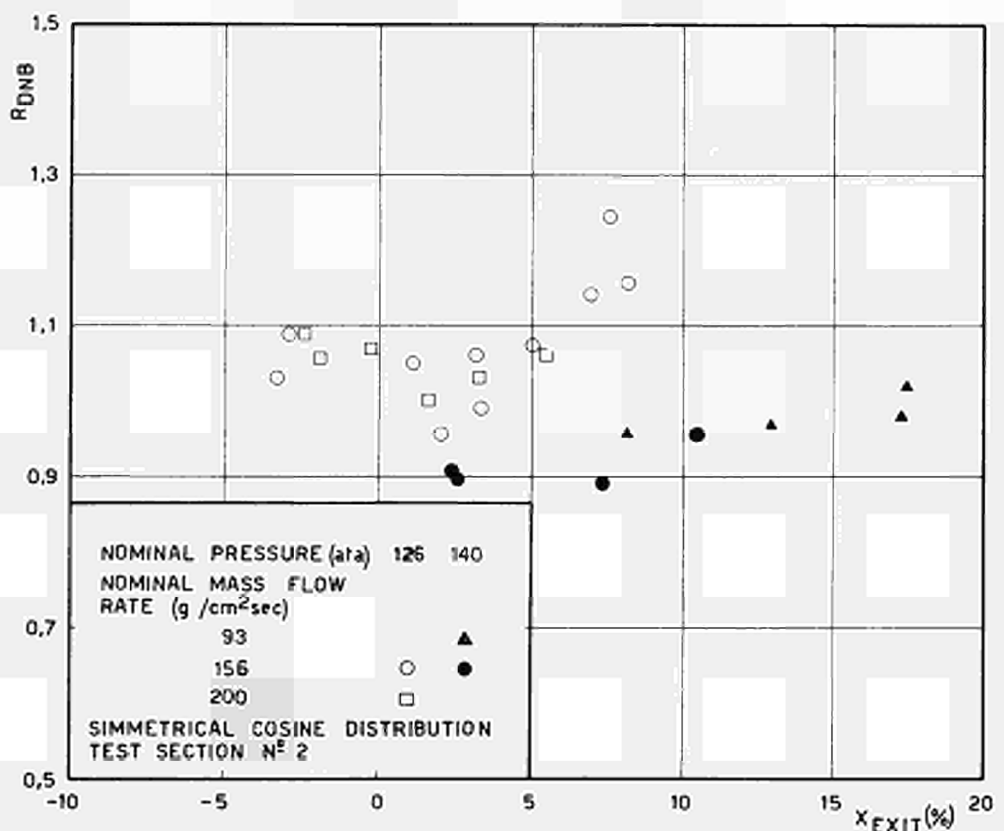


Fig. 23



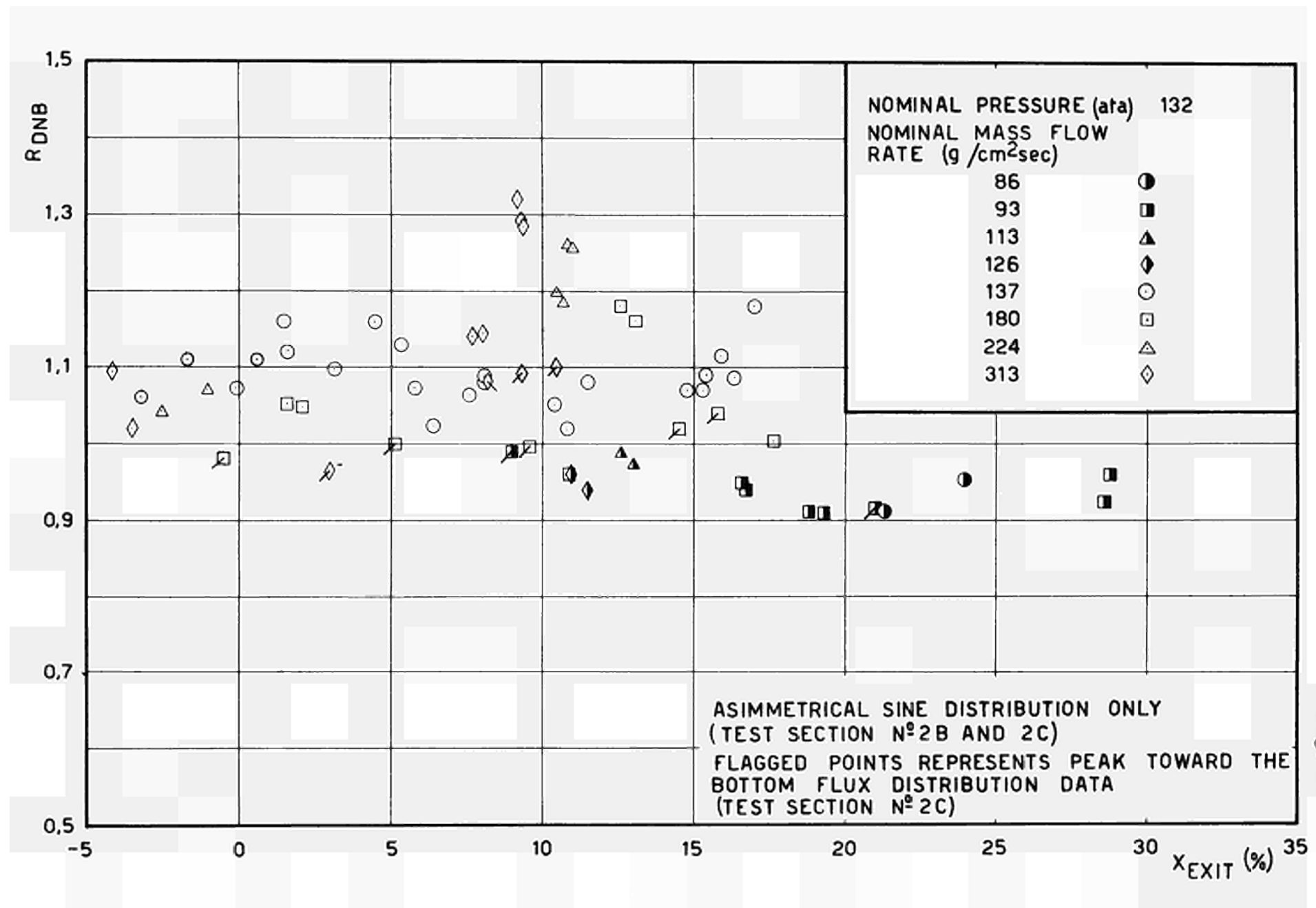


Fig. 24

Fig. 25

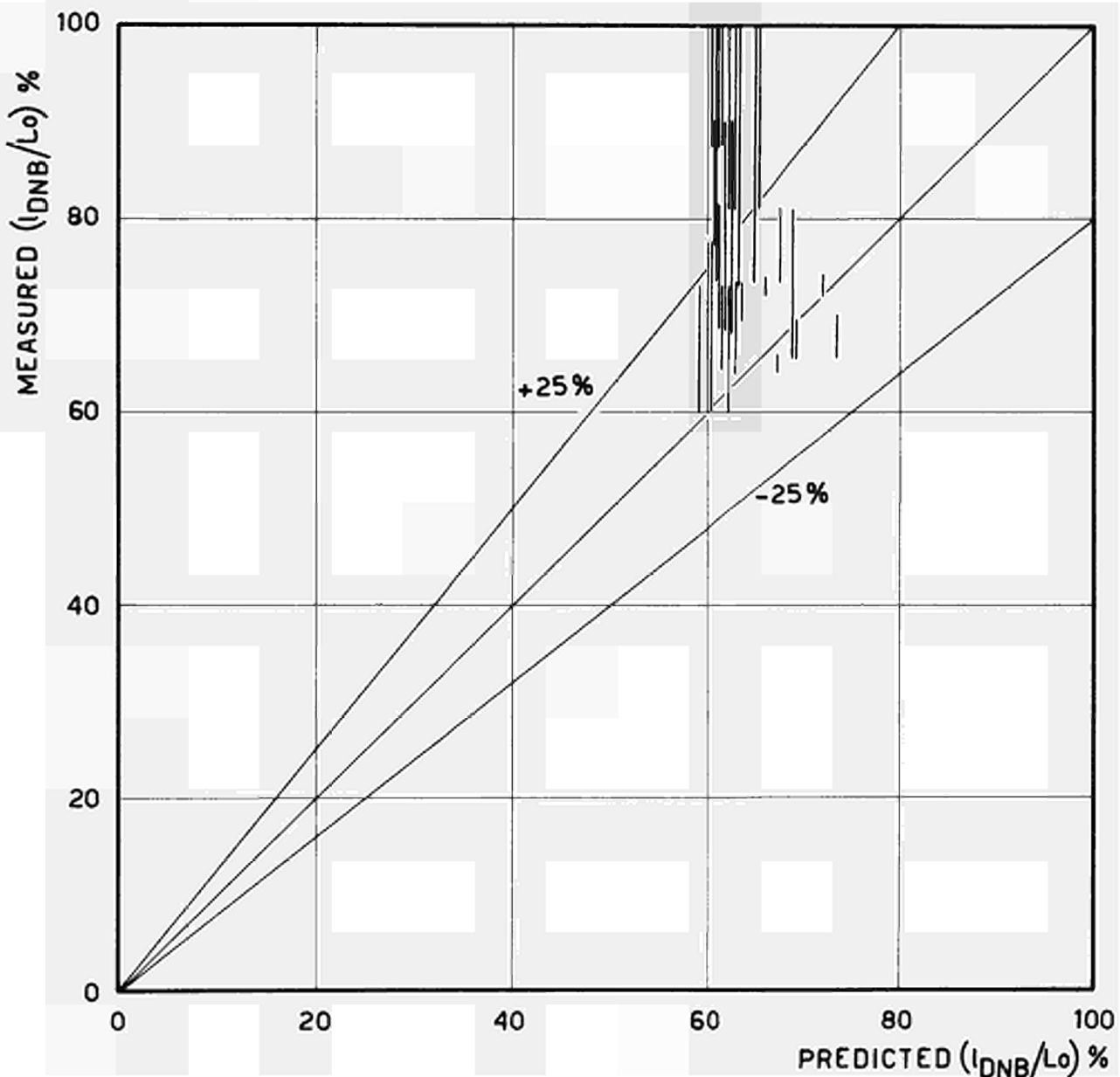


Fig. 26

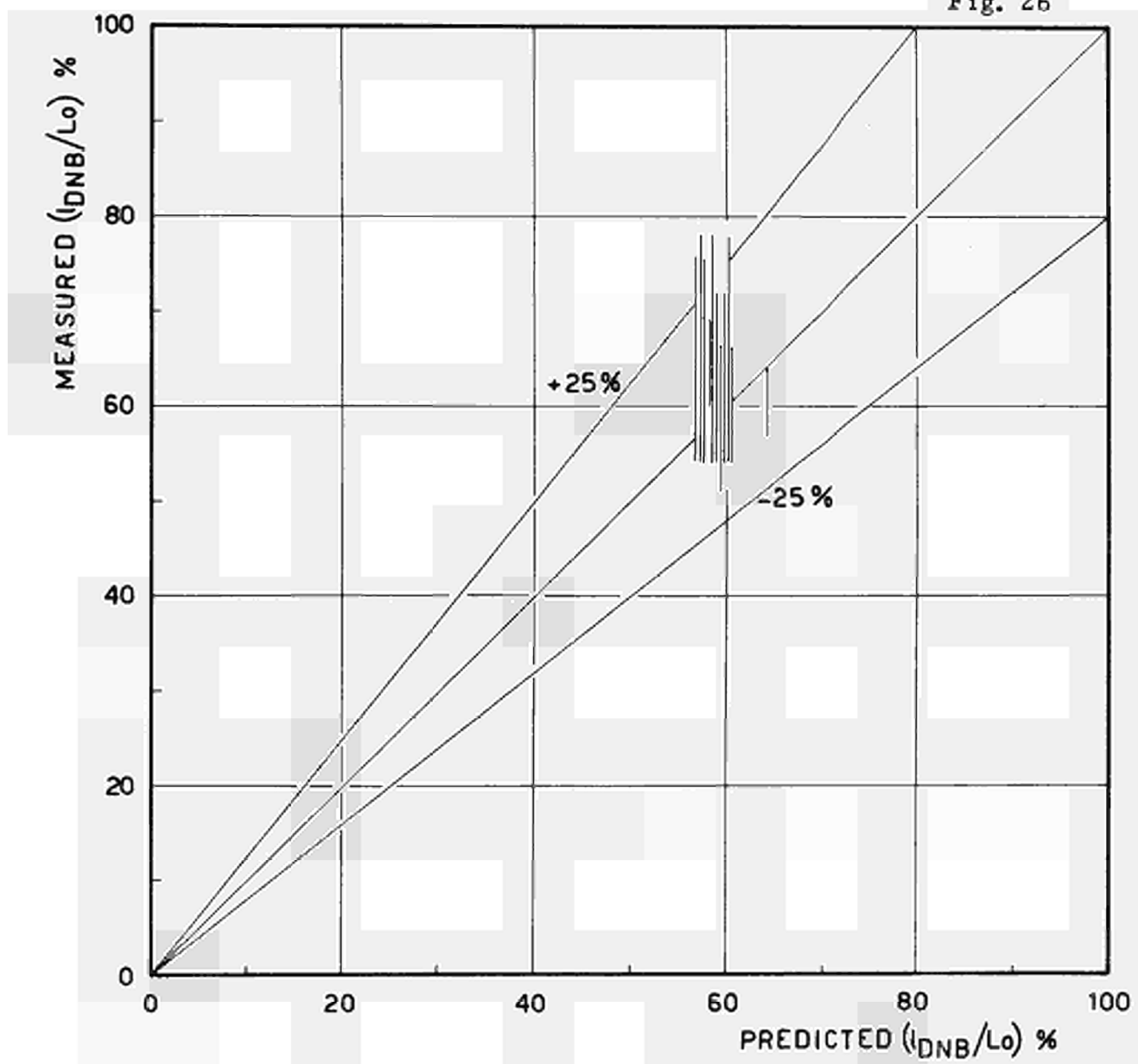


Fig. 27

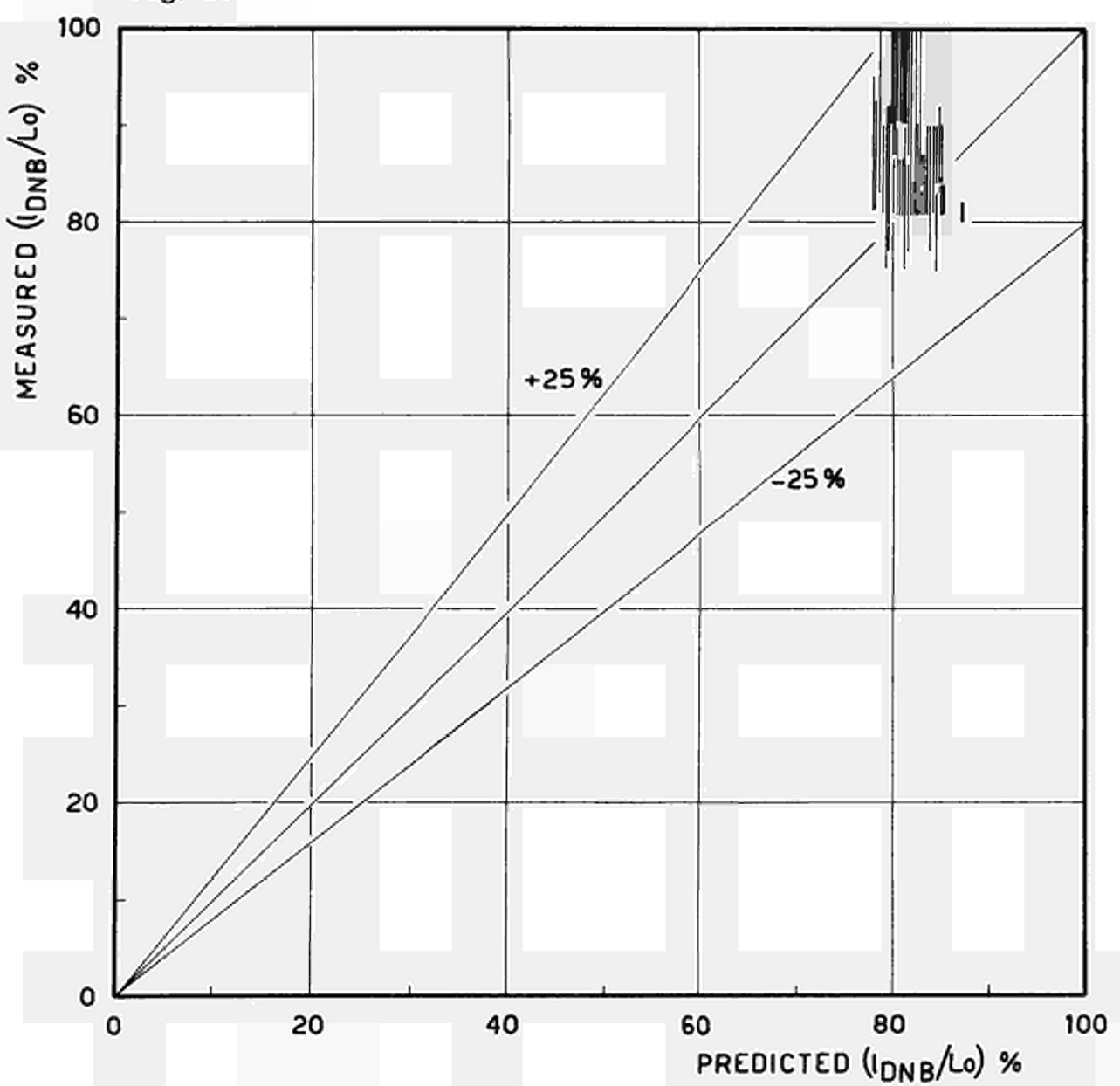


Fig. 28

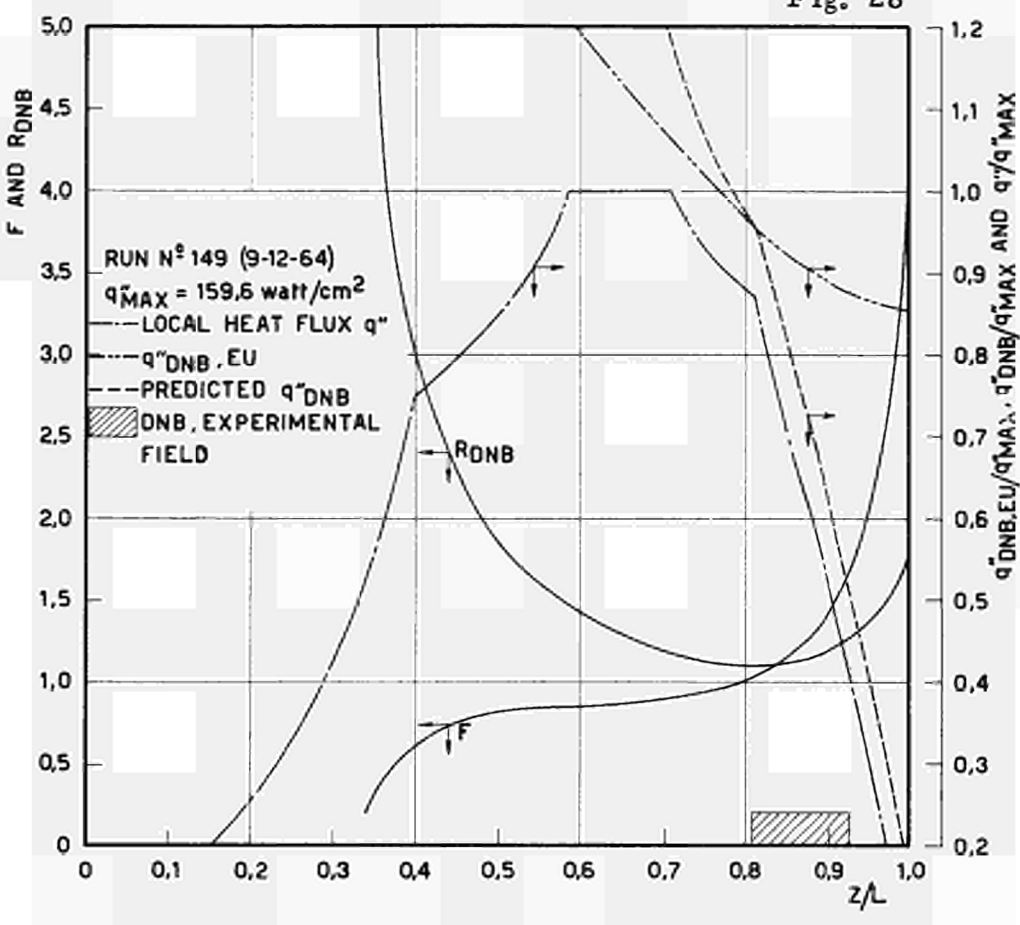


Fig. 29

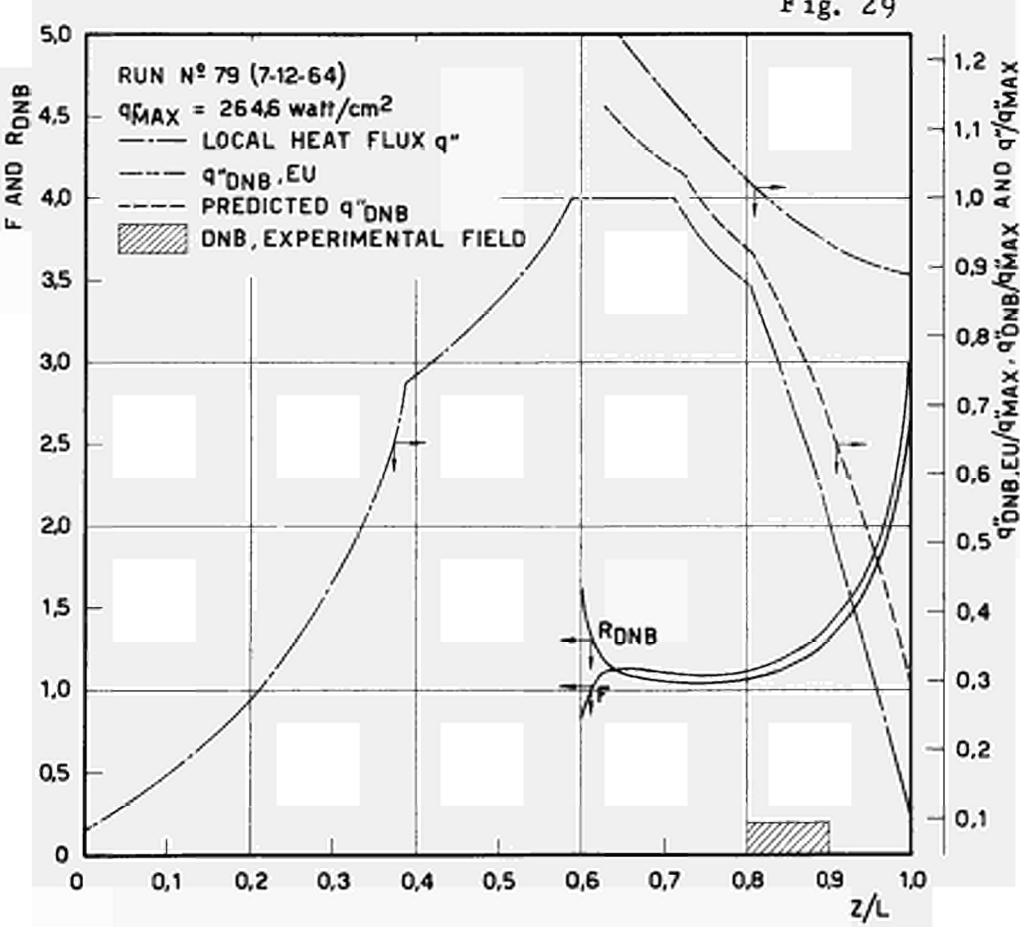
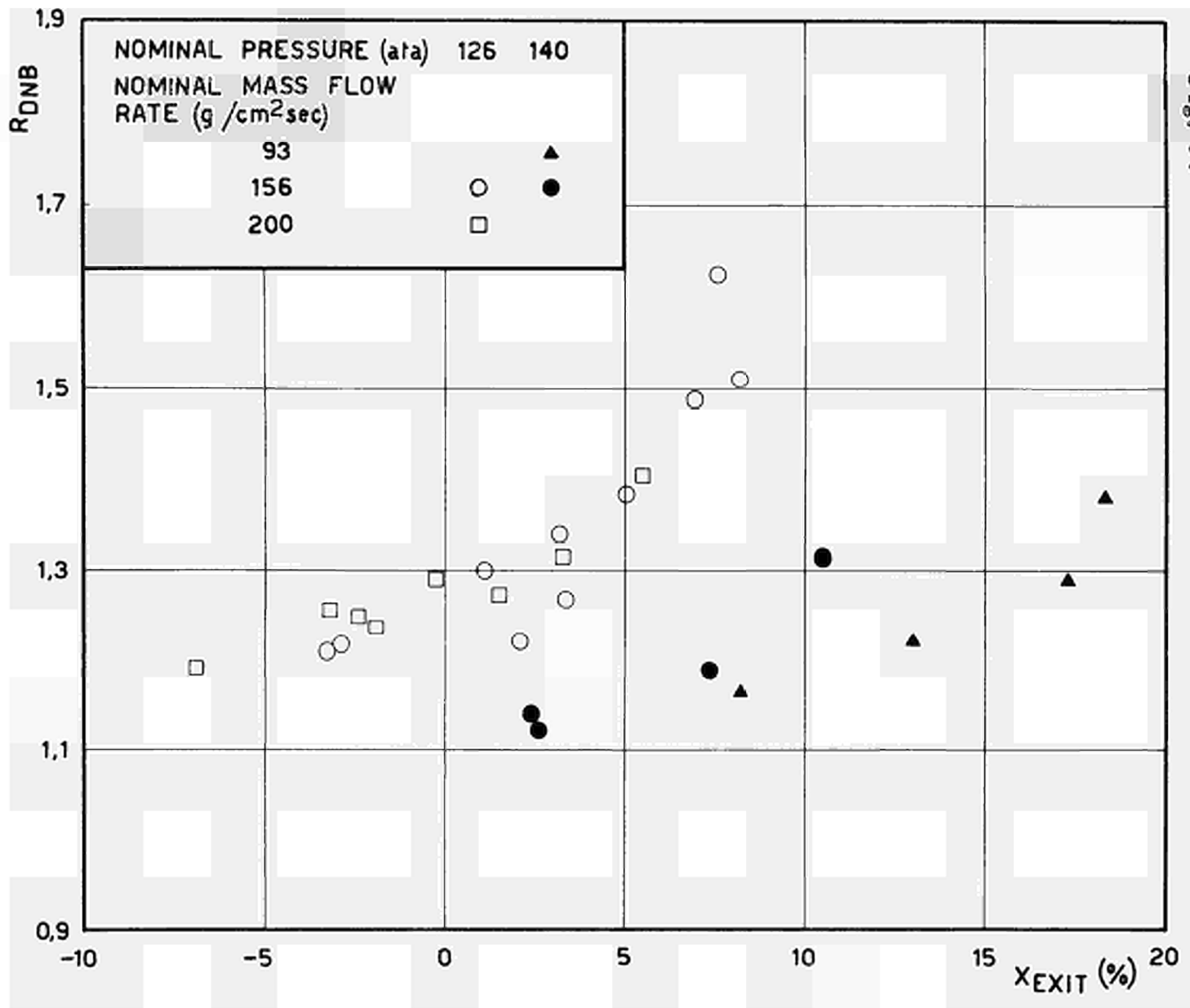


FIG. 30



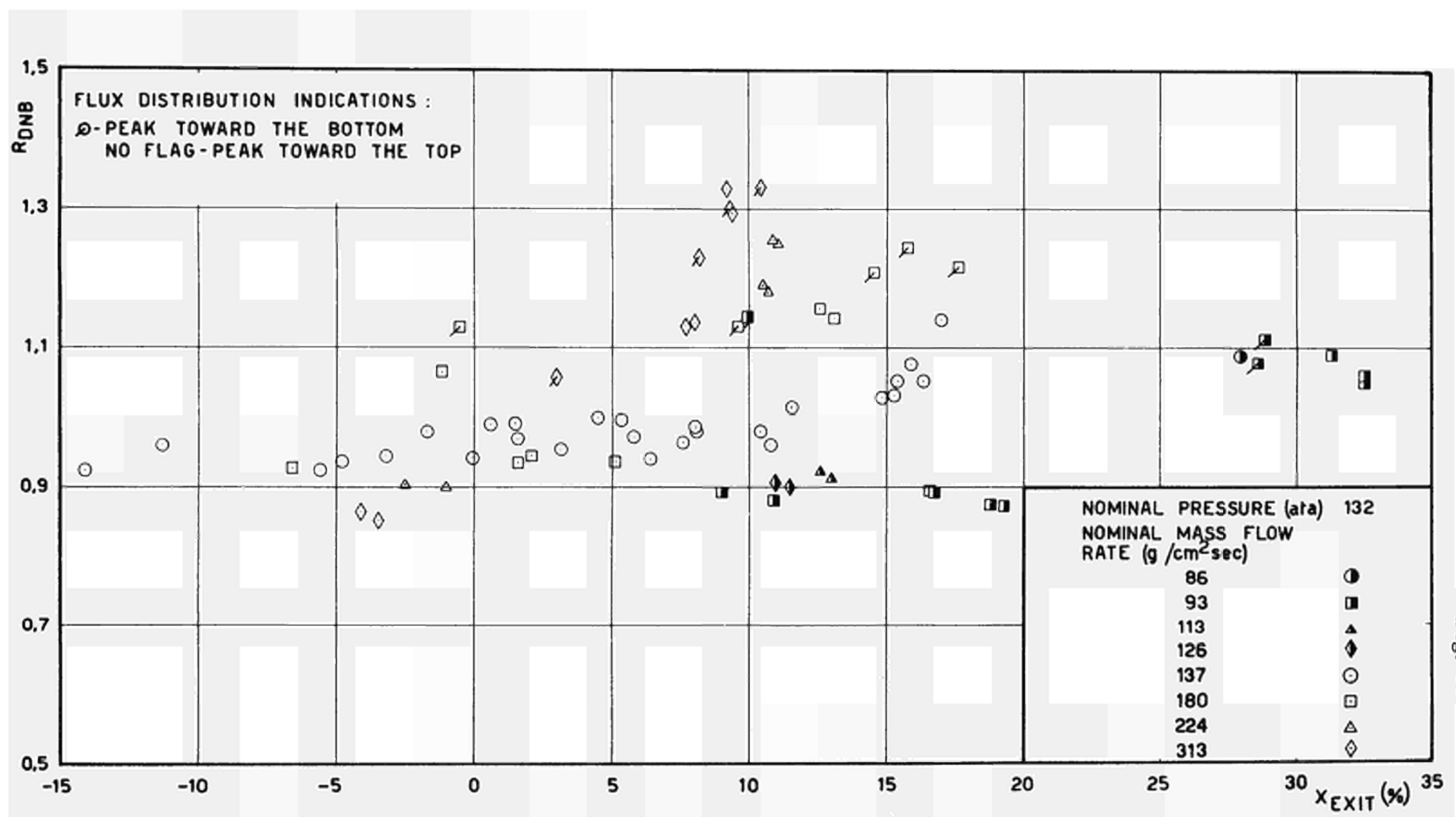
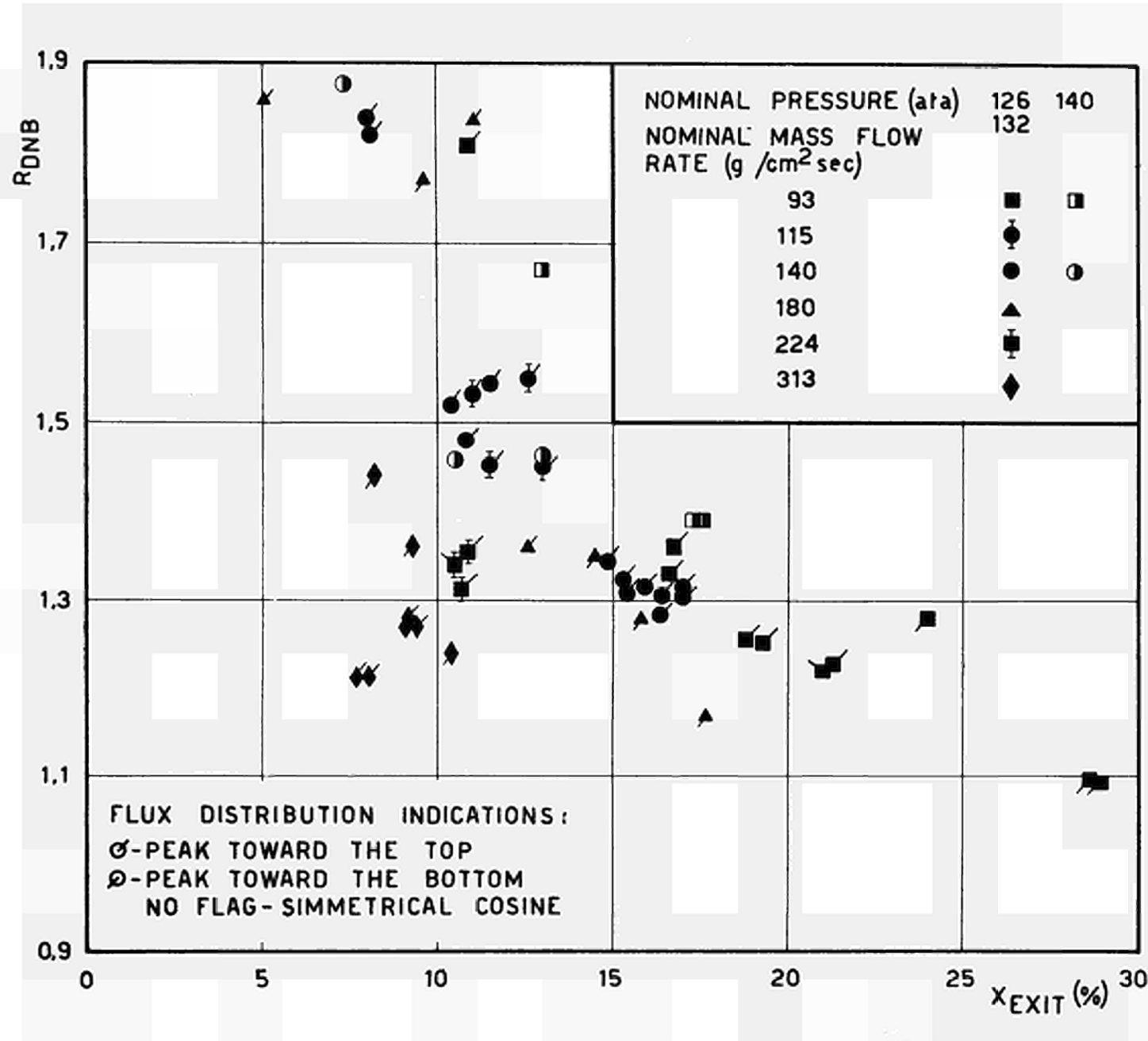


Fig. 31

Fig. 32



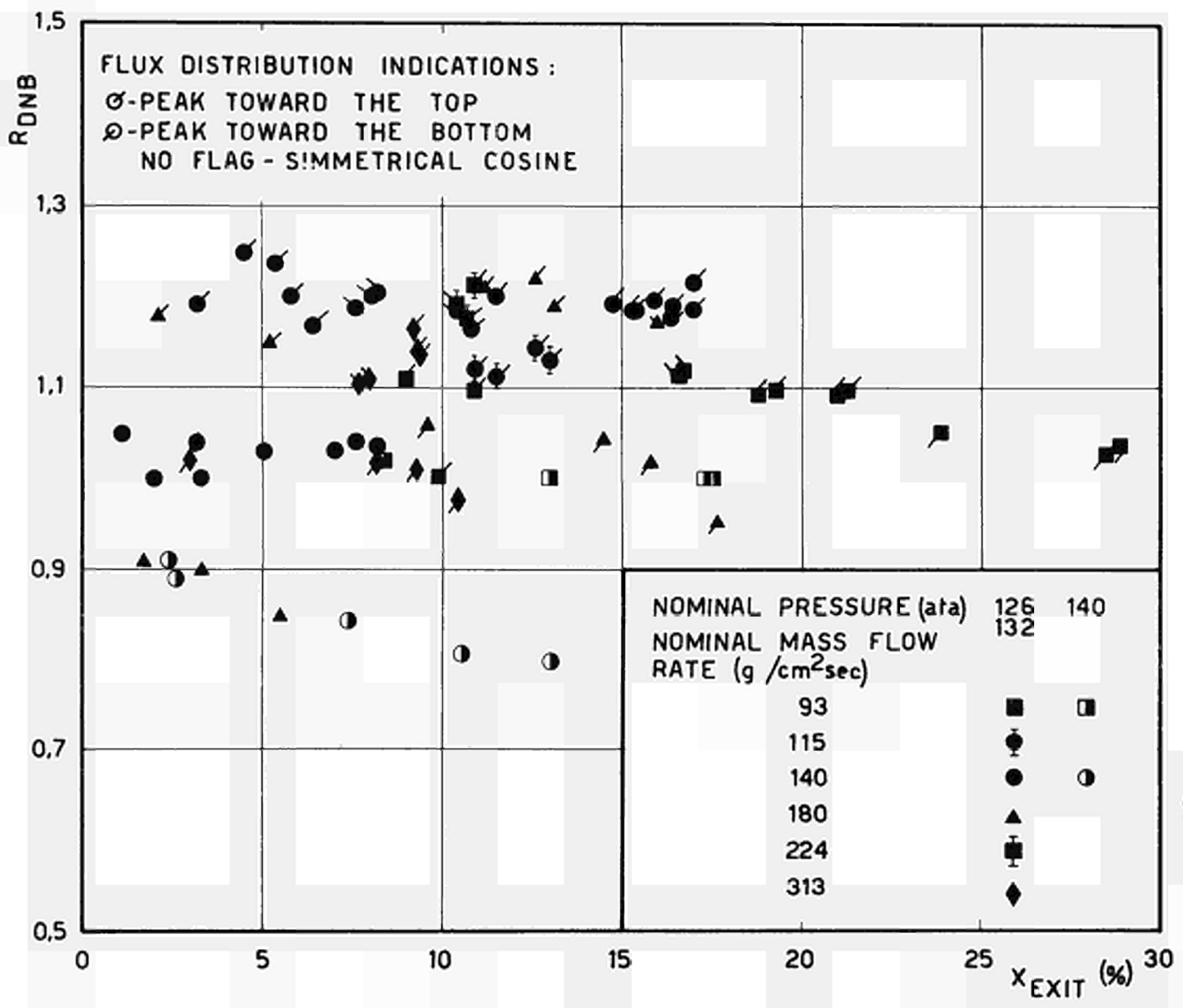


Fig. 33

Fig. 34

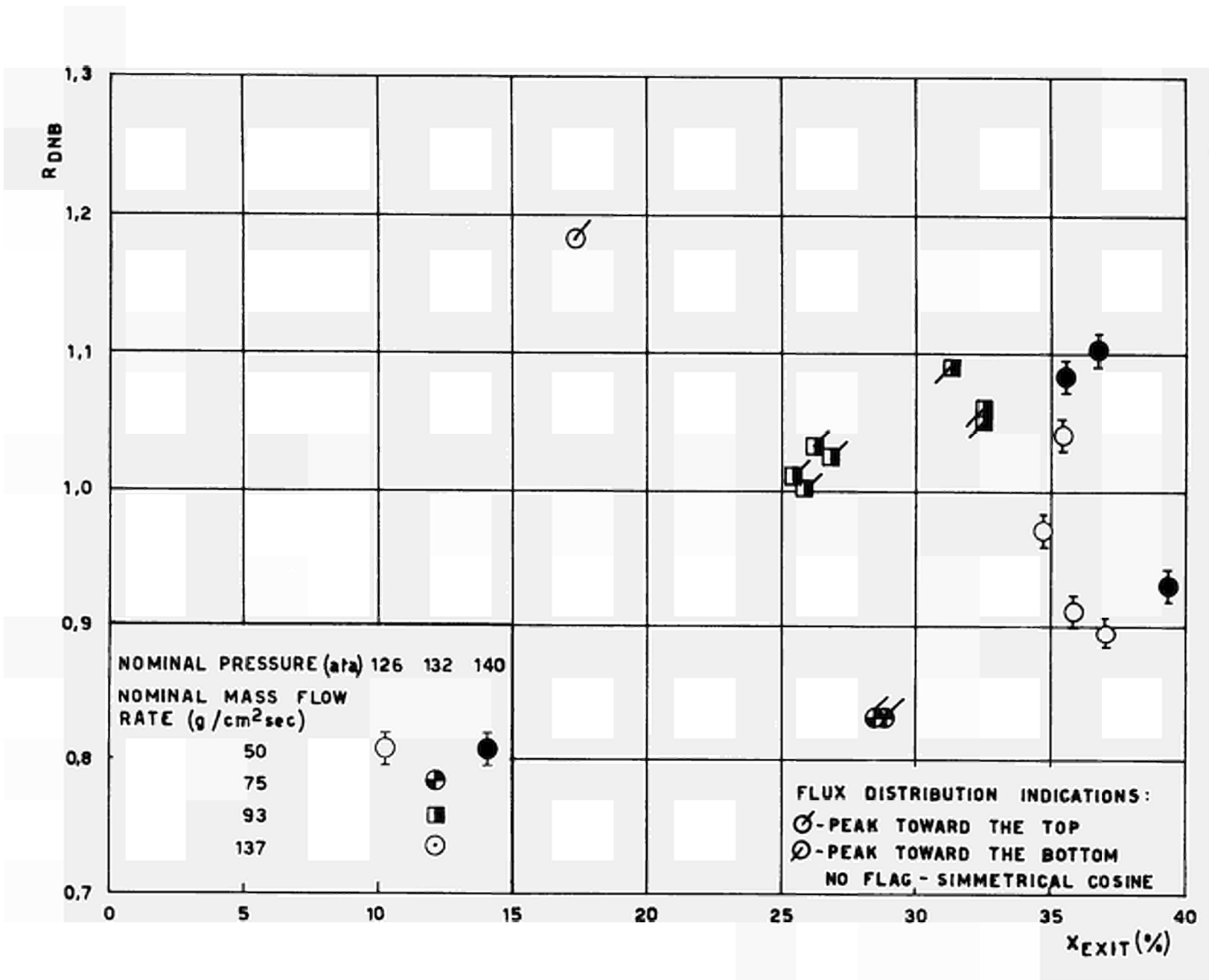


Fig. 35

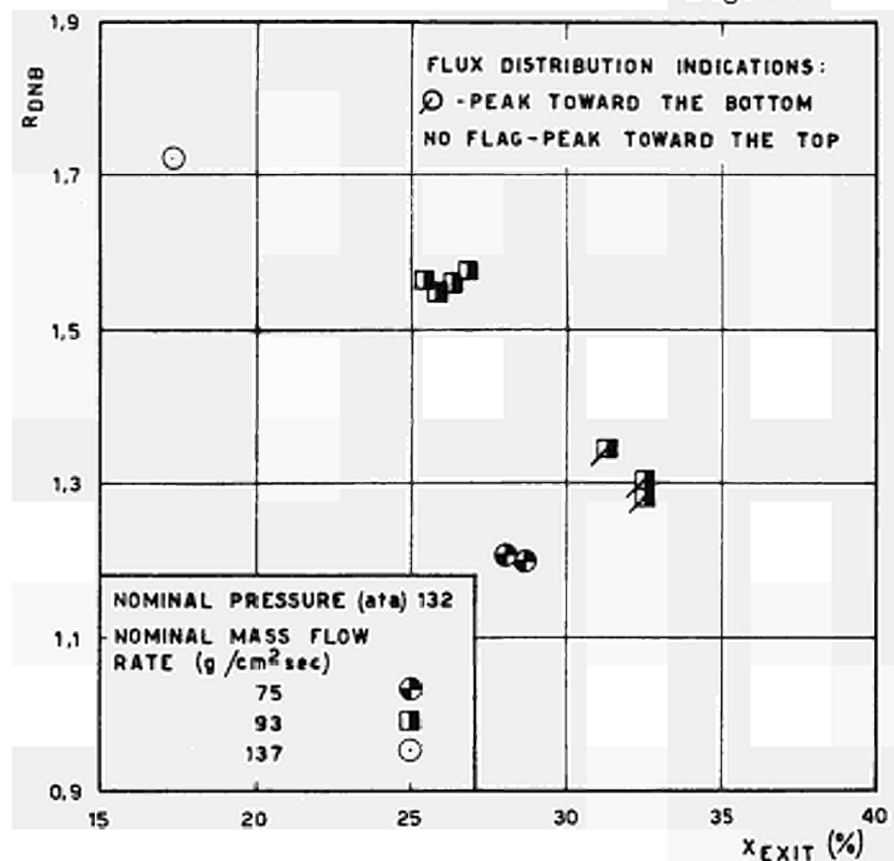


Fig. 36

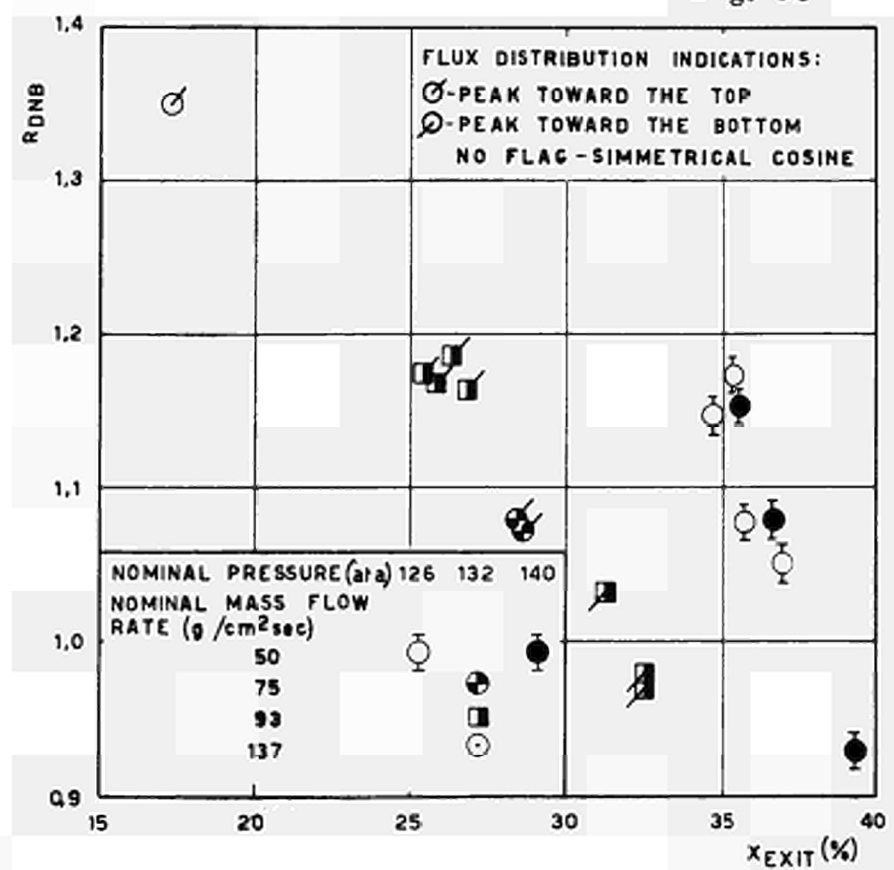


Fig. 37

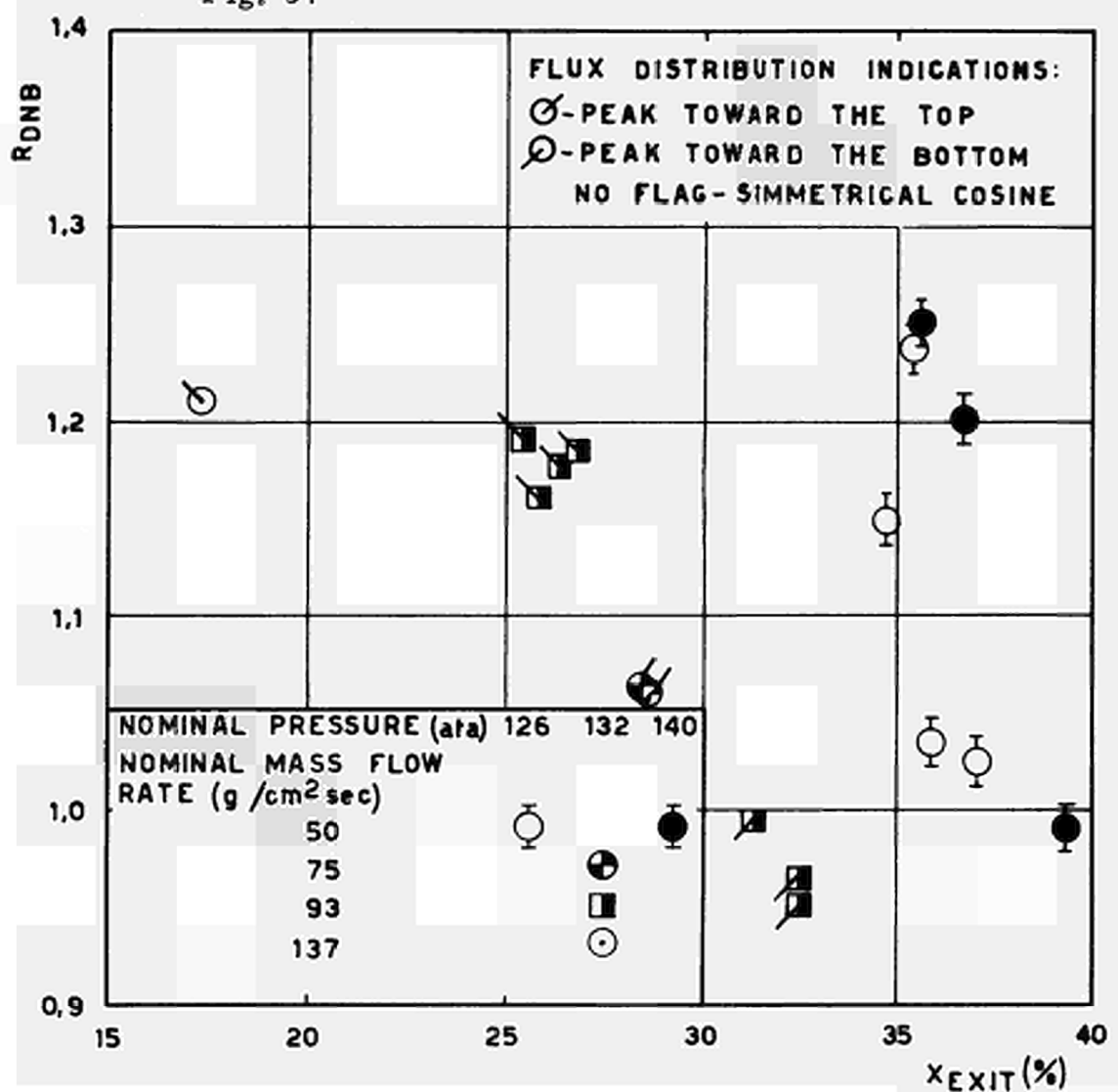
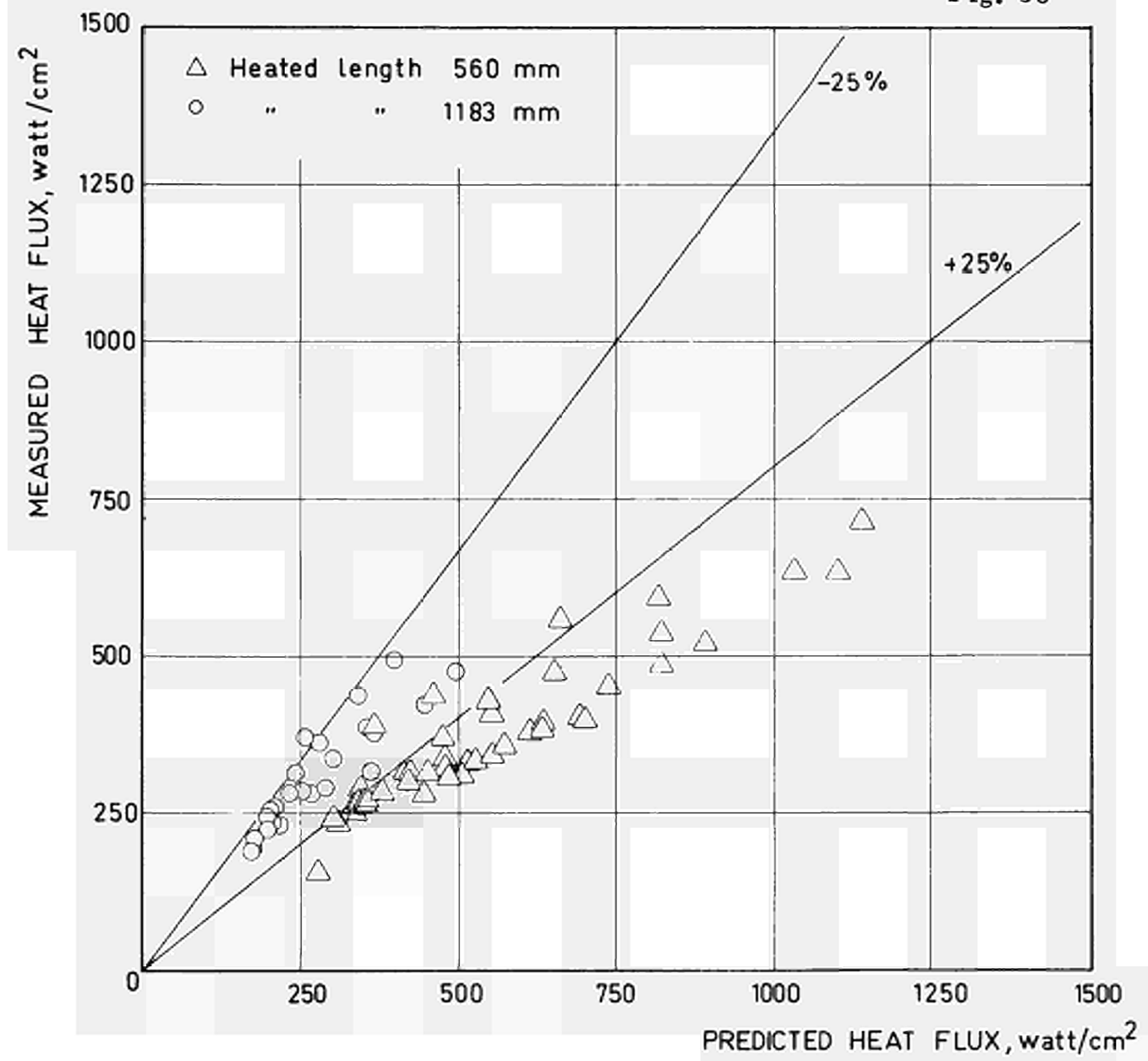


Fig. 38



MEASURED HEAT FLUX, watt/cm²

Fig. 39

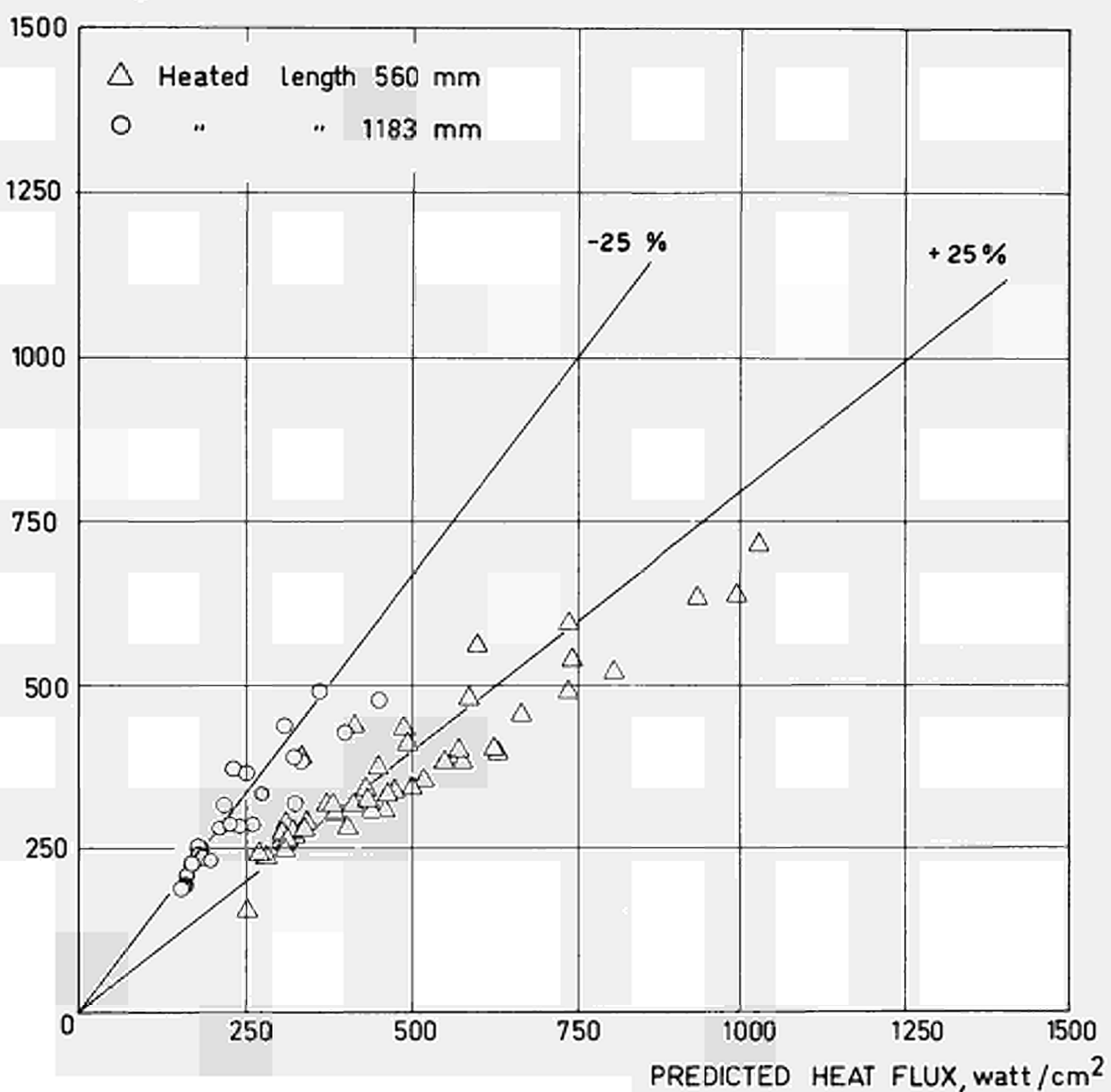


Fig. 40

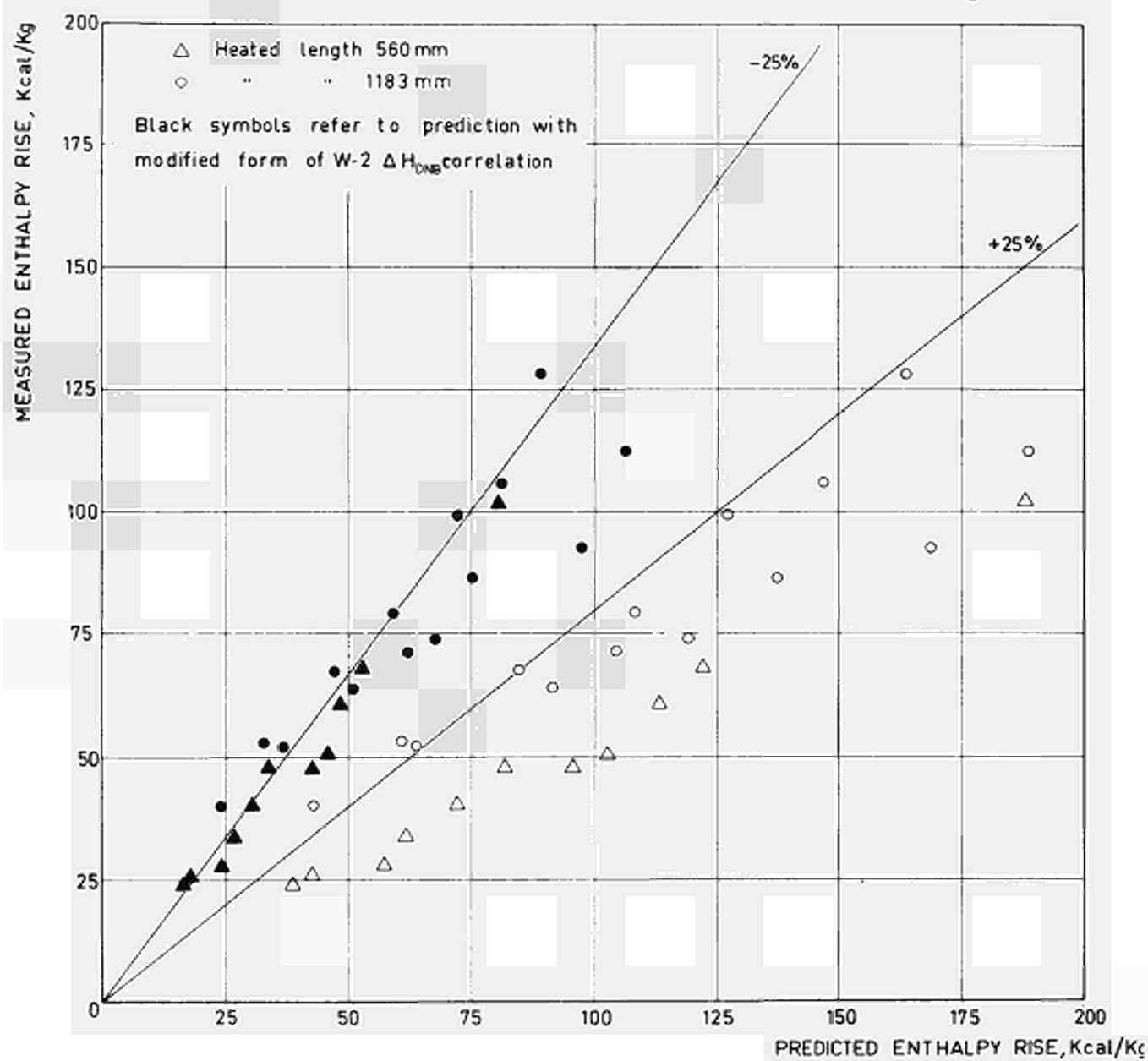


Fig. 41

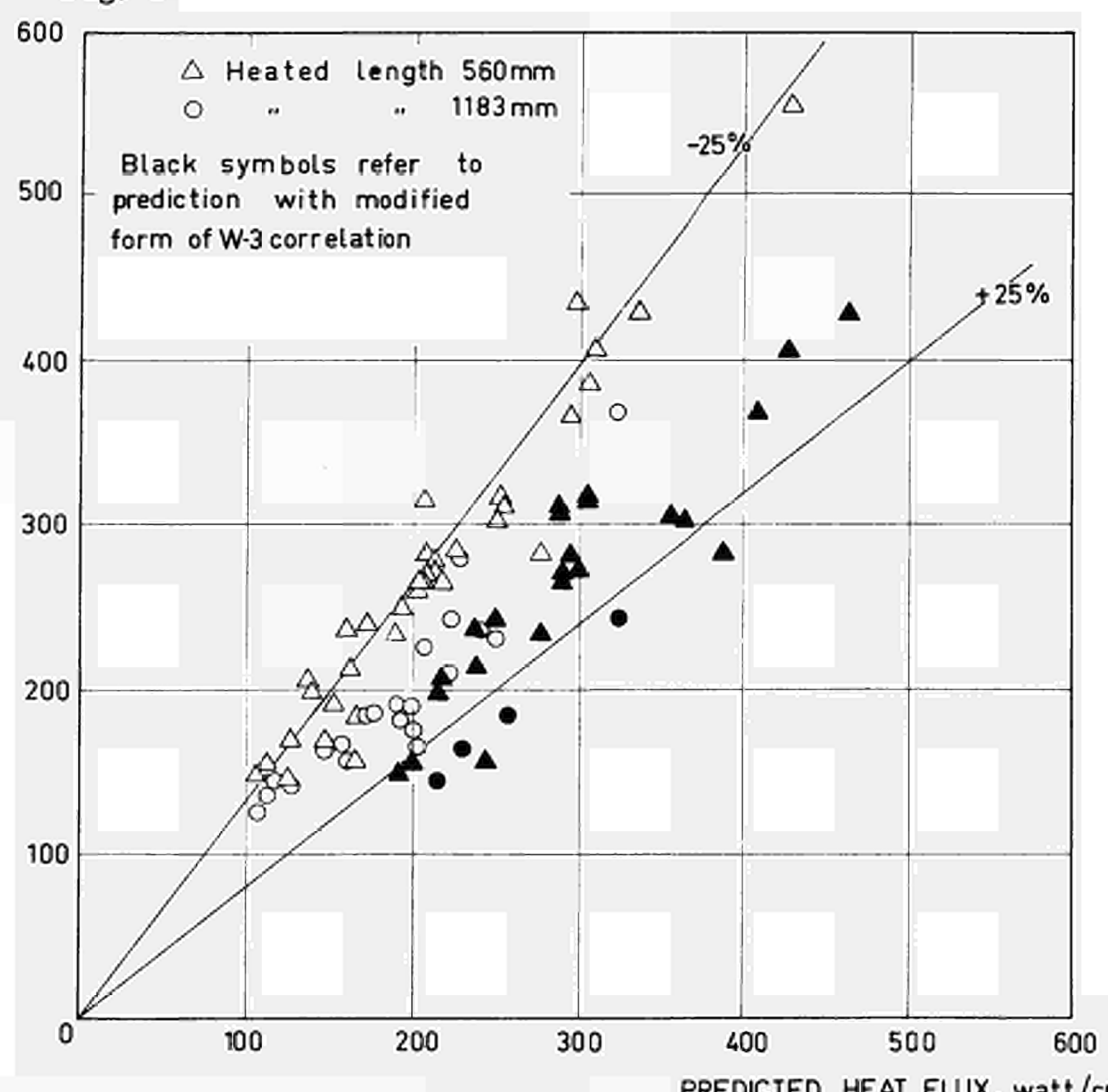


Fig.6

EFFETTO DELLA PARETE FREDDA - CONFRONTO TRA FLUSSO TERMICO CALCOLATO
(Correlazione W-3 modificata) E Sperimentale per distribuzione di potenza
UNIFORME

Fig. 42

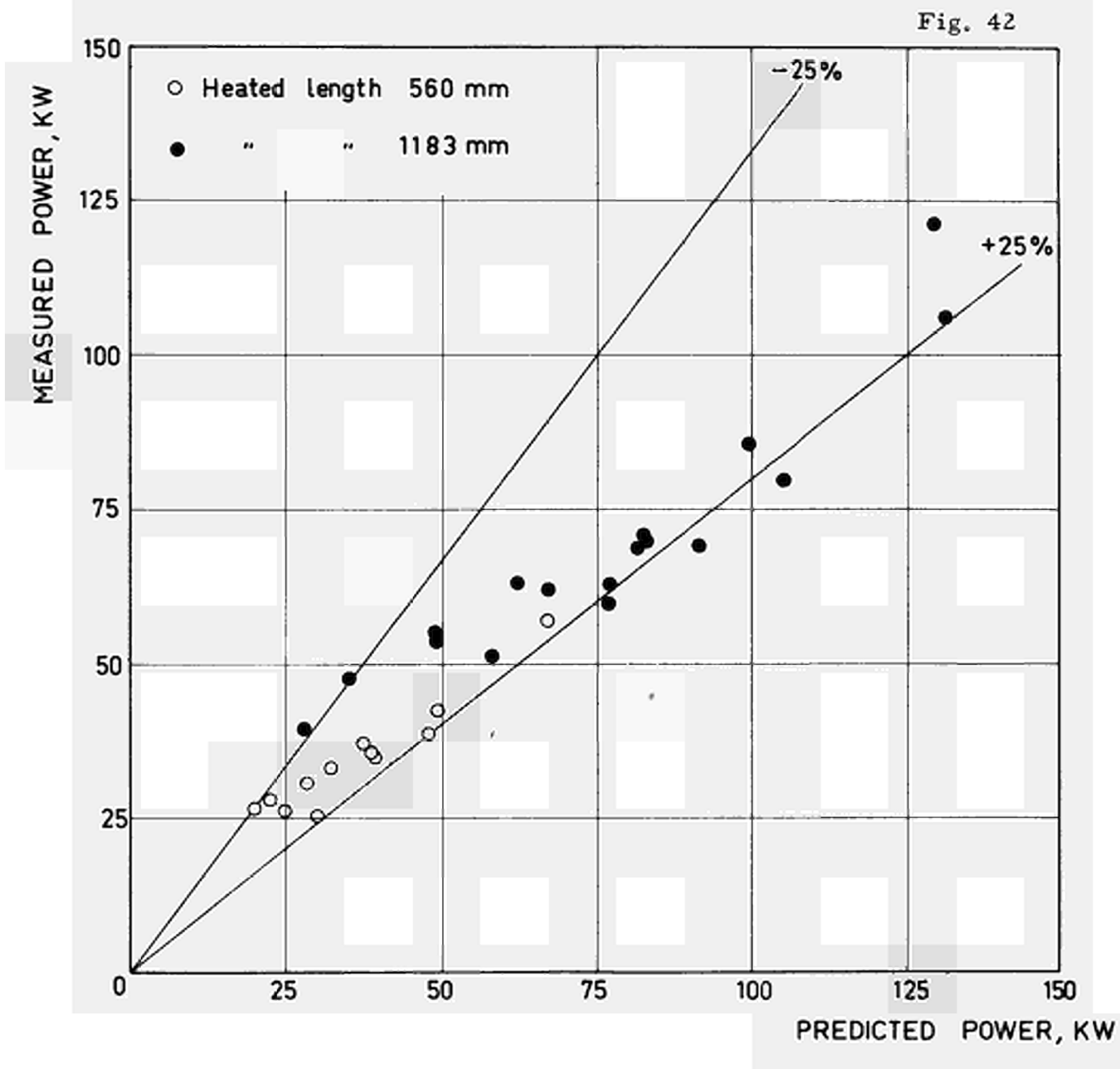
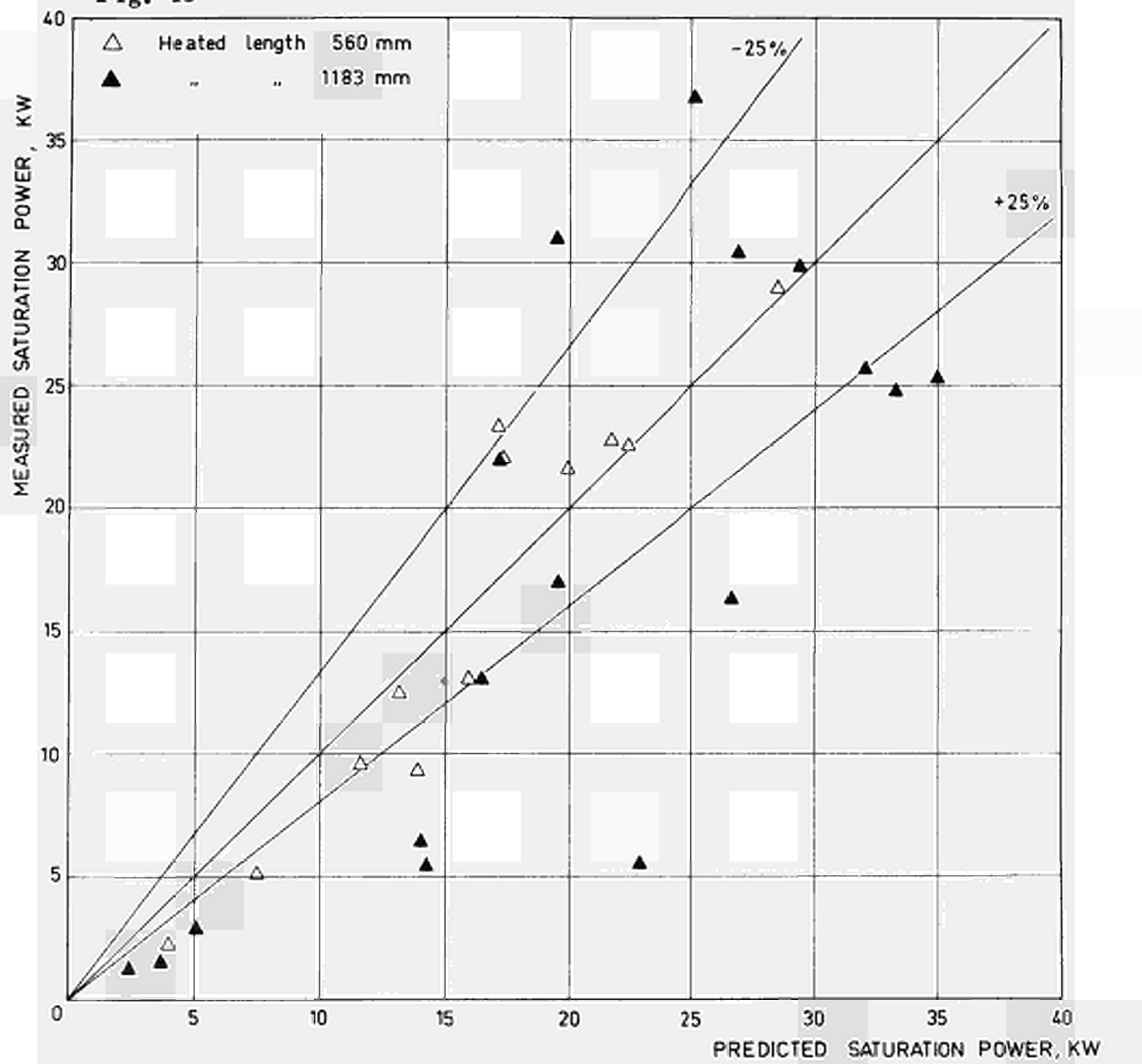


Fig. 43



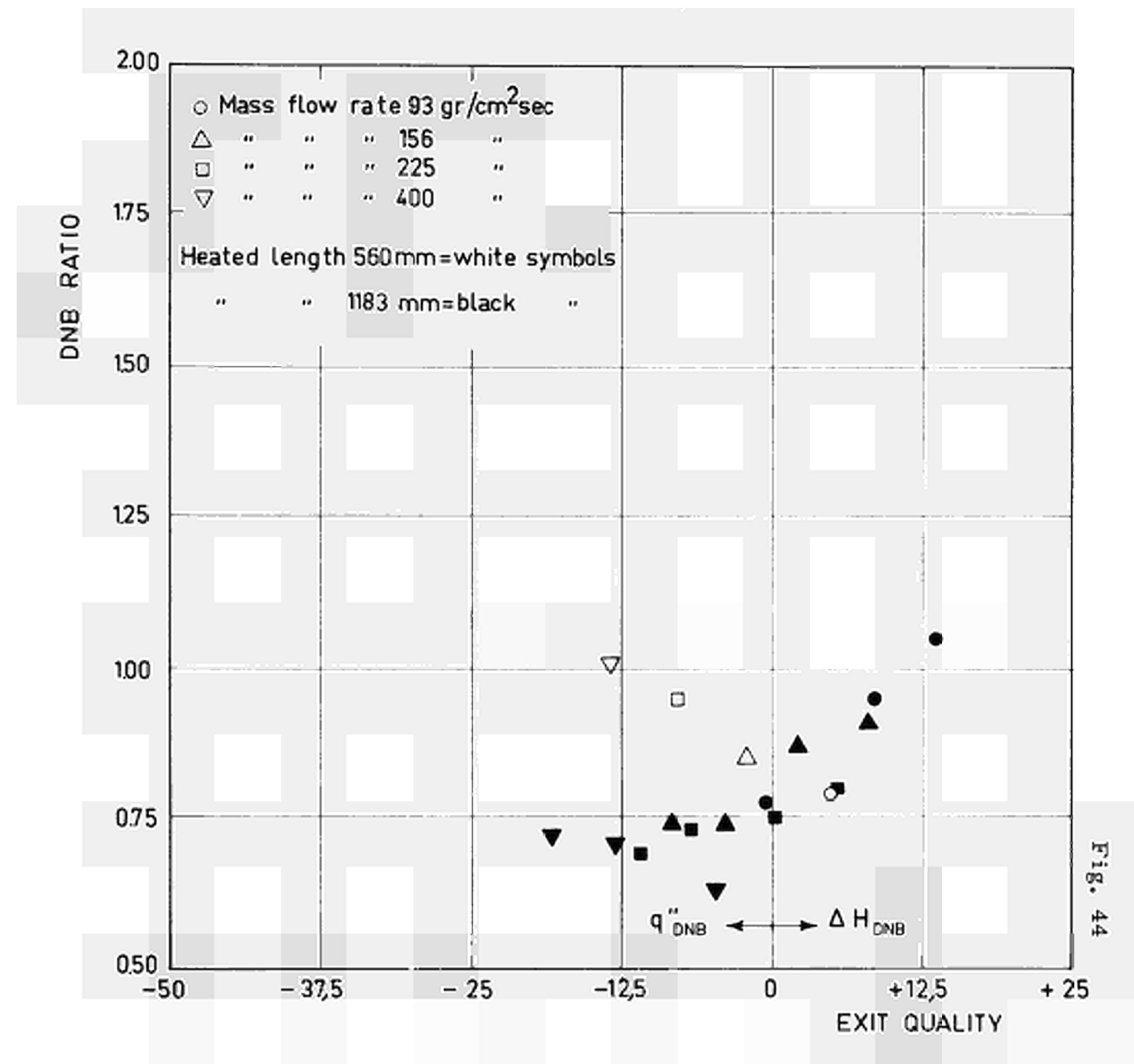
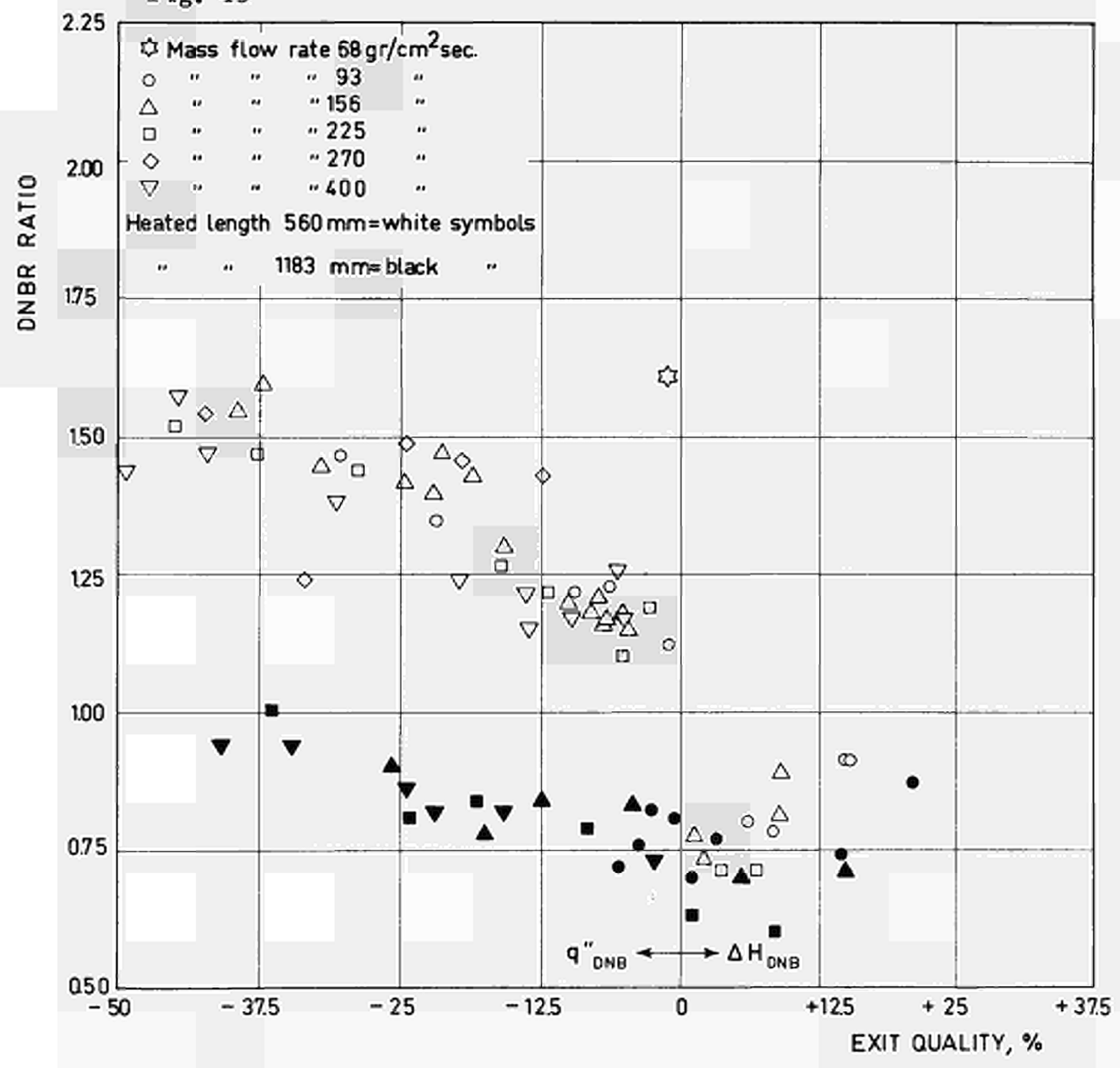


Fig. 45



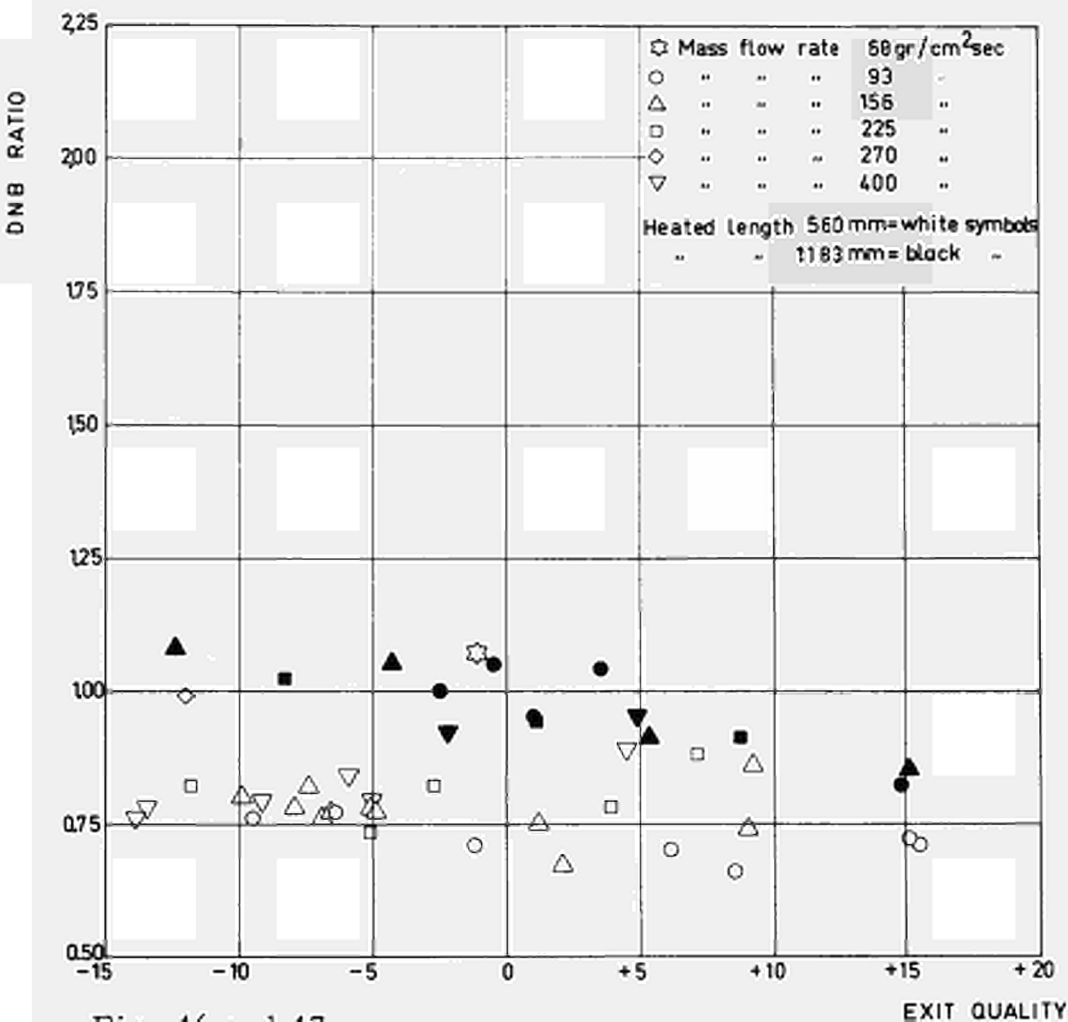


Fig. 46 and 47

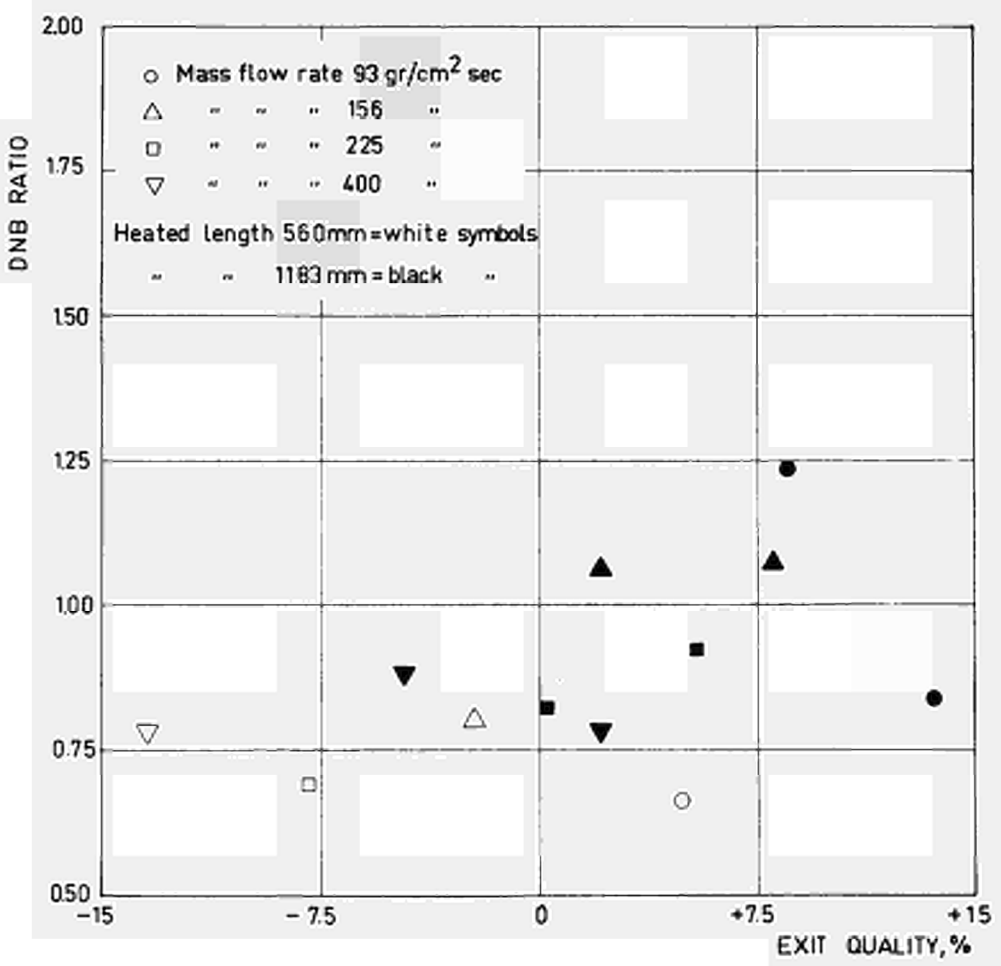


Fig. 48

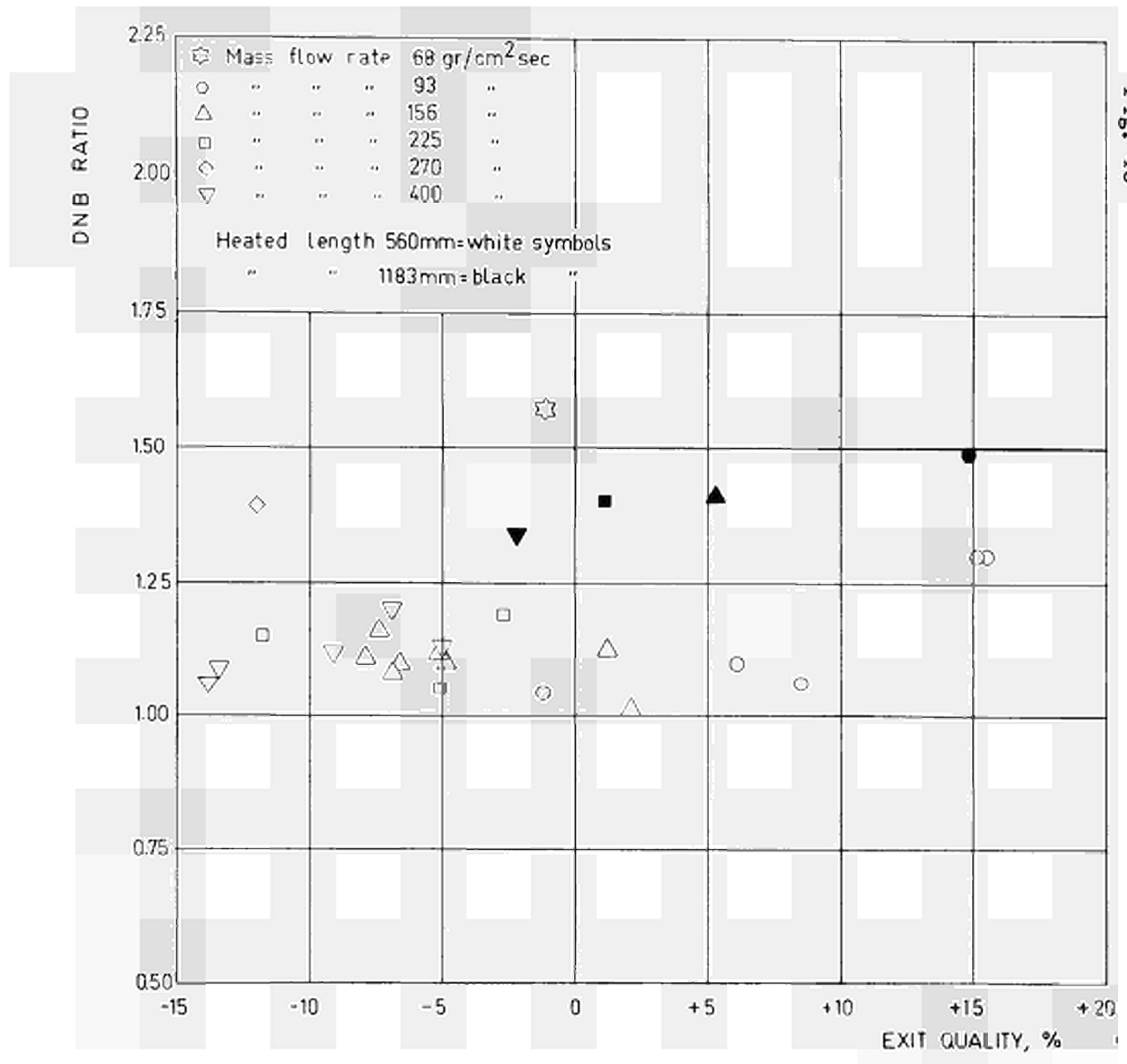


Fig. 49

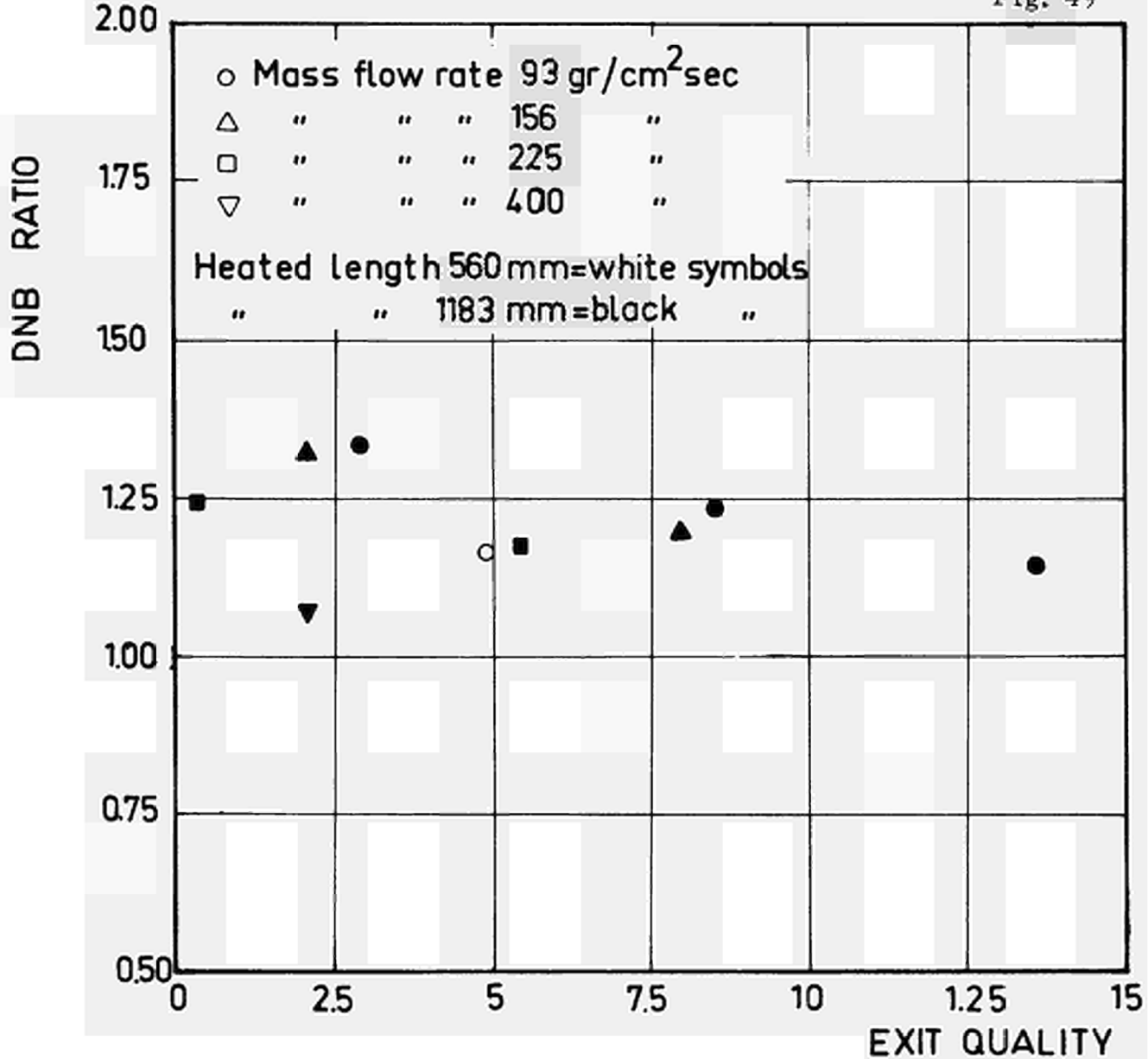


Fig. 50

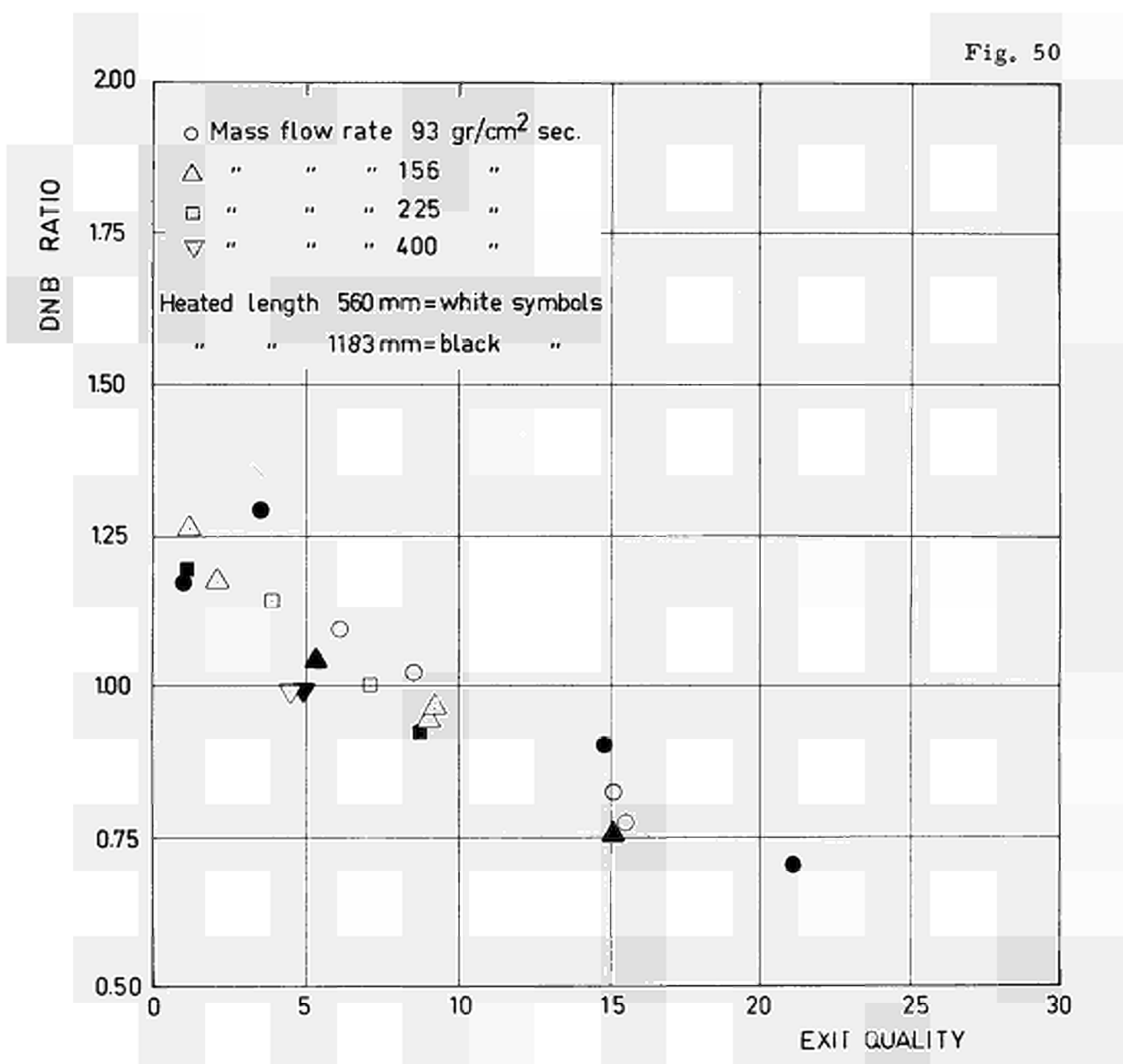
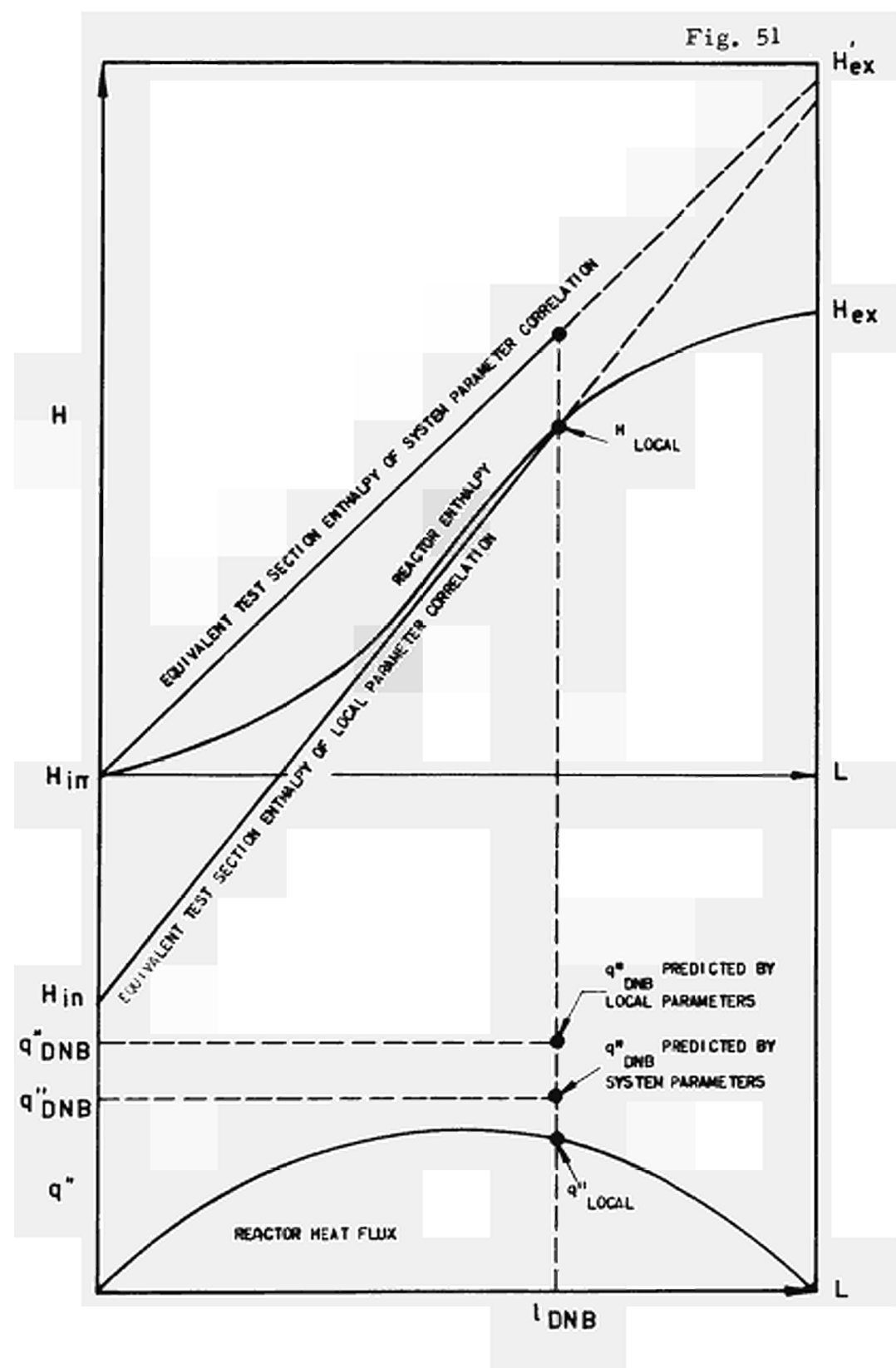


Fig. 51



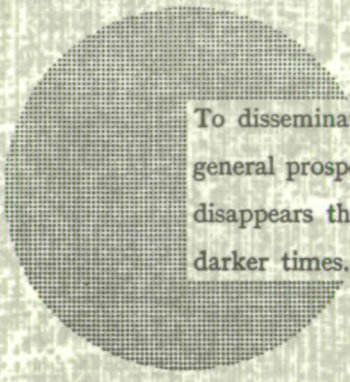
NOTICE TO THE READER

All Euratom reports are announced, as and when they are issued, in the monthly periodical **EURATOM INFORMATION**, edited by the Centre for Information and Documentation (CID). For subscription (1 year: US\$ 15, £ 5.7) or free specimen copies please write to :

Handelsblatt GmbH
"Euratom Information"
Postfach 1102
D-4 Düsseldorf (Germany)

or

**Office central de vente des publications
des Communautés européennes**
2, Place de Metz
Luxembourg



To disseminate knowledge is to disseminate prosperity — I mean general prosperity and not individual riches — and with prosperity disappears the greater part of the evil which is our heritage from darker times.

Alfred Nobel

CDNA03113ENC

SALES OFFICES

All Euratom reports are on sale at the offices listed below, at the prices given on the back of the front cover (when ordering, specify clearly the EUR number and the title of the report, which are shown on the front cover).

PRESSES ACADEMIQUES EUROPEENNES

98, Chaussée de Charleroi, Bruxelles 6

Banque de la Société Générale - Bruxelles
compte № 964.558,

Banque Belgo Congolaise - Bruxelles
compte № 2444.141,

Compte chèque postal - Bruxelles - № 167.37,

Belgian American Bank and Trust Company - New York
compte No. 22.186,

Lloyds Bank (Europe) Ltd. - 10 Moorgate, London E.C.2,
Postscheckkonto - Köln - Nr. 160.861.

OFFICE CENTRAL DE VENTE DES PUBLICATIONS DES COMMUNAUTES EUROPEENNES

2, place de Metz, Luxembourg (Compte chèque postal № 191-90)

BELGIQUE — BELGIË

MONITEUR BELGE
40-42, rue de Louvain - Bruxelles
BELGISCH STAATSBALD
Leuvenseweg 40-42 - Brussel

LUXEMBOURG

OFFICE CENTRAL DE VENTE
DES PUBLICATIONS DES
COMMUNAUTES EUROPEENNES
9, rue Goethe - Luxembourg

DEUTSCHLAND

BUNDESANZEIGER
Postfach - Köln 1

NEDERLAND

STAATSDRUKKERIJ
Christoffel Plantijnstraat - Den Haag

FRANCE

SERVICE DE VENTE EN FRANCE
DES PUBLICATIONS DES
COMMUNAUTES EUROPEENNES
26, rue Desaix - Paris 15^e

ITALIA

LIBRERIA DELLO STATO
Piazza G. Verdi, 10 - Roma

UNITED KINGDOM

H. M. STATIONERY OFFICE
P. O. Box 569 - London S.E.1

EURATOM — C.I.D.
51-53, rue Belliard
Bruxelles (Belgique)